EXPERIMENTAL STUDY ON BEHAVIOR OF WOOD AND STEEL SINGLE PILES

MASTER'S THESIS

NICHIRVAN RAMADHAN TAHER

Department: Civil Engineering
Program: Geotechnical

Supervisor: Assoc. Prof. Dr. H. Suha AKSOY

MARCH-2019

T.C.

FIRAT ÜNİVERSİTESİ

FEN BİLİMLERİ ENSTİTÜSÜ

EXPERIMENTAL STUDY ON BEHAVIOR OF WOOD AND STEEL SINGLE PILES

Yüksek Lisans Tezi

Nıchırvan Ramadhan TAHER

162115106

Tezin Enstitüye Verildiği Tarih : 06.03.2019

Tezin Savunulduğu Tarih: 12.04.2019

Anabilim Dalı: İnşaat Mühendisliği

Programı: Geoteknik

Danışman: Doç.Dr.H.Suha AKSOY

Doç.Dr.Muhammet KARATON

Dr.Öğr.Üyesi Abdulhakim ZEYBEK

NİSAN-2019

ACKNOWLEDGEMENTS

All praises and thanks be to Allah, we seek His help and mercy, the Almighty, who has created the heavens and the earth, and brought into being deep darkness as well as light. On whom we definitely depend for sustenance, guidance and help.

I would like to thank my thesis advisor, in Civil Engineering Department Assoc. Prof. Dr. H. Suha Aksoy for his support, patience, motivation, all along my research. Who has always helped me and his door was always open, and was ready to help anytime when I got a problem about my research and wish him long life with gladness. I also want to thank Res. Assist. Mesut GÖR and Res. Assist. Aykut ÖZPOLAT for their continuous help and support.This thesis was financially supported by BAP of Firat University, project number MF.18.39.

At the end I have to express my deepest gratitude to my drear parents and my whole family for their continuous support, motivation and encouragement throughout my years of study, and they had a great role and always supported me to continue my studying.

Nichirvan Ramadhan TAHER

Elaziğ, 2019

DECLARATION

I hereby declare that all information contained in this document has been achieved and presented in corresponding to academic rules and ethics. I also declare that, as required by these rules and behaviors, I have fully quoted and referenced all non-original documents and results used in this thesis.

Nichirvan Ramadhan TAHER

Elaziğ, 2019

TABLE OF CONTENTS

ÖZET

Ahşap ve Çelik Tekil Kazıkların Taşıma Güçlerinin Deneysel Olarak Belirlenmesi

Bu çalışmada, dört farklı rölatif sıkılıkta (10%, 40%, 65% ve 90%.) hazırlanmış kumlu bir zeminlerle ahşap ve çelik kazıklar arasındaki sürtünmenin belirlenmesi amaçlanmıştır. Ayrıca ahşap ve çelik tekil kazıklar eksenel olarak yüklenmiş ve sınır taşıma güçleri de belirlenmiştir. Bu araştırma kapsamında elde edilen deneysel sonuçların ışığında, sonlu elemanlar yöntemi kullanılarak eksenel yüklenmiş tekil kazıkların sayısal modellenmesi yapılmıştır.

Bu amaçla, farklı rölatif sıkılıktaki zeminlerin içsel sürtünme açısını elde etmek ve zeminle kazık malzemeleri arasındaki yüzey sürtünme açılarını belirlemek amacıyla 36 adet kesme kutusu deneyi yapılmıştır. 12 adet kesme kutusu deneyi 4 farklı sıkılıkta hazırlanmış zeminlerin içsel sürtünme açılarının belirlenmesi için yapılmıştır. 24 adet kesme kutusu deneyi ise kazık malzemeleri ile bu zeminlerin yüzey sürtünme açılarının belirlenmesi için yapılmıştır. Ayrıca ahşap ve çelik tekil model kazıkların eksenel yükleme deneyleri yapılmış ve yük oturma grafikleri elde edilmiştir.

Kesme kutusu deneyleri sonuçları incelendiğinde, kum zeminin rölatif sıkılığı arttıkça içsel sürtüne açısının arttığı görülmüştür. Yüzey sürtünme açılarının belirlenmesi için yapılan kesme kutusu deneyleri sonucunda, artan rölatif sıkılık değerleriyle yüzey sürtünme açısı değerlerinin %65 sıkılık değerine kadar arttığı belirlenmiştir. Ancak %90 rölatif sıkılık değerinde yüzey sürtünme açısı değerinde azalma gözlemlenmiştir. Bunun nedeninin, sıkı kumlarda artan deformasyonlarla beraber zemin kayma gerilmelerinin maksimum değere ulaştıktan sonra düşmesi ve daha sonra sabit bir değerde kalması olduğu düşünülmüştür.

Yapılan model deneylerinden ve sonlu elemanlar analizlerinden ise artan rölatif sıkılık değerleri ile taşıma gücünün arttığı belirlenmiştir. Deneysel ve nümerik sonuçlar karşılaştırıldığında, her iki yöntemde elde edilen sonuçların oldukça uyumlu olduğu görülmüştür.

Anahtar Kelimeler: Kesme kutusu, kum, içsel sürtünme açısı, yüzey sürtünme açısı, model kazık, sonlu elemanlar yöntemi.

SUMMARY

Experimental Study on Behavior of Wood and Steel Single Piles

The goal of this study is to investigate the friction between sandy soil and pile materials (wood and steel) in four different relative densities including 10%, 40%, 65% and 90%. It is also aimed to study the behavior and ultimate bearing capacity of the single model piles under axial loading for the same materials. Finite element method was also used in this research to study the behavior of the single model piles under axial loading.

For this purpose thirty-six direct shear tests were performed to study the internal friction angle of the sand and skin friction angle between sand and pile materials in different relative densities mentioned above. Twelve direct shear tests were conducted to investigate the internal friction angle of the sand, and twenty-four interface shear tests were performed to study the skin friction angle between the sand and pile materials. In addition, the axial load tests for pile models were conducted in the laboratory to study the behavior and load-settlement curve of single mode piles under action of axial loading.

The results from direct shear tests showed that the internal friction angle of the sand increases with increasing relative density. From the interface direct shear test, the skin friction angle between the sand and pile materials (wood and steel) increases with relative density up to 65% but in 90% relative density it started to decreases. Because in dense sand, the resisting shear stress increases with shear displacement until it reaches a failure stress, after failure stress is attained, the resisting shear stress gradually decreases as shear displacement increases until it finally reaches a constant value.

Also the results from experimental pile model tests and Plaxis 3D finite element programs indicated that the ultimate bearing capacity of the model piles increases with increasing relative density, and there is a good agreement between experimental results with finite element programs results.

Key words: Direct shear, sand, internal friction angle, interface friction angle, model pile, finite element method

LIST OF FIGURES

LIST OF TABLES

Page No

SYMBOLS LIST

IST	: Interface Shear Test
Dr	: Relative Density (%)
δ	: Skin Friction Angle between Sand and Pile materials
ϕ	: Internal Friction Angle of the Sand
δ’	: Effective Skin Friction Angle between Sand and Pile materials
ϕ’	: Effective Internal Friction Angle of the Sand
K	: Coefficient of Lateral Earth Pressure
K_p	: Rankine’s Passive Earth Pressure Coefficient
K_a	: Rankine’s Active Earth Pressure Coefficient
K_o	: Coefficient of Earth Pressure at Rest
σ'_v	: Vertical Effective over burden Pressure
A	: Area
A_p	: Pile Point Area
D	: Demeter of the Pile
L	: Length of the Pile
D_f	: Over Burden Depth of the soil
f**s**	: Unit Skin Friction
Q_f	: Shaft Friction Resistance of the pile
Q_u	: Ultimate Bearing Capacity of the pile
Q_p	: Point Bearing Capacity of the pile
N_q, N_γ, N_c	: Bearing Capacity factors
d_q, d_c, d_γ	: Depth factors
ASTM	: American Society for Testing and Materials
C_c	: Coefficient of Curvature
C_u	: Coefficient of Uniformity
D_{10}	: Effective Grain Size
D_{30}	: Particle size at 30 % finer
D_{50}	: Median Grain Size
D_{60}	: Particle size at 60% finer

e	: Void Ratio
$\mathbf{e_{max}}$	: Maximum Void Ratio
$\mathbf{e_{min}}$	: Minimum Void Ratio
Gs	: Specific Gravity
SP	: Poorly Graded Sand
USCS	: Unified Soil Classification System
γ_d	: Dry density
pH	: Degree of acidity or alkalinity
γ	: Soil Unit Weight
s_γ	: Shape Factor
L_b	: Embedment Depth of Pile
η'	: Effective Surface Angle in Radian at Pile Toe
Es	: Modulus of Elasticity of Soil
μ	: Poisson’s Ratio of Soil
p	: Pile Circumference or Pile Perimeter
L'	: Critical Pile Embedment Length ≤ 15D
D_{tank}	: Diameter or Short Dimension of Model Tank
LVDT	: Linear Variable Displacement Transducer
γ_d	: Dry Unit Weight
e	: Void Ratio
ASTM	: American Society for Testing and Materials
G_s	: Specific Gravity
$\gamma_{d\ min}$	: Minimum Dry Unit Weight
$\gamma_{d\ max}$	: Maximum Dry Unit Weight
e_{min}	: Minimum Void Ratio
e_{max}	: Maximum Void Ratio
D_{max}	: Maximum Grain Size
D_{min}	: Minimum Grain Size

1. INTRODUCTION

1.1. General Introduction

The vast majority of structures consist of two main parts, one above the ground level, it is called super structure and the other, below ground level, is called foundation.

The foundation is an important part of any engineering structure project. Therefore, special attention must be paid to its design and construction, as it supports all parts of the structure in case of failure of the structure as a whole. The foundation transmits super-structural loads and its own weight to the underground layers of soil, the soil on which the foundation rests is called a foundation bed.

The allowable bearing capacity of the ground on which the foundation rests must be greater than the stress exerted at the bottom of the foundation. Shear failure of the soil should not be allowed and the settlement expected from the foundation should be tolerable.

The foundation is built at the base of any structure to carry out and satisfy the following significant purposes.

- To spread the structure's load on a considerable large bearing area.
- To apply the load over the bearing surface area uniformly so that differential settlement is avoided.
- To forbid the sideward movements of the all materials supported by the foundation.
- To get high stability degree of the whole structure.

In general, foundations can be divided into two sub-categories: shallow foundations and deep foundations. Figure 1.1 shows the classification of foundation system, this classification is based on how the foundation transmits the load of the structure to the ground. If the depth of the foundation is less than its width ($D < B$), it is called shallow foundation. The shallow foundation transmits the load of the superstructure vertically to the shallow depth of the ground. There are about five types of shallow foundations; they are classified according to the design as:

- Continuous wall footing (strip footing)
- Isolated spread footing
- Combined footing

- Cantilever (strap footing)
- Mat (raft foundation)

Deep foundations are foundations where the depth of the foundation is greater than its width (D>B), the ratio (D/B) is generally 4-5 for deep foundations. In contrast to shallow foundations, deep foundations vertically transmit the load of the superstructure into the rock or into deep, deep soil layers below the ground. A deep foundation must be used when the capacity of the shallow foundation is not sufficient to support the loads of the structure. The deep foundation can be further classified into the following types:

- Pile foundation
- Pier (caissons) foundation

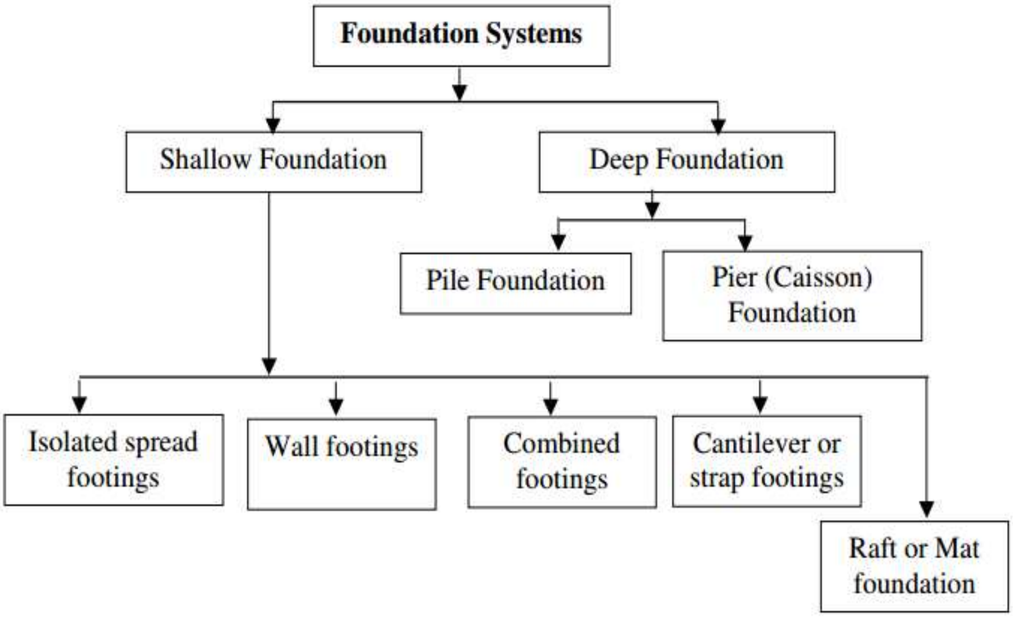

Figure 1.1. Classification of foundation system (Das and Sivakung, 2016)

1.2. Pile Foundations Introduction

Piles are used to construct pile foundations; they are structural members fabricated from timber, concrete, steel and composite materials. Piles are considered a deep foundation because the width or diameter of the pile is much smaller compared to its depth. Despite the cost of more expensive piles than shallow foundations, it is often necessary to use them to ensure the safety and protection of the structure. The following list identifies some of the situations requiring the use of pile foundations (Vesic, 1977).

1. While one or more layers of the ground soil are extremely compressible and too poor to carry the load which is transferred through the superstructure, piles are utilized to convey the loads of the superstructure to underlying bedrock or very potent soil layers, see Figure 1.2a, at the point when the bedrock is not met at a sensible depth beneath the ground surface, piles can be used to transfer the structural load in a gradual way to the ground soil layers, the structural load resistance is mostly obtained from the friction developed in between pile-soil interface as shown in Figure 1.2b.

2. When the structure exposed to a lateral forces Figure 1.2c, in this case pile foundations can resist the exposed horizontal loads by bending in the same time supporting vertical loads coming from the superstructure. This kind of situation is usually met in the construction and design of foundations of high rise buildings and earth-retaining structures which are subjected to high degree horizontal forces.

3. In lots of instances, the existing soil on the site of a proposed structure is collapsible and expansive soil, this type of soil may be extended into a greater depth underneath the ground surface. As the water content of expansive soils increase or decrease those soils start to swell or shrink, the swelling pressure can be extremely significant and considerable, in such conditions, if shallow foundations be used the proposed structure may subject to a great damage. Nevertheless, the pile foundations can be thought about as an alternate while the piles can be extended below the active zone, in which where swelling and shrinking take place as shown in Figure 1.2d. Soils like loess are collapsible by nature, as the water content of these types of soils rises, the failure may happen to their structures. Unexpected or sudden decrease of void ratio of the soil will cause a considerable settlements of the structures which are supported by shallow foundations, in such conditions, this type of problems can be solved by using pile foundations while piles are extended deep into the stable soil layers below the zone in which moisture content will increase or decrease.

4. In some cases, the foundations of structures subject to uplifting forces such as offshore platforms, transmission towers and basement mats below the water table, in this types of problems pile foundations are used to resist the uplifting forces. See Figure 1.2e.

5. Pile foundations are generally used under piers and abutments of bridge to stay away from the loss of bearing capacity due to soil erosion at the surface of the ground in which shallow foundations might suffer from it, as shown in Figure 1.2f.

Although, in the past, many researchers conducted theoretical and experimental studies to understand the behavior of the piles in granular (cohesionless) and cohesive soils under different types of loading. The mechanisms have not been fully understood so far and may not be forever. Because of uncertainties involved in subsoil conditions, the pile foundation analysis and design might be considered a little bit of an art.

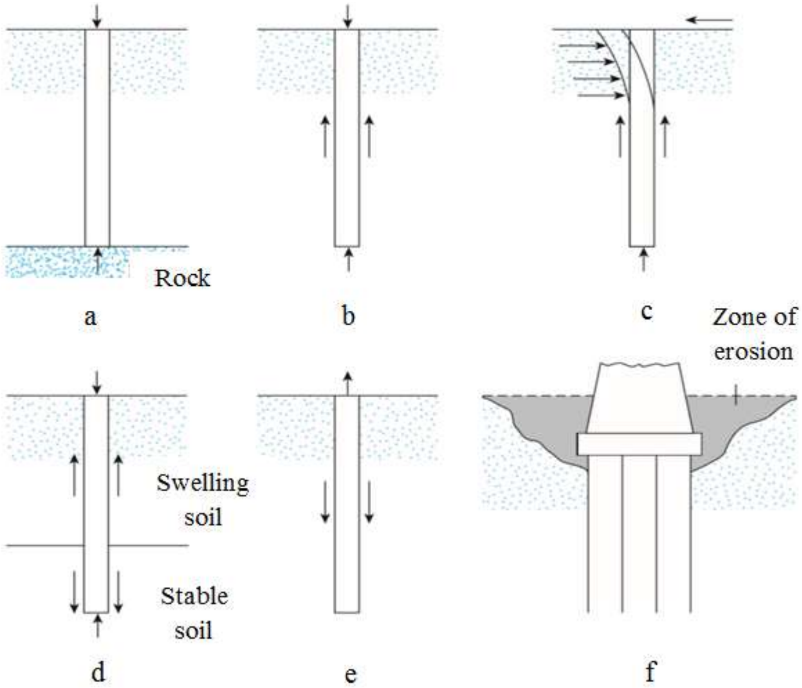

Figure 1.2. Conditions that require the use of pile foundations

1.3. Deep Foundation Types and Terminology

Engineers and contractors have developed many types of deep foundation systems using different installation techniques. Each foundation type and installation system is most suitable to a specific ground soil properties, the location of the water table and loading conditions because the method which is used for installation of deep foundation has a great effect on behavior, analysis and design of them. Because of that, deep foundations are classified into groups and sub-groups by their installation methods and techniques. Deep foundation systems are widely classified into three which are piles, caissons and pile-supported mats.

Piles are structural elements they are long and slender which enter profound into a ground, a wide range of various pile technologies are accessible, every one of which is most appropriate for a specific situations. The most widely used three types of foundations are:

- **Driven piles**, they are also called displacement piles are prefabricated structural members and can be made of steel, timber and concrete, they are driven into the ground to the desired design depth by pounding or vibration by using appropriate machineries and apparatus.
- **Drilled shafts or bored piles** are also known as non-displacement piles; they are cast-in-place deep foundation members and have high capacity. Drilled shaft piles are constructed by drilling a hole in the ground and inserting the reinforcement steel into the hole afterwards filling the hole with the concrete.
- **Continuous flight auger piles (CFA)**, are also well-known as augur-cast-in place and augur pressure grout piles, they are constructed by drilling a hole using continuous flight augur machine when the desired depth is reached the augur is withdrawn in a gradual way and in the same time the cement ground is pumped into the drilled hole through the hollow center of the augur pipe, if needed, the steel reinforcement is placed into the hole immediately after withdrawn of the augur.

A number of other different pile technologies are available in spite of the fact that they are not used widely but each of those technologies and methods has its special and unique advantageous which can be used in specific conditions, these cover:

- **Jacked piles,** they are just like driven piles with the exception of the pile are pushed instead of beating into the ground.
- **Franki piles,** they are built via beating a wet concrete right into a cased hole which shapes an enlarged base at the bottom of the pile and compacts the neighboring soils.
- **Micro piles,** they are similar to the drilled shaft foundation but with small diameter and high strength steel casing or threaded bar.
- **Helical screw piles,** they are made of steel with helices like screws and progressed into the ground by twisting.
- **Anchors,** is a vast term which refer to as deep foundation and they are basically proposed to withstand a tensile loads.

Pile foundations are usually straight they have a constant cross-section along their depth, some of them are tapered which means pile cross-section is decreased with depth as shown in Figure 1.3b. Some of the piles have an enlarged base at the bottom of the pile they are also known as belled piles see Figure 1.3c. The axis of the foundation is a line passes through the centroid of the pile is parallel its longest dimension

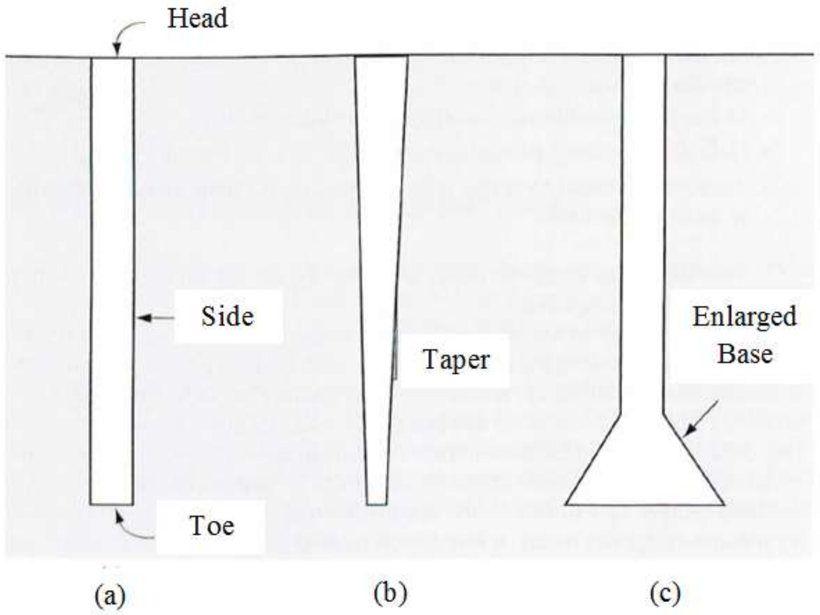

Figure 1.3. Parts of the deep foundation: (a) Straight foundation; (b) Tapered foundation; (c) Enlarged base foundation

1.4. Behavior of Piles Materials and Deterioration Problems

1.4.1. Steel Piles

In 1890 steel had to be extensively on hand and plenty of structures were built by using this new material. Using steel as piles was a natural evolution, for the first time in 1899 steel I-beam section was used as a driven pile, in the same year steel pipe piles with 30 cm diameter were used. The pneumatic hammer was used for driving steel pipe piles and filled with concrete. In 1908 H-section steel piles were introduced by Bethlehem. From 1930 up to now using both H-and I-section steel piles are common. (Parkhill, 2001).

Steel piles usually can be pipe piles or H-section piles, steel pipe piles might be driven into the ground with open or closed end. I-section and wide flange steel beams can also be utilized as piles. Nevertheless, H-section piles are more preferred this is because the thicknesses of their flange and web are equal. In lots of cases, after the steel pipe piles are driven into the ground then they are filled with concrete.

While necessary or long steel piles are required, they can be spliced together by welding or by riveting. During the site exploration and taking boreholes from the ground site of the proposed area if hard soil layers are found such as dense gravel, soft rock and shale, the driving process will subject hard conditions, therefore driving shoes or pints can be fitted with bottom of the steel piles.

Steel piles also may expose to corrosion problems. For instance, peats, swamps and organic soils are corrosive. When the pH of the soil is greater than 7 the soil is considered not very corrosive.

At the present time, many industrial companies have attempted to decrease the rate of steel corrosion to the minimum value. For instance, the corrosion of steel has been estimated by British Steel Corporation in industrial environment which is up to 0.2 mm/year. Nevertheless, in the tough soil environment, maximum corrosion rate recorded for an extracted steel pile after 25 years was 0.03 mm/year. (Han et al., 2003).

To reduce the effect of corrosion, extra steel thickness is added over the actual design cross-section. Using epoxy coating is also satisfactory against steel corrosion. The epoxy coating can't be easily vandalized during pile driving.

- **Advantageous**

a) It is easy to deal with cutoff and extending deep to the required depth.

b) Can sustain high level of driving stress.

c) Can be penetrated through dense soil layers such as soft rock or dense gravel.

d) High capacity to carry loads.

- **Disadvantageous**

a) Fairly high priced.

b) High noise degree while driving.

c) Exposed to corrosion.

d) May be subjected to deformation or damage from the vertical while driving into dense soil layers.

1.4.2. Timber Piles

The history of using timber piles dates back to at least as far as the age of stone. The dwellers of alpine lake in Europe used timber piles as support for their house platforms 4000 to 5000 years ago. Alexander the Great used driven wood piles in the Tyre city 332 B.C., and the Romans also utilized them widely. Timber piles also have been used as a foundation for the bridges in china for the time of the Han Dynasty (200 BCE-200 CE). In the middle of ages, people utilized pulleys and leverage for lifting heavy weights. (Chellis, 1961).

Construction techniques updated very fast through the Industrial Revolution, particularly while the steam power being invented. Bigger and very powerful equipment were invented, so driving pile abilities was improved. The steam hammer was first used in Devonport England in 1845. These improvements were continuous through the nineteenth and twentieth centuries. In 1940 Diesel hammer was invented and for the first time appeared in North America in 1952, and in 1961 for the first time vibratory hammer was used. (Parkhill, 2001)

Timber piles are considered one of the oldest types of pile foundations. They have been used for hundreds and thousands of years and are still an excellent choice for many applications. They are made from straight trunks with their bark and perfectly cut branches. To be used as a pile, the wood must be healthy, straight and free from defects. Because the trees are naturally raised and tapered, they are thus penetrated into the soil upside down. Timber piles are high displacement piles because when they are driven into the ground they displace their whole volume of soil.

According to the American Society of Civil Engineers, No. 17 (1959) practice manual, classifying wooden piles into three classes

1. Class A piles are used to transfer heavy loads. The minimum diameter of the butt should not be less than 356 mm (14 in.).
2. Class B piles can be used for carrying medium loads. The minimum butt diameter should be 305 to 330 mm (12 to 13 in.).
3. Class C piles which are used in provisional construction work. They also can be used forever for structures when the whole pile is located under the water table. The minimum butt diameter should be 305 mm (12 in.).

Timber piles are not very strong enough, so they can’t resist high stress during driving; as a result, timber piles generally have limited capacity. Steel shoes are used at the tip (bottom) of the pile to keep it away from damage. Timber piles may also subject to damage at the tops of the piles while driving process, the impact of the hammer blows can cause brooming (crushing wooden fibers) and splitting, to reduce the damage at the top of the piles, cap or metal band may be used.

It is better to avoid splicing for timber piles, especially when they are designed to resist lateral loads and tensile forces. Nevertheless if it is necessary to do splicing, they can be spliced together by using sleeves or metal straps and bolts, as shown in Figure 1.4.

When timber piles used in marine environment, they subject to retrogradation problems because of marine organisms attack. This type of problem revert to historical utilize of timber in piers and other offshore facilities.

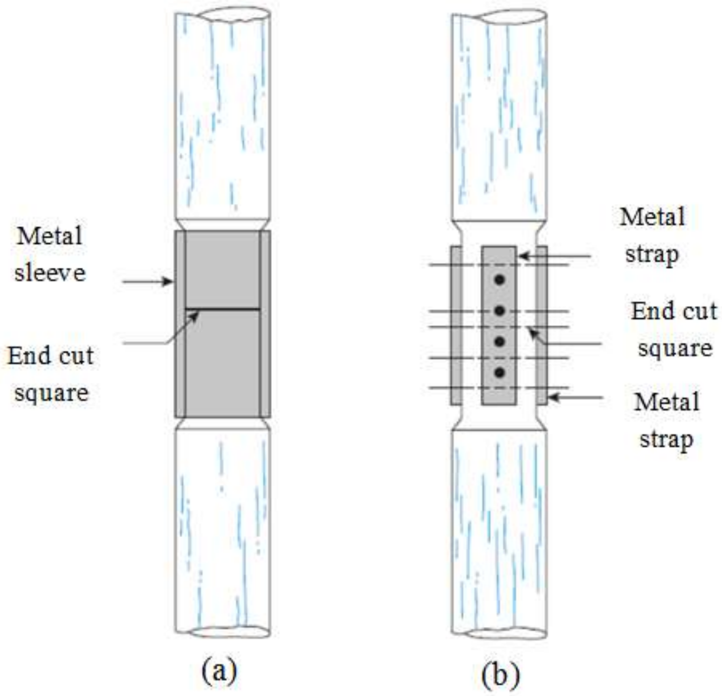

Figure 1.4. Splicing for timber piles (a) Use of pipe sleeves; (b) Use of metal straps and bolts

In general wood in waterfront structures expose to deterioration due to two major groups of organisms which are; fungi and marine borer. When timber used above the water-line area it is attacked by wood degrading fungi because there is an adequate oxygen which allows them to remain alive and deteriorate the wood, but marine borers mostly attack timber when they are completely submerged in marine water or in the tidal zone. (Lopez-Anido et al., 2004).

Timber-boring organisms which make a damage to timber piles in saltwater are classified into; (1) Moulluskan borers (ship worms and pholads); and (2) Crustaceam borers which contain several species generally known as gribbles. (Groodel, 2000).

Polymer (FRP) composite shells can be used as an encased for timber piles which supplies shear transfer possibility in between the timber pile and encasing FRP composite shells and it gives strength to the damaged portion of the pile, this repairing system also decrease the rate of retrogradation in future by making barrier around the wood pile which keep it safe from the attack of marine borers. (Lopez-Anido et al., 2003, 2004).

Wooden piles can last indefinitely and remain undamaged if they are completely submerged below the water table and surrounded by saturated soil. Nevertheless, when used in marine environment wooden piles are exposed to attack by numerous different organisms and might be damaged easily in a couple of months, they are also subject to attack by insects when located above the water table and susceptible to decade. Timber piles can be treated with preservatives like creosote to make their lives longer for decades (ASCE, 1988).

Creosote has been favorite preservative choice since 1850 because of its strength and ability to resist organisms attack and it is the unique oil-type which is currently used as a recommended wood preservative for saltwater. Creosote is a mixture of numerous chemical ingredients and their ratios which can be vary with the manufacturers but the basic ingredients are polycyclic aromatic hydro carbons (PAHs). A lot of PAHs are poisonous to marine life and some of them are carcinogenic to humans, therefore special care and precaution are required for workers who are exposed to working with creosote while the process of pile treating and installing. (Perkins and Robert, 2009).

1.4.3. Concrete Piles

Concrete piles can be classified into two main categories: precast concrete piles and cast-in-place concrete piles. Precast concrete piles are usually fabricated in special manufacturing facilities then being transported to the construction area. Ordinary reinforcement is used in precast piles to withstand bending moment while lifting and transportation. They are cast to the required design length and cured then shipped to the proposed work area. Driven concrete piles are generally fabricated with square or octagonal cross sections, as shown in Figure 1.5.

Besides, prestressed concrete piles can be made using high tensile and high strength steel cables. Before starting to concretize the piles, the cables are pre-tensioned, and then concrete is poured around them after hardening. The cables are cut, which creates a compressive force on the piles. The advantages and disadvantages are the same as prefabricated concrete piles.

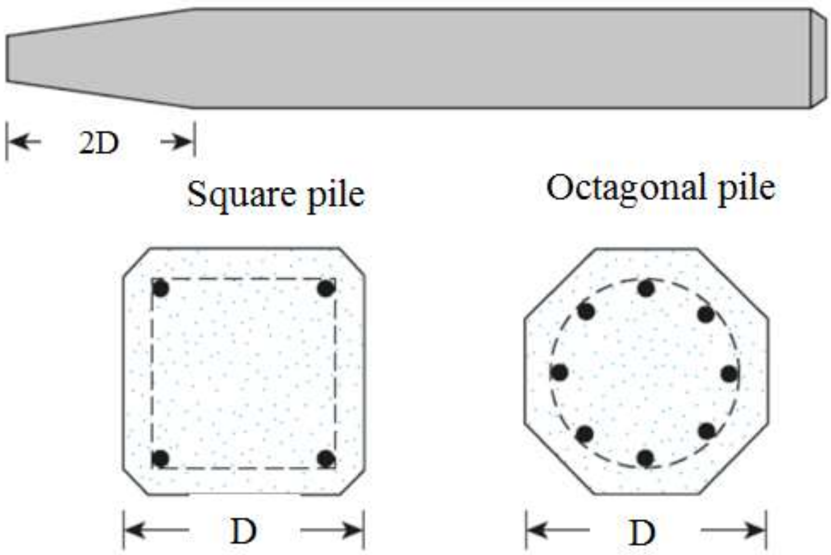

Figure 1.5. Precast concrete pile cross section

- **Advantageous**

a) Can withstand high driving stress.

b) Non-corrosive.

c) It is easy to combine them with concrete superstructures.

- **Disadvantageous**

a) Not easy to get appropriate cutoff

b) Hard to transport to the construction site

The cast-in-place concrete piles are constructed by drilling a hole in the ground, then pouring concrete to the hole and reinforcement can be placed after pouring concrete immediately.

Concrete is very common and significant construction material which is used at the present time. It has high resistant to compression forces but weak under tension forces.

Steel bars are used with it to improve its properties and withstand tension forces. Concrete protects steel bars from corrosion because it surrounds steel bars and acts like a barrier and partially insulates steel surfaces from external environment.

The durability of reinforced concrete piles rely on many factors such as the environment, time, properties of concrete and mainly its permeability. Concrete with low permeability has high durability and vice versa. (Lea, 1949).

Concrete deterioration take place mostly at low levels of PH particularly when high concentration of sulfate and chloride salt composition are available in ground soil or ground water. (Fleming et al., 2008).

The chemical reaction inside the concrete is the main cause of internal damage, differences in the chemical and physical properties of aggregates and cement paste, and in particular its permeability, which cause a change in the volume of the concrete. (Buenfeld, 1986).

1.4.4. Composite Piles

To reduce or solve the deterioration problems concerns to conventional pile foundation materials especially in water front structures, the commercial composite piling (i.e., Plastic based-materials composite piling) indicates to the most recent uprising in the pile foundation manufacturing and offer commercial productions as a replacement of traditional pile foundation materials. Modern industrial evolutions have been advanced to use fiber reinforced polymer (FRP), recycled plastic materials, and other suitable materials for this purpose.

FRP is a compound material which includes fibre that can supply high tensile strength and it is also recognized as fibre-reinforced plastics (Bank and Wiley, 2006). FRP is widely known for its great strength ratio to its weight and also has its longitudinal/transverse young and shear modulus of elasticity and high corrosion resistance in marine application (Pecce, 2001). FRP composite piles are still have a limited use in a number of seaport or offshore structures and mostly used in fendering usage and also FRP piles have been utilized for supporting piers (Bowders et al., 2000)

Composite materials (recycled plastics and reinforced fibers) also show a good compatibility due to their specific characteristics such as lightweight, long-term durability and high specific strength, high corrosion resistance for chemicals and environmental conditions and have lower repair costs than traditional piles, plastic material is mostly used as sheet piles in water front structures.

However, many studies have been conducted on the composite piles, and it has been approved that these types of piles can be used instead of conventional piles in corrosive environments, but because lack of sufficient knowledge in the data base of these piles, and design guide lines that conventional piles have. In addition to drivability of these piles, the machines which are used for driving the conventional piles they have an impact stress on the pile head during driving and cause the damages in both top and bottom of the pile. In conventional piles everything has been documented such as creep behavior under axial loading, while the creep behavior of composite piles is not well understood especially for such a case like plastic materials. Because of the reasons mentioned above the composite piles remain in a limited application and they have not been a good alternative instead of conventional piles. Therefore the conventional piles such as wood and steel are used often in the construction of pile foundation so far.

1.5. Load Transfer Mechanism of the Pile Foundation

Unlike the shallow foundation, the mechanism of transferring the load through the pile to the soil layers is complicated. In general, the axial loads applied to the piles are transferred into the ground by two mechanisms: the end bearing and the skin friction. Figure 1.6 illustrates the load transfer mechanism of the pile foundation under different types of loads.

Where rocky soils or very heavy soil layers are expected during soil exploration at the site with sensible depth, the tip of the piles can be rested on the rock surface in this case most or entire applied axial loads on the piles is carried by underlying rock layer, these types of piles are called end-bearing piles as shown in Figure 1.7 a and b.

Where rock layers or rock-like materials are not available at the proposed site at a reasonable depth, the length of the pile will become very long and the end bearing piles will not be economical. In this case, the piles can be driven into the ground at a given depth. This type of pile is called a friction pile because most of the resistance comes from the side friction between the pile materials and the surrounding ground, as shown in Figure 1.7c.

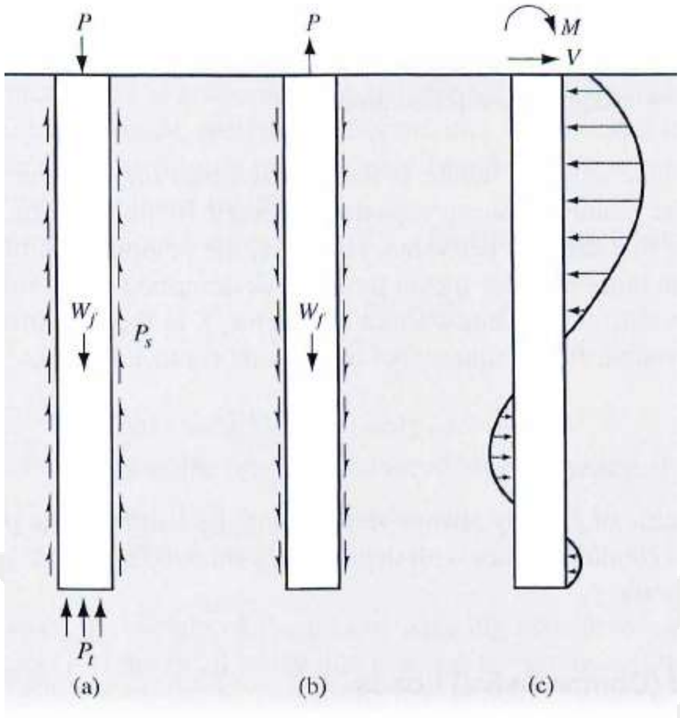

Figure 1.6. Load transferring from pile to the ground soil (a) Axial downward (compressive) loads, (b) Axial upward (tensile) loads; (c) Lateral loads

The determination of pile capacity is not simple and it is quite complex, a lot of theories and empirical methods are available at the present time but they will not give the same value of bearing capacity especially for friction piles because there are many uncertainties in soil properties and soil-pile materials interface. (Mijena, 2012).

There are many methods and empirical equations achieved from experimental work are available for calculation of ultimate bearing capacity of pile foundations and most of them are based on shallow foundation equations (i.e., Terzaghi (1943), Hansen (1970), Janbu (1976), Meyerhof (1976), Vesic (1977), and Coyle and Castello (1981).

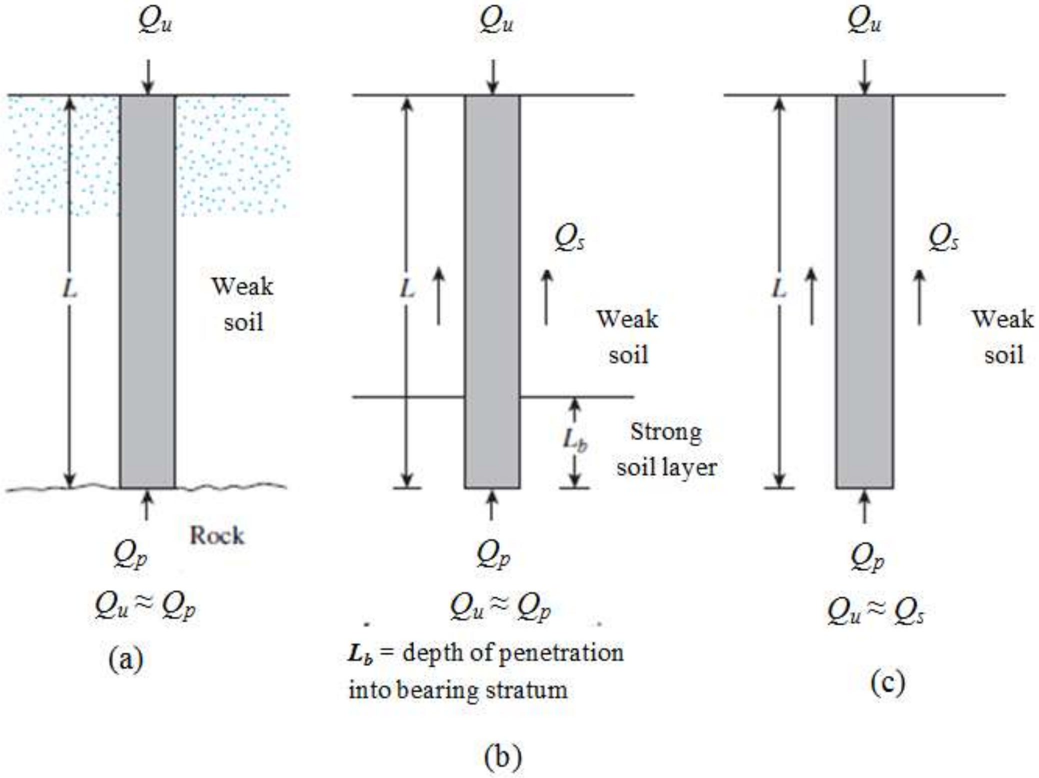

Figure 1.7. (a) and (b) End bearing piles; (c) Friction piles

The ultimate load-carrying capacity Q_u of a pile is given by the equation bellow:

$$Q_u = Q_p + Q_f \tag{1.1}$$

Where;

$Q_u =$ ultimate bearing capacity of the pile

$Q_p =$ end(point) bearing capacity of the pile

$Q_f =$ Shaft friction resistance capacity of the pile

The side friction of piles is a parameter which is related to the displacement of the pile shaft, the skin friction of piles is not easy or constant value for any kind of soil. Single pile load tests have shown that the side friction resistance of the piles increases to the maximum value at a specific settlement point and beyond this point it starts to decrease to residual strength. (Wada, 2004).

A general equation used for estimating the skin friction pile capacity suggested by Burland (1973) and this equation is based on the effective stress method from bored pile load tests, It is a function of skin friction angle (δ) between pile materials and surrounding soil and the coefficient of lateral earth pressure (K) this equation generally used for cohesionless soil:

$$f_s = K\, \sigma'_v \tan \delta' \tag{1.2}$$

Where f_s: is a skin friction, K: is coefficient of lateral earth pressure, σ'_v: is an effective over burden pressure at any depth and δ': is an effective skin friction angle between soil and pile materials.

The pile shaft friction resistance can be estimated by multiplying the unit skin friction f_s by surface area of the pile.

$$Q_f = f_s\, PL \tag{1.3}$$

Where; Q_f is shaft friction resistance of the pile, P is perimeter of the pile and L is an embedded length of the pile

The soil pressure coefficient K is the most difficult factor to find. Numerous field tests have shown that the value of K depends on the degree of stress, the density, the angle of friction of the soil, the roughness and the diameter of the pile. It was observed that K is not a constant value along the length of the pile. (Gavin and Gallagher, 2005).

The American Petroleum Institute (API, 1984) has recommended that the value of K = 0.8 be used for the design and construction of friction piles.

The magnitude of K may vary with the depth, near the head of the piles, it is approximately equal to the pressure coefficient of passive Rankine earth, K_p at the greatest depth may be less than the pressure coefficient of the earth at rest, table 1.1 are K values recommended based on the available results (Braja M. Das, 2014).

Many authors tried to estimate the value of K from several pile test program. Table 1.2 is a summary of several values of K which are suggested by some authors, from the table one can realize that there is no very fine agreement what to use for K value.

Table 1.1. Recommended values for K by (Braja M. Das, 2014)

Pile type	K
Bored or jetted	$\approx K_0 = 1 - sin\phi'$
Low-displacement driven	$\approx K_0 = 1 - \sin\phi'$ or $1.4(1 - \sin\phi')$
High-displacement driven	$\approx K_0 = 1 - \sin\phi'$ or $1.8(1 - \sin\phi')$

The ultimate resistance of the friction pile is mainly based on the mechanical properties between the pile materials and the surrounding soil. The skin friction angle (δ) between the soil and the pile materials plays an important role in the calculation of the ultimate bearing capacity of the piles. The researchers tried to evaluate the angle of friction of the skin between the ground soil and common pile materials such as wood, steel and other types of materials.

Table 1.2. Summary of a number of pile tests for estimating the lateral earth-pressure coefficient

	Pile type					
Source	H-piles	pipe	Precast concrete	timber	tapered	Tension tests
Mansur and Hunter (1970)	1.4-1.9	1.2-1.3	1.45-1.6	1.25		0.4-0.9 All types
Tavenas (1971)	0.5		0.7		1.25	
Ireland (1957)						1.11-3.64
API (1984)		0.8 or 1.0				

Numerous studies have been conducted in the past to estimate the internal friction angle between sand and various pile materials. Several different types of apparatus have been used in the literature such as direct shear test (Potyondy, 1961 and Reddy et al., 2000), simple shear apparatus (Uesugi and Kishida, 1986 and Paikowsky et al., 1995) and soil-pile-slip test also has been utilized for this purpose (Reddy et al., 1998).

Many geotechnical engineers consider the skin friction angle (δ) as equal to 2/3 of the internal friction angle (ϕ) of soil in their designs (Terzaghi and Peck 1948). However, it is clear that skin friction angle (δ) can vary in the event of frictions between the same soil and different materials. Even today, skin friction angles (δ) between soil and pile materials are not exactly obvious and known and designs are made with the use of approximate values. δ values used in designs are of prime importance in the determination of pile number, diameter and length. A low δ value prevents making economic designs and increases project costs considerably. On the other hand, a high δ value leads to security problems.

1.6. Research Aim

The main goal of this research is to study the skin friction angle between sandy soil and pile materials (timber and steel) and also to study the skin friction mobilized on timber and steel model piles in sand under axial loading and to determine their ultimate bearing capacities especially their frictional shaft resistances in the laboratory.

For this purpose the interface direct shear test will be used to study the skin friction angle between sand and pile materials, and static axial load test will be conducted by using a special loading machine system designed for this purpose, piles are embedded in sand in four different relative densities 10%, 40%, 65% and 90% axial load will be applied and settlement rate is kept approximately about 1 mm/minute. The applied load and settlement values are recorded by the computer program system.

It is also aimed to calculate the ultimate bearing capacity of the model piles by common geotechnical theoretical methods in the literature and also to do finite element analysis by finite element software Plaxis 3D. The results of experiments will be compared to common theoretical methods and finite element analysis.

2. LITERATURE REVIEW

2.1. General

Friction between ground soil and common construction material is extremely important because it plays a significant role in the design of soil-structure interaction problems such as retaining walls, deep foundation and earth reinforcement. The behavior of sandy soil interface friction is highly counted on the surface roughness of the construction materials, and particle shape and size, the strength of the particle which is concerning to the soil crushability, the grading and the shear deformation level up to an interfacial critical state (Yasufuku and Ochiai, 2005)

2.2. Interface between Sand and Pile Materials

Shear interface parameters between sand and pile materials are usually determined in laboratory by conduction normal direct shear interface test apparatus, however some researchers have performed shear interface test with large direct shear test to investigate the effect of scale on the shear interface between sand and common pile materials.

Potyondy (1960) used direct shear test to investigate the internal friction angle between soil and common pile materials such as timber, steel and concrete, he also tried to make a relation between skin friction angles (δ) with the internal friction angle of the soil (ϕ). He discovered that there are several factors which affect the value of skin friction angle (δ) between soil and pile materials which include properties of soil and pile materials. Soil properties such as density, soil particle shape and size and gradation, material properties like hardness and surface roughness.

Uesugi and Kishida (1986) analyzed the friction between mild steel and dry sand by using interface shear test IST in their study. They determined that the type and mean grain diameter of sand (D_{50}) had important effects on friction between sand and steel material.

Some researchers worked on large scale direct shear box tests to determine skin friction of soil and various structural materials (Liu et al. 2009, Laskar and Dey 2011, Khan et al. (2014).

Aksoy et al., (2016) used direct shear test to relate skin friction angle (δ) between soil and common pile materials which included wood, steel and FRP. For this purpose they used sand-clay mixture with mixing ratios of 100:0, 80:20, 70:30, 60:40, 55:45, the internal friction angle of sand-clay mixture were 43°, 39.5°, 41.5°, 35°, 28° consecutively. They gave a design chart for determination of skin friction angle for the mentioned materials, with known value of internal friction angle of soil.

2.3. Field and Model Piles Bearing Capacity

Piles are structural members used for construction of pile foundation they transfer the super structural loads deep into the soil layers. Determination of ultimate bearing capacity of piles is quite complex many researchers have tried to find the determination of the ultimate bearing capacity of single pile by conduction model pile load tests in laboratory and in the field.

Mansur and Hunter (1970) conducted a pile load test in the field, they used pipe steel pile with 40 cm diameter and 16.8 m embedded into the sand, after performing the analysis they concluded that the unit skin friction along the pile shaft is progressed at very smaller displacement compared with the end bearing resistance.

Chen, (1987) stated that the side friction resistance of piles increases over time, while no change happened to the end bearing of the piles. Also (Chen,. 2006) indicated that the bearing capacity of friction piles can be increased more than 10% of the ultimate bearing capacity of friction pile.

According to (Okahara et al., 1990) the ultimate bearing resistance of non-displacement piles can be clearly displayed when the settlement of the pile reaches about 10% of the pile's diameter.

Several studies have been conducted on increasing bearing capacity of friction pile over time, they concluded that there are two major causes of increasing friction resistance of piles over time which are; soil ageing (Schmertmann, 1991) and stress relaxation (chow et al., 1996).

Wada (2004), conducted several load tests on non-displacement piles, the piles diameters were between (80 ~ 150) cm and the piles length between (14 ~ 40) m long. He studied the skin friction resistance of non-displacement piles for this purpose he used strain gauge and extensometers. Through his research on pile load tests he concluded that the skin friction of non-displacement piles has the following properties:

1. It is not easy to estimate the skin friction value of the piles because it is produced by shaft displacement.
2. The skin friction resistance of the piles increases to its maximum strength value at a specific displacement beyond this point it starts to decrease to its residual strength.
3. The maximum skin friction was noticed mainly at 5 to 15 mm settlement and by increasing axial load on the piles, the major depth of active skin friction region is moved to downwards.
4. The side friction of the piles is a factor of pile shaft settlement that's why the active skin friction won't reach 100% of the theoretical skin friction value.
5. The share proportion of the skin friction indicates nearly constant value even if the applied load been increased from 100% to 300% of the design load.

Al-Mhaidib et al,. (2006) conducted a series on direct shear tests to investigate the effects of shearing rate on the internal friction angle of sand and skin friction angle between sand and steel. For this purpose they used two steel samples with smooth and rough surfaces and performed a total forty five tests by utilizing normal direct shear equipment which was deformation controlled with dimensions 10 cm x 10 cm. the tests were carried out under three different normal stresses and five different shearing rates used in the tests (0.9 mm/min , 0.4 mm/min, 0.08 mm/min, 0.048 mm/min, 0.0048 mm/min). The sand relative density used in all tests was 64% with unit weight 16.5 kN/m^3. Fifteen direct shear tests were performed for studying the internal friction angle of the sand (ϕ) and thirty were conducted to study the skin friction angle (δ) between sand and steel samples fifteen on smooth surface steel sample and others for rough. After completing all direct shear tests they also tried to study the skin friction angle (δ) of sand-steel by using the uplift steel piles model embedded in the sand with diameter 2.5 cm and length 55 cm. Two types of model piles were used one with smooth surface and other with rough. The steel material used for the pile models was the same materials used in the interface direct shear tests and same sand with same relative density of direct shear tests used in the uplift model piles tests. Ten tests were carried out five on smooth surface and other on rough, the vertical load applies by the loading machine with same five different five shearing rates used for interface direct shear tests, the loading was also deformation controlled like direct shear apparatus, after completing their research they concluded the following important points:

1. The required settlement for the model pile to mobilize the ultimate uplift resistance were between 2 mm to 3 mm which was nearly about 10% of the pile model diameter.
2. It was obvious from the tests results that with increasing the shearing rate the value of internal friction angle (ϕ) also increases.
3. It was also noticed that the skin friction angle (δ) between sand and both steel samples (smooth and rough) also increase with increasing the shearing rate values.
4. The skin friction angle values (δ) which were determined from direct shear interface were lower than those values achieved from uplift pile models tests.

Rahil et al., (2015) studied the influence of the relative density of sands and embed length on ultimate bearing capacity of single piles under axial loading. The pile models used in the experiments has square steel sections with dimensions (1.8 x1.8) cm and different embedded length (L_b) in sand (32, 42 and 52) cm. Tests were performed with three different relative densities of sand (33%, 60% and 80%) matching to loose, medium and dense, the axial load were applied by using hydraulic jack with constant settlement rate 3 mm/min. It was found that the ultimate bearing capacity of model pile increases with increasing the relative density of the sand, when changing relative density from loose to medium the ultimate bearing capacity of piles increased approximately 96% while from medium to dense it increased about 81%. Also it was investigated that the pile capacity increases with increasing embedded length of the pile in the sand

Adejumo, (2015) studied the influence of shape and installation methods on the ultimate bearing capacity of pile foundations in layered sand and clay soil. He used three different shapes of piles which were square, tapered conical and cylindrical sections and also used different installation techniques for installing piles included driving (hammering and vibration) and boring method. He conducted field and laboratory tests, the results showed that the bearing capacity of tapered conical piles is 1.5 – 2 times higher than prismatic (square) piles and 2-3 times higher than cylindrical piles respectively.

2.4. Finite Element Analysis

Usually the boundary conditions for the design of geotechnical engineering structures may be very complex because of the condition of soil variability and it is not possible to conduct traditional analysis by applying simplified theories and equations. In this case numerical modeling become very useful and can be used in the designs of pile foundations, retaining walls, dams, and other earth-supported structures. Many researchers have tried to study the behavior of single piles under axial loading by using finite element programs such as plaxis 3D finite element program, ABAQUS and ANSYS programs.

Naghibi et al., (2014) investigated the expecting elastic settlement of single friction pile under vertical loading, for that purpose they performed a linear finite element program on the piles established in a homogenous soil, they made a regression model and then developed an easy mathematical expression for determining the elastic settlement of friction pile in a homogenous soil. Their mathematical expression display a good agreement with FE results and also fits well with analytical solution derived by Randolph and Worth for predicting the piles settlement. The most important advantage of their mathematical expression is that pile length can be easily estimated with given value of settlement and of course this can be used in pile design process and their serviceability limit.

Kishanrao and Prasad., (2016) studied the behavior, settlement and load transfer mechanisms of single pile under axial loading in layered soil by using two dimensional finite element program Plaxis 2D which offers a very good method to investigate the behavior of soil-pile interface and its response to applied axial load. For this purpose they used single piles with three different slenderness ratio (L/D= 7.5, 10, 12.5) and embedded in two different layered soil system, sand underlying clay and vice-versa and single pile was modeled in 2D plaxis with axis-symmetric situation. The results achieved from finite element analysis in the shape of load-settlement curve. It was observed that the ultimate bearing capacity of single pile increases with increases pile slenderness ratio and also it was noticed that the pile with same slenderness ratio has a remarkably higher ultimate resistance in situation of sand overlying the clay than in case of clay overlying the sand.

Han et al., (2017) studied the behavior and response of the non-displacement piles under action of axial loading embedded in sand; the piles were analyzed by using three-dimensional finite element software (ABAQUS) to estimate the end-bearing capacity and shaft resistance of pile. The analysis area near the pile were carefully meshed in a way that the shaping and development of shear bands adjoining to the pile shaft and close to the base of the pile were properly captured. A lot of soil profiles and different pile shape geometries were used in the analysis process. The analysis results exhibited that the coefficient of earth pressure K increases with increasing relative density of sand and lowering initial confining stress, and also the ultimate bearing resistance of pile base increases with increasing sand relative density and initial confining stress neighboring the pile base. On the basis of analysis results an equation have been suggested which is useful for predicting the maximum shaft resistance and ultimate resistance of pile base of non-displacement piles embedded in sandy soil.

3. THEORETICAL BACKGROUND

3.1. Introduction

The determination of pile capacity is not simple and it is quite complex. A lot of theories and empirical methods are available at the present time but they will not give the same value of bearing capacity, because there are many uncertainties in soil properties and soil-pile materials interface.

There are many methods and empirical equations achieved from experimental work are available for calculation of ultimate bearing capacity of pile foundations and most of them are based on shallow foundation equations (i.e., Terzaghi (1943), Hansen (1970), Janbu (1976), Meyerhof (1976), Vesic (1977), and Coyle and Castello (1981).

In conventional geotechnical engineering application, the calculation for the pile design is based on a combination of previous experiences and experimental methods. While theoretical methods cannot be well found in the literature. The complication of the pile foundation behavior has led to Terzaghi and Peck (1967) stated that the "…theoretical refinements in dealing with pile problems are completely out of place and can be safely ignored…". The experimental methods based on theoretical methods are the last effort to guess the bearing capacity of a single pile. The estimation of axial capacity is the most important step in the design of a pile foundation based on experimental relationships (Paul, 1989).

Douglas (1989) reported that it is necessary to conduct the pile load tests to minimize the influence of the limitations in assessment procedures among all methods used in pile design, such as theoretical, experimental and numerical computer modeling studies. Randolph (2003) stated that the bearing capacity of the single pile under axial loading embedded in different soil situations cannot be precisely assessed more than about 30%. So that's why while construction of pile foundations, it is necessary to perform pile field load tests to assure the final design of pile foundations. Time and expenses are two most important constraints in field load tests that lead the researcher to invent dependable design methods of empirical, analytical or numerical methods, to estimate the pile bearing capacity of the pile foundation.

Many researchers have tried to execute model-pile load test studies interestingly in term of axial load versus displacement or deflection in case of lateral loads in various soil environments (Vesic 1963, Tavenas 1971, Hanna and Tan 1973, Tan and Hanna 1974, Beringen et al. 1979, Olson and Dennis 1983, Yazdanbod et al. 1984, Briaud and Tucker 1988, Kraft 1991, Randolph et al. 1994, and Igoe et al. 3011). The end bearing capacity of pile foundations is normally calculated on the basis of conventional shallow foundation equations (i.e., Terzaghi (1943), Hansen (1970), Janbu (1976), Meyerhof (1976), Vesic (1977), and Coyle and Castello (1981). The shaft friction resistance is determined based on the shear strength parameters of the soil which is determined from the direct shear test.

This chapter provides an adequate theoretical background and methods to evaluate the pile bearing capacity (i.e., end bearing and shaft friction resistance) in sand, and all he methods are based on evaluation procedures of conventional pile bearing capacity equations.

3.2. Bearing Capacity of Pile

When the rock or rock-like materials are not encountered at a reasonable depth as our study, the ultimate bearing capacity of a single pile can be determined from the contribution of pile end point capacity and shaft friction resistance. The axial capacity of a single pile is usually derived from the relationship below:

$$Q_u = Q_p + Q_f \tag{3.1}$$

Where;

Q_u = ultimate bearing capacity of a single pile,

Q_p = end (point) bearing capacity at the pile

Q_f = shaft friction resistance of the pile

3.2.1. End Bearing Capacity of Pile

The ultimate end (point) bearing capacity of a single pile is usually calculated based on the most common bearing capacity equations of the shallow foundation (i.e., Terzaghi (1943), Hansen (1970), Janbu (1976), Meyerhof (1976), Vesic (1977), and Coyle and

Castello (1981). From many field load tests, it has been noticed that a pile displacement of 10-25% of its diameter is required to fully mobilize pile end-bearing capacity (Das, 2015).

This section will present common methods which are frequently used by geotechnical engineers to estimate the end bearing capacity of the single pile subjected to axial load.

3.2.1.1. Terzaghi (1943)

Terzaghi (1943) is considered the first one who offered a thorough theory for calculation of ultimate bearing capacity of the rough shallow foundation and his theory is usually extends to estimate the pile bearing capacity. Nevertheless, the Terzaghi equation is known to give conservative results but is still used by many geotechnical engineers due to its simplicity. Terzaghi suggested that when a foundation with its depth (D_f) equal or less than its width (B) is considered to be a shallow foundation, however, many researchers then proposed that a foundation with its depth equal to (3-4) times of its width is also defined as a shallow foundation. In Terzaghi`s theory, shear strength parameters of the overburden soil are ignored in the estimation of foundation bearing capacity and only its weight is considered. Terzaghi suggested that when the foundation is loaded, the triangular zone immediately under the foundation is moved downward and the other soil volumes at the left and right side are moved outward and upward with the failure surface at the bottom of the foundation.

Terzaghi derived his equation based on that for a continuous, or strip foundation (i.e., which its width to length ratio approximately zeros). He used equilibrium principles to derive the ultimate bearing capacity of continuous shallow foundation considering the triangular wedge ACD as shown in Figure 3.1. An equivalent surcharge was used instead of the soil above the bottom of the foundation, $q_u = \gamma D_f$ (where γ is the unit weight of the soil). The failure zone under the foundation can be separated into three parts (see Figure 3.1):

1. The ACD triangular which is directly located under the foundation.

3. CDE and ADF were indicated as radial shear zones, the curves DE and DF were considered as arcs of a Logarithmic spiral.

3. AFH and CEG are two triangular Rankine passive zones

The ultimate bearing capacity, q_u, of the foundation obtained by considering the equilibrium of the triangular wedge ACD

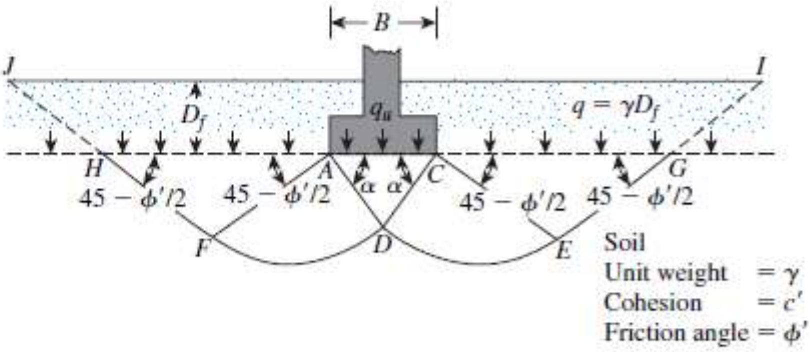

Figure 3.1. Illustration of the Terzaghi bearing capacity theory.

Terzaghi bearing capacity equation for circular foundation in sand can be expressed as below:

$$Q_p = A_p\ (qN_q + 0.5\ \gamma\ B\ N_\gamma\ S_\gamma) \tag{3.2}$$

Where;

Q_p = Ultimate point bearing or end-bearing capacity of the pile,

A_p = pile point area,

q = soil pressure above the pile toe (γ x D_f),

γ = unit weight of foundation soil at the pile toe,

B = pile diameter,

N_q and N_γ = bearing capacity factors,

S_γ = Shape factor.

The shape factor S_γ in the last term of Terzaghi's bearing capacity equation was invented by Golder et al. (1941) based on empirical or semi-empirical consideration. Table 3.1 present the shape factor for different foundation shapes.

Table 3.1. Shape factor (S_γ) in the last term of Terzaghi's equation**.**

Shape	Circular	Square Foundation	Strip
S_γ	0.6	0.8	1

By plugging Sγ for circular foundation in the (equation. 3.2) Terzaghi bearing capacity equation can be rewritten as below:

$$Q_p = A_p\ (qN_q + 0.3\ \gamma\ B\ N_\gamma) \tag{3.3}$$

It is not simple to estimate the exact values of the bearing capacity factors N_q and N_γ, so Terzaghi found these factors based on an approximate method (soil weightless theory). These dimensionless bearing capacity factors rely only on the angle of internal friction of the foundation soil and they can be calculated analytically based on the principle of soil weightless. This approximation was also used by other researchers such as (Meyerhof 1951, Vesic 1973, Chen 1975, Bolton and Lau 1993). These researchers evaluated the bearing capacity factors nearly the same with some differences except for Nγ. However, many researchers have made the considerable effort in this area; but still, the differences in the value of Nγ from various researchers confirm the theoretical uncertainty in this shear strength parameter (Ukritchon et al., 2003). Table 3.2 presents the bearing capacity factors at various internal friction angles. The following equations can be used to make an approximate evaluation for bearing capacity factors:

$$N_q = \frac{e^{3\left(\frac{3\pi}{4} - \frac{\phi'}{3}\right)\tan\phi'}}{3\ cos^3(45 + \frac{\phi'}{3})} \tag{3.4}$$

$$N_\gamma = \frac{1}{3}\ tan\ \phi'\ (\frac{K_{p\gamma}}{cos^3\phi'} - 1) \tag{3.5}$$

Where;

φ' = effective internal friction angle of the soil at the pile toe,

$K_{p\gamma}$ = coefficient of passive earth pressure, some back computed typical values of Kpγ are given in (Table 3.2.).

Table 3.2. Terzaghi's bearing capacity factors with some typial values of $K_{p\gamma}$ (adopted from Bowles 1996).

Values of Nγ for Φ of 0, 34, and 48º are original Terzaghi values and used to back compute Kpγ				
φ, deg	N_c	N_q	N_γ	Kpγ
0	5.7*	1.0	0.0	10.8
5	7.3	1.6	0.5	12.2
10	9.6	2.7	1.2	14.7
15	12.9	4.4	2.5	18.6
20	17.7	7.4	5.0	25
25	25.1	12.7	9.7	35.0
30	37.2	22.5	19.7	52.0
34	52.6	36.5	36.0	
35	57.8	41.4	43.4	82.0
40	95.7	81.3	100.4	141.0
45	172.3	173.3	297.5	298.0
48	258.3	287.9	780.1	
50	347.5	415.1	1153.2	800.0
$^*N_c = 1.5\pi + 1$ (Terzaghi, 1943)				

3.2.1.2. Meyerhof (1976)

According to Meyerhof (1948) the failure mechanism in the shallow foundation proposed by Terzaghi does not correspond to the observed ground movement, and the Terzaghi equation offers conservative values, and as well the shear strength parameters of the overburden soil is not considered in the estimate of soil shearing resistance. In (1951, 1963) Meyerhof proposed a general bearing capacity equation for estimating the bearing capacity of the shallow foundation. For the vertically loaded foundation, he proposed the depth factor (d_c) with the term N_c, shape (s_q) and depth (d_q) factor with the term Nq and depth (d_γ) factor with the term N_γ. Meyerhof (1976) suggested that pile point capacity is increased with increase pile embedment into the bearing stratum to a critical depth of $(L_b/D)_{cr}$. The pile point capacity remains constant when the embedment ratio reaches

$(L_b/D)_{cr}$ even if the $L_b<L$, and L_b is equal L in the case of homogeneous soil (Figure 3.2). Field load tests showed that $(L_b/D)_{cr}$ = 16 to 18.

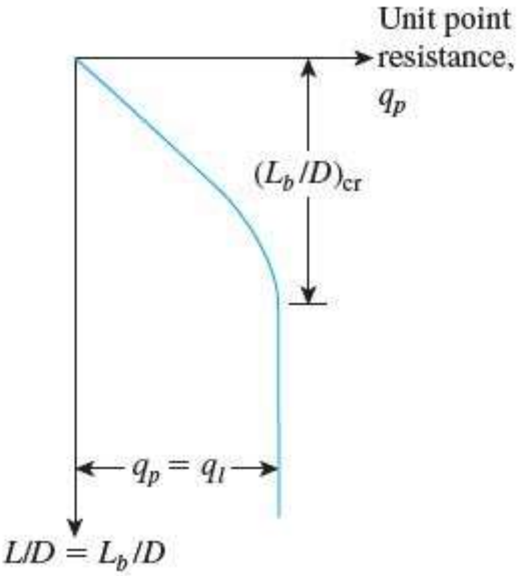

Figure 3.2. The nature of variation of unit point resistance in homogeneous sand

Meyerhof's general bearing capacity equation for cohesionless soil can be written below:

$$Q_p = A_p(q' N_q d_q s_q + 0.5\, \gamma' B\, N_\gamma d_\gamma s_\gamma) \tag{3.6}$$

Where;

Q_p= ultimate point bearing or end-bearing capacity of the pile,

A_p= pile point area,

q' = effective overburden soil pressure at the pile toe,

γ' = unit weight of the foundation soil at the pile end,

B = pile diameter,

N_q and N_γ = bearing capacity factors,

d_q and d_γ = depth factors,

s_q and s_γ = shape factors.

For φ >10°

$$d_q = d_\gamma = 1 + 0.1\sqrt{K_p}\,(\frac{D}{B}) \tag{3.7}$$

$$s_q = s_\gamma = 1 + 0.1\, K_p \frac{B}{L} \tag{3.8}$$

$$K_p = tan^3(45 + \frac{\varphi'}{3}) \tag{3.9}$$

Where;

K_p = coefficient of passive earth pressure,

φ' = effective internal friction angle of the soil at the pile toe,

$$N_q = e^{\pi \tan \varphi'} tan^3(45 + \frac{\varphi'}{3}) \tag{3.10}$$

$$N_\gamma = \left(N_q - 1\right) tan(1.4\, \varphi') \tag{3.11}$$

The second term in the equation above (Equation 3.6) for piles is very small compared to the other term so that it can be neglected. So the end-bearing capacity equation proposed by Meyerhof can be expressed as below:

$$Q_p = A_p q_p = \ A_p q' \ N_q^* \tag{3.12}$$

Where;

Q_p = ultimate point bearing or end-bearing capacity of the pile,

A_p = Pile point area,

q' = effective overburden pressure,

N_q^* = Meyerhof's bearing capacity factor for pile foundations (1976).

Meyerhof's bearing capacity equation from φ'= 20 to 45º are given in Table 3.3. based on Meyerhof's theory.

Meyerhof (1976) proposed that the pile point or end-bearing capacity should be equal or less than the limiting value:

$$Q_p = A_p q_p = A_p q' \ N_q^* \leq A_p 0.5\ p_a N_q^* \tan \phi' \tag{3.13}$$

Where;

p_a = atmospheric pressure (100 kN/m^3),

φ' = effective soil internal friction angle of the bearing soil at the pile point level.

Table 3.3. Meyerhof's bearing capacity equation with φ' from 30 to 45º (adopted from Das 2015).

φ', deg	N_q*	φ', deg	N_q*	φ', deg	N_q*
20	12.4	29	46.5	38	231.0
21	13.8	30	56.7	39	276.0
22	15.5	31	68.2	40	346.0
23	17.9	33	81.0	41	420.0
24	21.4	33	96.0	43	525.0
25	26.0	34	115.0	43	650.0
26	29.5	35	143.0	44	780.0
27	34.0	36	168.0	45	930.0
18	39.7	37	194.0		

3.2.1.3. Coyle and Castello (1981)

Coyle and Castello presented the end-bearing capacity equation for a driven pile based on a 34 large-scale field tests. They expressed their equation as below:

$$Q_p = A_p q' N_q^* \quad (3.14)$$

Where;

Q_p = ultimate point bearing or end-bearing capacity of the pile,

A_p = Pile point area,

q' = effective overburden pressure,

N_q^* = Bearing capacity factor.

Figure 3.3 shows the variation of Coyle and Castello's bearing capacity factors with embedment ratio as a function of soil internal friction angle at the pile tip.

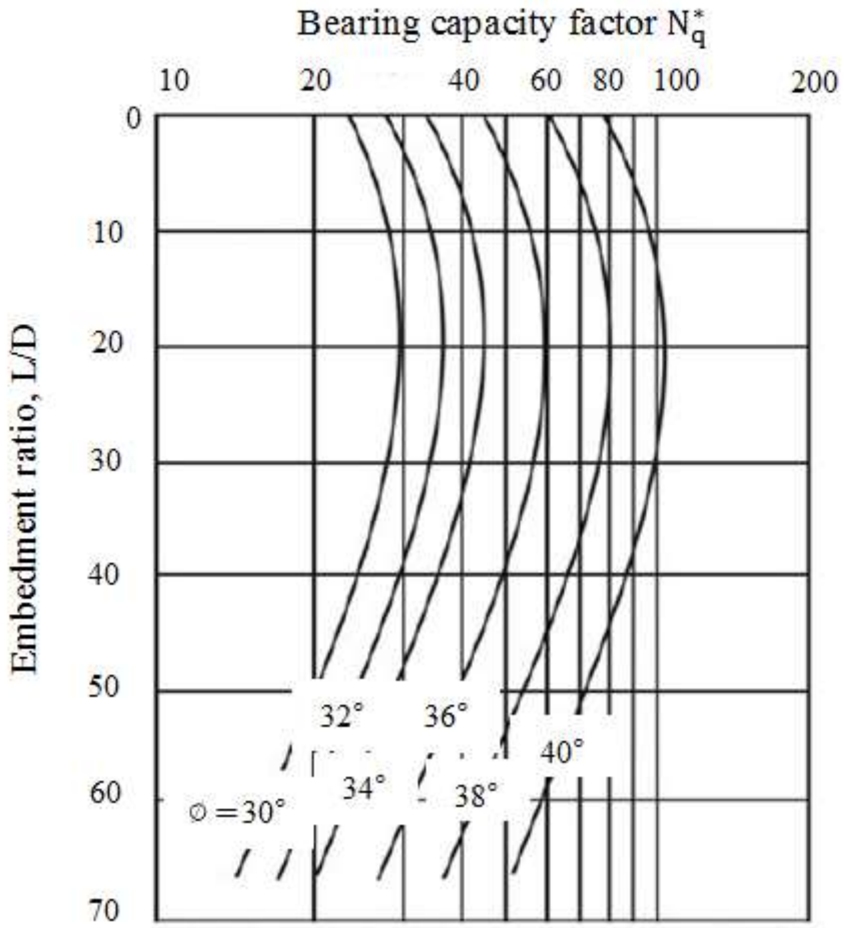

Figure 3.3. Variation of N^*_q with embedment ratio (Coyle and Castello 1981).

3.2.1.4. Janbu (1976)

Janbu suggested that the failure surface of deep foundation is different from shallow foundation and will not be extended only to the level of pile base. Janbu proposed another value for N_q^* with including surface failure angle at the pile tip. Janbu's equation can be expressed in the relationship below:

$$Q_p = A_p q' N_q^* \tag{3.15}$$

Where;

Q_p = ultimate point bearing or end-bearing capacity of the pile,

A_p = Pile point area,

q'=effective overburden pressure at the pile end,

N_q^* = Bearing capacity factor.

Janbu's bearing capacity factors can be written as follow:

$$N_q^* = (\tan\phi' + \sqrt{1 + tan^2\,\phi'}\,)^2\;(e^{2\eta'\tan\phi'}) \tag{3.16}$$

Where;

φ'= effective soil internal friction angle at the pile end,

η' = effective surface angle in radian at pile end.

The surface soil angle ranges from 60° for soft clay to 105°for dense sand. Usually, for practical purposes, the surface angle is suggested between 60° to 90°. In the current study pure model-sand is used at different relative densities, so 70°, 75°, 83° and 90° are considered in the calculation for relative density 10%, 40%, 65% and 90%, respectively.

Figure 3.4. Shows the variation of Janbu's bearing capacity factors with soil internal friction angle as a function of soil surface angle.

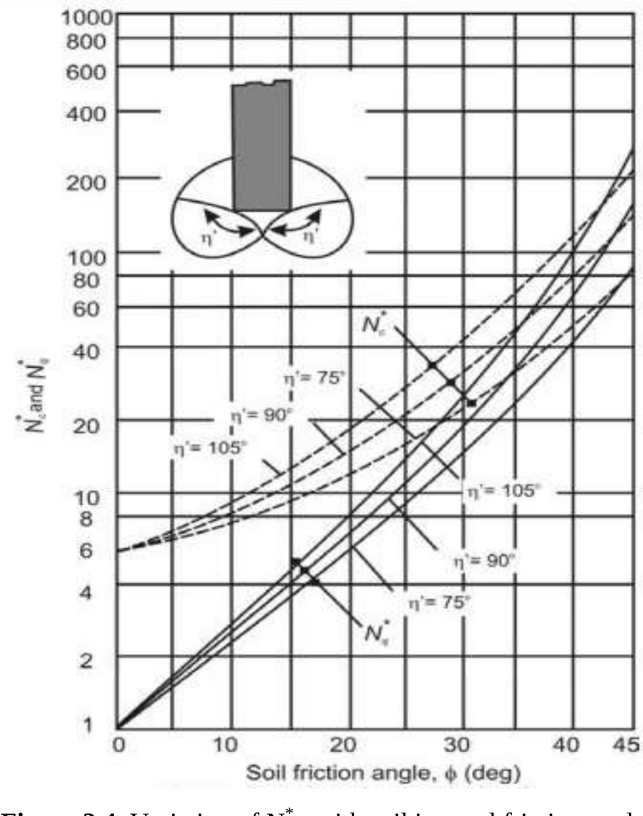

Figure 3.4. Variation of N^*_q with soil internal friction angle (Janbu 1976).

3.2.1.5. Hansen (1970)

Hansen (1970) proposed a more comprehensive equation to estimate the ultimate bearing capacity of both shallow and deep foundation. Because the Hansen equation includes the depth factor in the term D/B thus it can be used for shallow and deep foundations. The principle of Hansen's theory is that any load that is applied to the soil foundation is divided and acts into two components (i.e., horizontal and vertical components) and both components are combined into one resultant force which is called (Load Center). Figure 3.5 shows the Hansen’s bearing capacity factors versus internal friction angle. Full-scale load tests emphasized that Hansen's general bearing capacity equation is more accurate than Terzaghi’s equations. Hansen's equations can be given as below:

$$Q_p = A_p(q'N'_q d_q s_q + 0.5\,\gamma' B'\,N_\gamma d_\gamma s_\gamma) \tag{3.28}$$

Where;

Q_p = ultimate point bearing or end-bearing capacity of the pile,

q'= effective overburden pressure at the pile toe,

d_q = depth factor,

γ' = dry unit weight of soil,

B' = pile diameter (note; B'=B there is no eccentricity in vertical load),

N'_q , N_γ = bearing capacity factors.

$$N_q = e^{\pi \tan\varphi'} \tan^3(45 + \tfrac{\varphi'}{3}) \tag{3.29}$$

$$N_\gamma = 1.5\left(N_q - 1\right)\tan\varphi' \tag{3.30}$$

For all φ ;

$$s_q = 1 + \frac{B'}{L'}\sin\varphi \tag{3.31}$$

And for all φ when $\frac{D}{B} > 1$;

$$d_q = 1 + 3\tan\varphi\,(1-\sin\varphi)^3 \tan^{-1}\frac{D}{B} \tag{3.33}$$

Note; tan -1 D/B should be calculated in radians

Where;

D = pile embedment length,

B = pile diameter.

For all φ ;

$$s_{\gamma} = 1 - 0.4\,\frac{B'}{L'} \geq 0.6 \quad (3.33)$$

$$d_{\gamma} = 1 \quad (3.34)$$

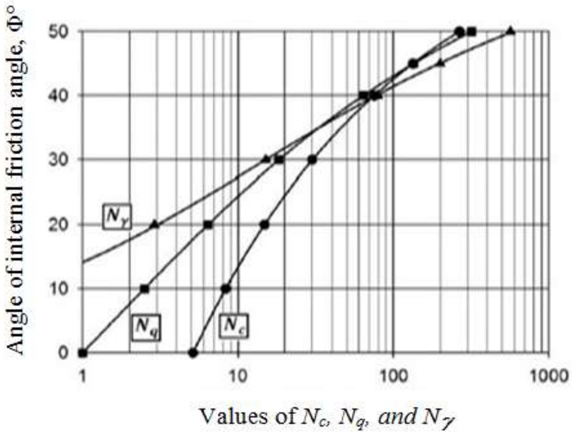

Figure 3.5. Variation of bearing capacity factors with soil internal friction angle (Hansen 1970).

3.2.2. Shaft Friction Resistance

It is not quite easy to determine a unit skin friction resistance of pile shaft f, in estimating the shaft resistance of pile some significant factors have to be considered:

1. The pile installation method, for example in case of driven pile in sand, the effect of driving process causes the densification of the sand around the pile as much as 2.5 the diameter of the pile thus increasing the frictional resistance of the pile. Figure 3.6a shows a typical pile in sand.

2. Another important parameter of the friction pile is design length because it has been noticed in the variation of the friction resistance is approximately linear as shown in Figure 3.6b, the skin friction resistance increases with a depth to appoint L' and beyond this point it becomes a constant. The critical value of L' could be 15 to 20 times the diameter of the pile.

3. At the same depth the jetted or bored piles have less skin friction resistance than driven piles and also at the similar depth the frictional resistance of high displacement piles in loose sand is greater than the low displacement piles in dense sand.

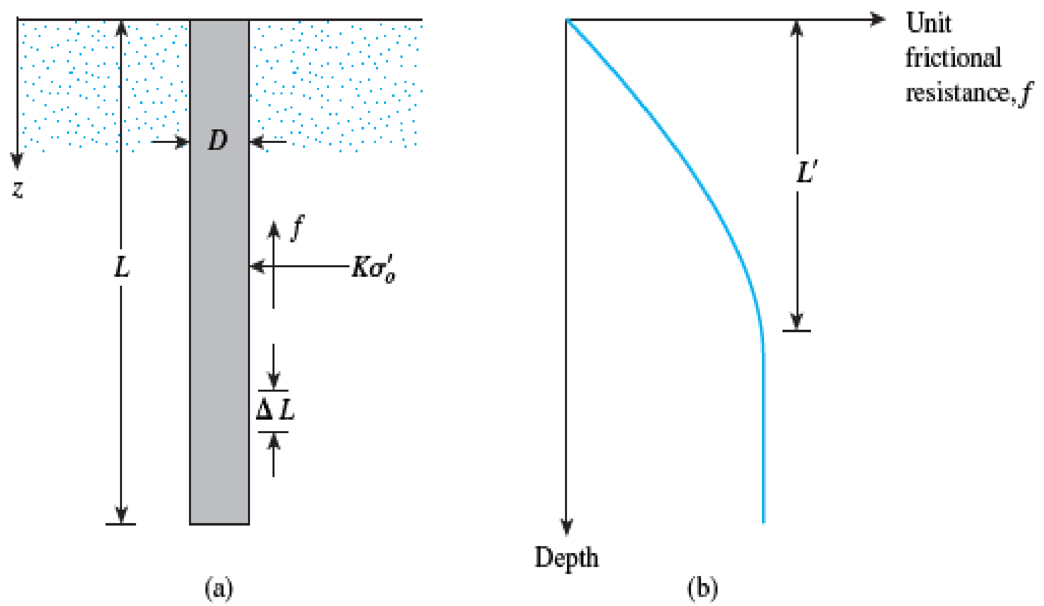

Figure 3.6. (a) Typical piles in sand (b) Shaft friction resistance behavior with pile depth.

The general equation of shaft friction resistance (Q_S) for a pile installed in sandy soil can be derived from the behavior of the pile-soil interface as below:

$$Q_s = \Sigma\, p\, \Delta L\, f_{av} \tag{3.35}$$

As shown in Figure 3.6b it can be seen that shaft friction capacity increases with pile embedment to a depth of 15-20 times pile diameter and then remains constant. For a conservative estimate, L' ≈15D is usually used.

The simplified unit skin friction can be expressed in the relationship below:

$$f_{av} = K\sigma_0' \tan \delta' \tag{3.36}$$

Where;

f_{av} = unit skin friction resistance,

K=coefficient of lateral earth pressure,

σ_0' = mean effective vertical pressure at the desired depth,

δ' = pile-soil interface friction angle.

In order to estimate the resistance of pile shaft friction resistance in sandy soils, many methods have been developed. In this study, Burland (1973) was used to estimate friction resistance, with considering different value of K and Coyle and Castello (1981) method.

3.2.2.1. Coyle and Castello (1981)

Coyle and Castello proposed an equation to evaluate the unit skin friction resistance as below:

$$Q_s = f_{av}\, pL = (K\sigma_0' \tan \delta' \, pL') \tag{3.37}$$

Where;

K = coefficient of lateral earth pressure,

σ_0' = mean effective vertical pressure at the desired depth,

δ' = pile-soil interface friction angle,

p = pile circumference,

L' = critical pile embedment length ≤ 15D

D = pile diameter

In fact, the K value changes with depth but depends on the existence of the available results, the following approximate values presented in Table 3.4 are suggested for K. However, based on different studies, the interface friction angles appear to range from 0.5 φ' and 0.8 φ', but in the present study the real measured interface friction angles from direct shear test are used. Figure 3.7 shows variation of K with L/D (redrawn after Coyle and Castello, 1981).

Table 3.4. Approximate values of *K* (adopted from Bowles 1996).

Pile type	K	K
Bored or jetted	$\approx K_0 = 1 - sin\phi'$	$K = K_a = tan^2(45 - \frac{\varphi}{2})$
Low-displacement driven	$\approx K_0 = 1 - \sin\phi'$ or $1.4(1 - \sin\phi')$	$K = K_p = tan^2(45 + \frac{\varphi}{2})$
High-displacement driven	$\approx K_0 = 1 - \sin\phi'$ or $1.8(1 - \sin\phi')$	$K = K_p = tan^2(45 + \frac{\varphi}{2})$

Bhusan (1983) proposed an equation to estimate K and δ for high displacement pile. Bhusan's equation can be expressed in the relationships below:

$$K \tan \delta = 0.18 + 0.0065 D_r \tag{3.38}$$

$$K = 0.5 + 0.008 D_r \tag{3.39}$$

Where;

D_r = relative density %.

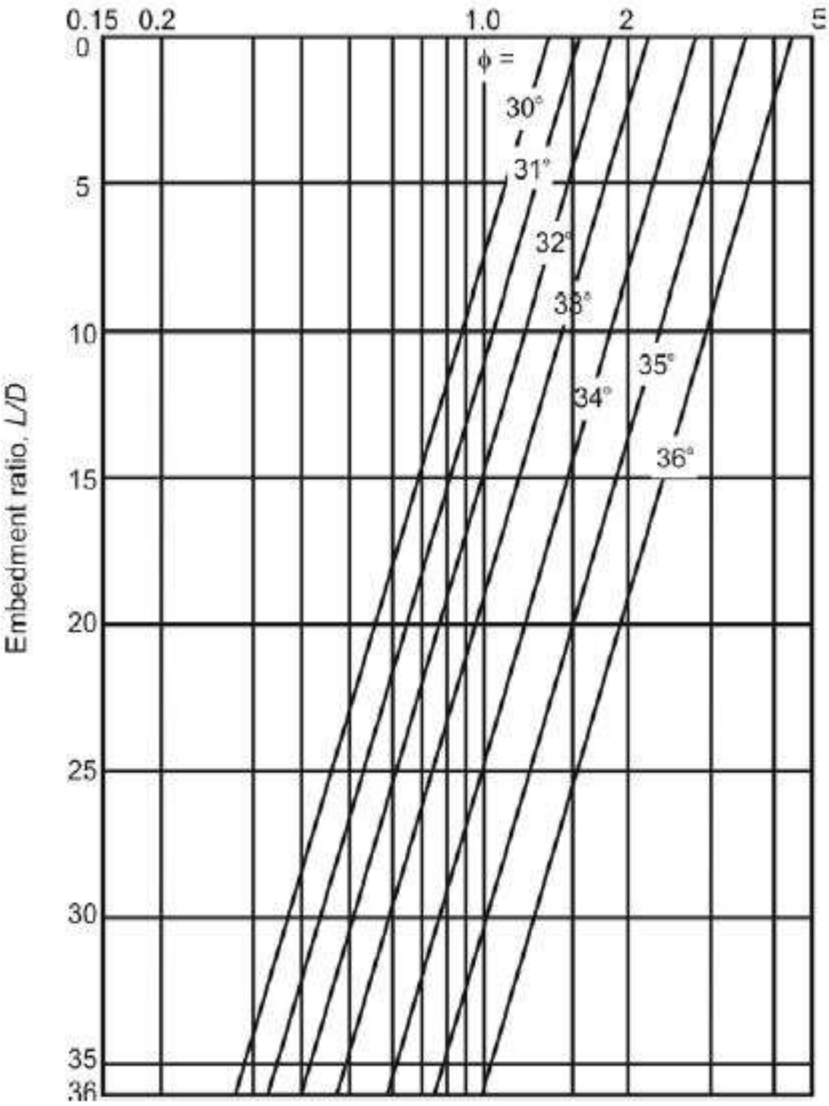

Figure 3.7. Variation of K with L/D in the function of soil internal friction angle (redrawn after Coyle and Castello, 1981).

4. EXPERIMENTAL STUDY

4.1. General

This chapter will provide an explanation of all the properties of the materials and equipment used in this study. Moreover, it will also explain more details about all test procedures which have been done for this study, such as direct shear test for determination internal friction angle (ϕ) of sand and skin friction angle (δ) between sand and pile materials (wood and steel), and it will also present all experimental pile model load tests and apparatus used for performing static load test on behavior of single pile under axial load.

4.2. Materials and Equipment

This section presents a detail of the materials and their properties which have been used in this study and also will give details of the methodology and equipment used for this purpose.

4.2.1. Sand Properties

The sand used in the experiments of this study was river sand with uniform gradation brought from the Murat River in Elazığ at Turkey. The sand has been washed and oven dried and sieved by passing 1 mm opening sieve and retained on the sieve #200 (0.075 mm). The sieve analyses and specific gravity tests were performed according to standards (ASTM D422-63 and ASTM D854-14). Relative density of the sand was determined according to (ASTM D4254-16). The sand is classified as poorly graded sand (SP) according (USCS) which is refer to Unified Soil Classification System according to ASTM D2487. Figure 4.1 illustrates the grain size distribution curve of the sand. Physical properties of the sand are summarized in the table 4.1.

Table 4.1. Physical properties of the sand used in the study.

Property	Value
Effective size, D_{10}, D_{30},D_{50}, D_{60} (mm)	0.19, 0.325, 0.475, 0.55
Coefficient of uniformity, C_u	2.895
Coefficient of curvature, C_c	0.980
Classification (USCS)	SP
Specific gravity, G_s	2.77
Maximum dry unit weight, γ_d (max.) kN/m^3	17.66
Minimum dry unit weight, γd (min.) kN/m^3	14.32
Maximum void ratio, e_{max}	0.898
Minimum void ratio, e_{min}	0.539
Maximum – Minimum grain size, D_{max}-D_{min} (mm)	1 - 0.074

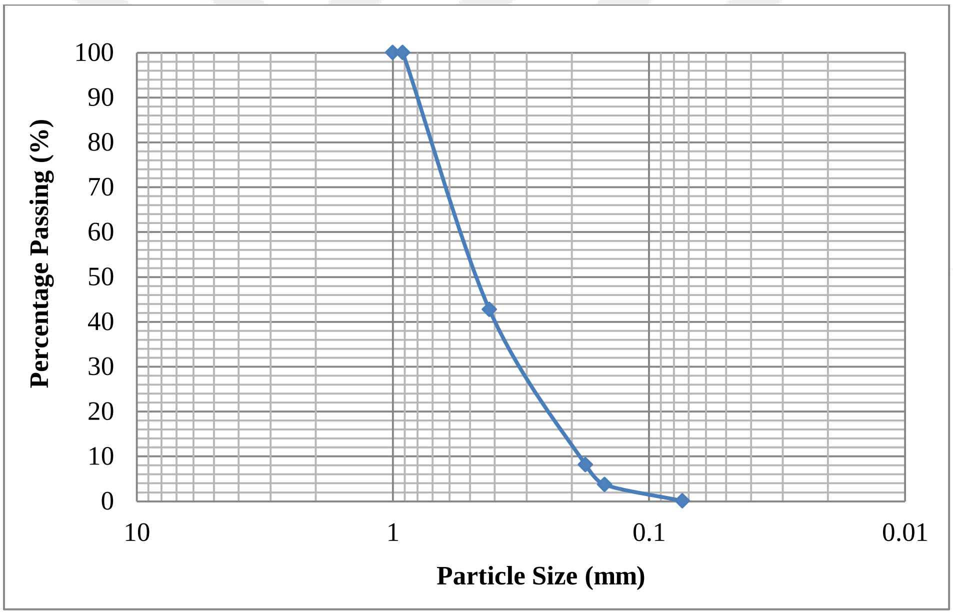

Figure 4.1. Grain size distribution of the sand

4.2.2. Model Pile Materials Properties

In this study, two model piles were used timber pile and closed end steel pipe pile, the diameter of the piles is 50 mm and length of 600 mm (500 mm embedded in sand) during test. The steel pile was made of steel st-37 and timber pile is made of oak white. Figure 4.2 shows the model piles which have been used in this study.

Figure 4.2. Timber and steel model piles

4.2.3. Determination of Surface Roughness of Pile Materials

Roughness is an important parameter when trying to find out whether a surface is suitable for a certain purpose. Rough surfaces often wear out more quickly than smoother surfaces. Rougher surfaces are normally more vulnerable to corrosion and cracks, but they can also aid in adhesion.

Mutitoyo SJ-201 surface roughness tester was used to determine the surface roughness of the steel and wood materials, figure 4.3 shows the determination of surface roughness parameters. The mean surface roughness parameters obtained as a result of the measurements performed are shown in Table 4.2.

Table 4.2. Values of R_a, R_y of pile materials

Model Pile	R_a	R_y
Wood	4.17	24.45
Steel	0.55	3.43

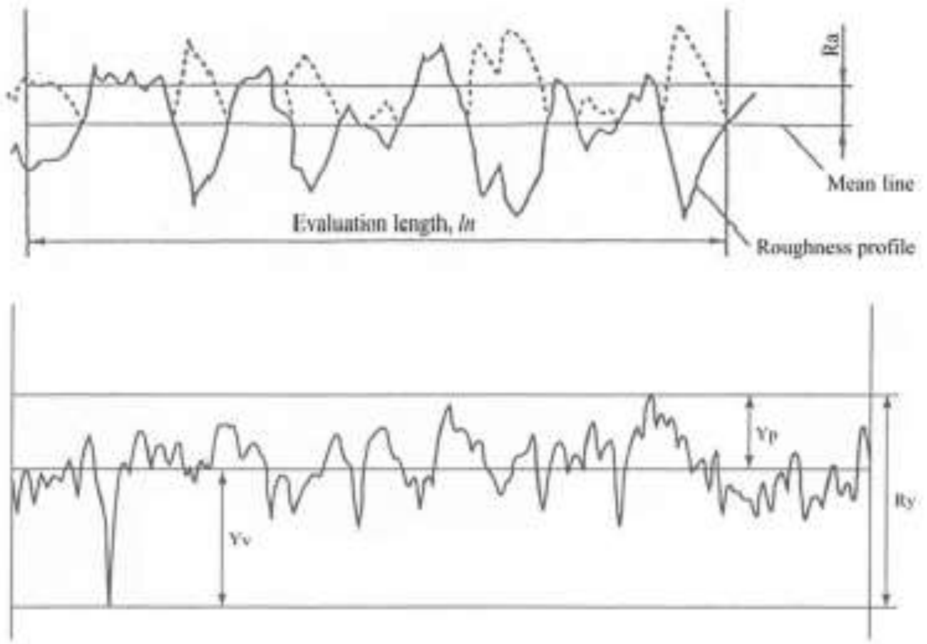

Figure 4.3. Determination of surface roughness parameters (R_a and R_y)

4.3. Calibration of Relative Densities of Sand Model Experiments

In this study, hand compactor was used to obtain four relative densities of sand which are required to be used in pile-sand model experiments. For this purpose a Proter brand electro-pneumatic hammer was used, a steel tamper plate with dimensions (15 cm x 15 cm) was manufactured for compaction the sand, in order not crush the sand particles a plastic base with same dimensions of steel plate was attached to the bottom of the steel base by screw bolts. Figure 4.4 shows the Proter brand hammer which was used in this study.

For determination of relative densities of sand a wooden box with dimensions (42 x 27.8 x 11.2 cm) was used. Calibration was performed in the laboratory by conducting of a series trial tests, four relative densities were found (Dr= 10%, 40%, 65% and 90%). 10% relative density of sand was obtained just by normally pouring the sand into the box at a height of 15 cm by using plastic hose, 40% relative density was achieved by pouring sand into a box every 10 cm and compacted by hammer by one moment, 65% relative density was obtained by pouring sand into a box every 10 cm and compacting by hammer for 2 seconds, 90% relative density was gained by pouring the sand into a box every 5 cm and compacting every layer for 8 seconds. At the end of each trial test a sample was taken to determine its moisture content because it was required to find the dry unit weight. Figure 4.5 shows the calibration of relative density in the laboratory. Table 4.3 indicates the summary of determining the dry unit weights of the sand corresponding to relative densities, void ratios and compaction process.

Figure 4.4. Proter brand electro-pneumatic hammer

Figure 4.5. Calibration of relative densities in the laboratory

Table 4.3. Dry unit weights of the sand corresponding to relative densities and compaction process

Compaction Process	Average Dry Unit Weight (γ_d), (kN/m^3)	Void Ratio (e)	Relative Density (Dr,%)
The model sand usually pours from a height of 15 cm until the model tank is filled to a required depth.	14.6	0.86	10
Each point (15 cm x 15 cm) of each 10 cm of soil layers is compacted for less than a second (for a moment only) after pouring the sand from a height of 5 cm.	15.5	0.75	40
Each point (15 cm x 15 cm) of each 10 cm of soil layers is compacted for 2 seconds after pouring the sand from a height of 5 cm.	16.3	0.66	65
Each point (15 cm x 15 cm) of each 5 cm of soil layers is compacted for 8 seconds after pouring the sand from a height of 30 cm.	17.3	0.57	90

4.4. Direct Shear Test

In this study normal direct shear box test equipment was used which has dimensions (6 x 6 x 2) cm, for determination of internal friction angles (ϕ) of sand and skin friction angles (δ) between sand and pile materials (steel and timber) at each relative densities. All tests were performed with strain controlled direct shear test machine with constant shearing rate 0.5 mm/min.

4.4.1. Internal Friction Angle of Sand

Direct shear tests were conducted for determination of friction angle (ϕ) of sand of relative densities (Dr= 10%, 40%, 65% and 90%). The samples were prepared in direct shear box, for each relative density three direct shear tests were performed under three different normal stress (54.5, 109, and 163.5 kPa) according to ASTM D3080-72(1989). Table 4.4 shows the internal friction angles of the sand obtained by direct shear test corresponding to the relative density of the sand. It was observed that the internal friction angle of the sand increases with increasing relative density of the sand. Figure 4.6 shows relationship of the internal friction angle of the sand versus the relative density of the sand.

Table 4.4. Internal friction angles of the sand corresponding to relative densities.

Relative density of the sand (Dr = %)	Internal friction angle of the sand (ϕ)
10	41.0°
40	44.3°
65	48.7°
90	52.4°

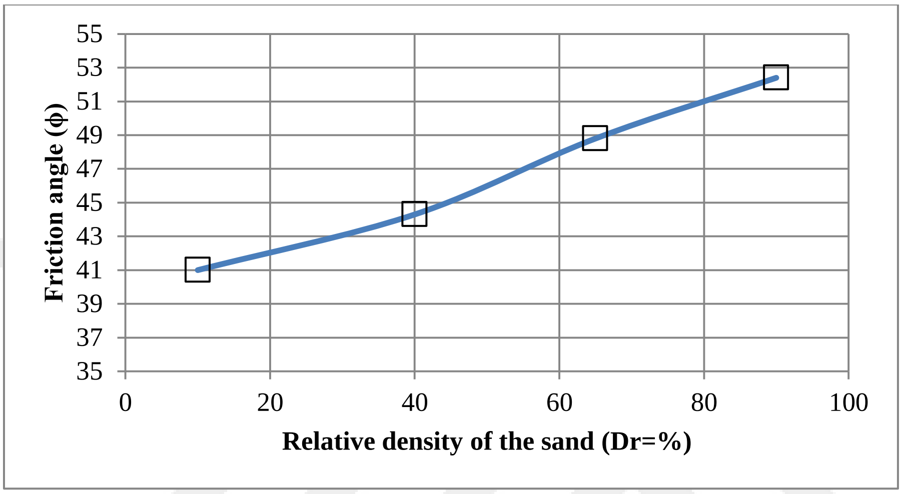

Figure 4.6. Relative densities of the sand versus internal friction angle

4.4.2. Interface Shear Test

In order to determine the skin friction angle (δ) between sand and pile materials (steel and timber) for each relative density, a total of twenty four interface shear tests were performed, twelve for steel-sand interface and the others for timber-sand interface. In each test a pile model specimen was put in the lower halve of the shear box and the sand poured in the upper halves with required relative density and sheared at constant rate 0.5 mm/min. Table 4.5 show the skin friction angle between sand and pile materials. Figure 4.7 shows the skin friction angles obtained by interface shear test corresponding to relative densities of the sand. It was observed that the skin friction angle increases with increasing relative density up to Dr=60% but for relative density Dr = 90% it started to decreases as shown in Figure 4.7.

Table 4.5. Skin friction angles between sand and pile materials corresponding to the relative density.

Relative density of the sand (Dr = %)	skin friction angle (δ) of sand-timber material	skin friction angle (δ) of sand-steel material
10	35.1°	18.04°
40	36.2°	19.28°
65	37.9°	20.7°
90	35.3°	18.8°

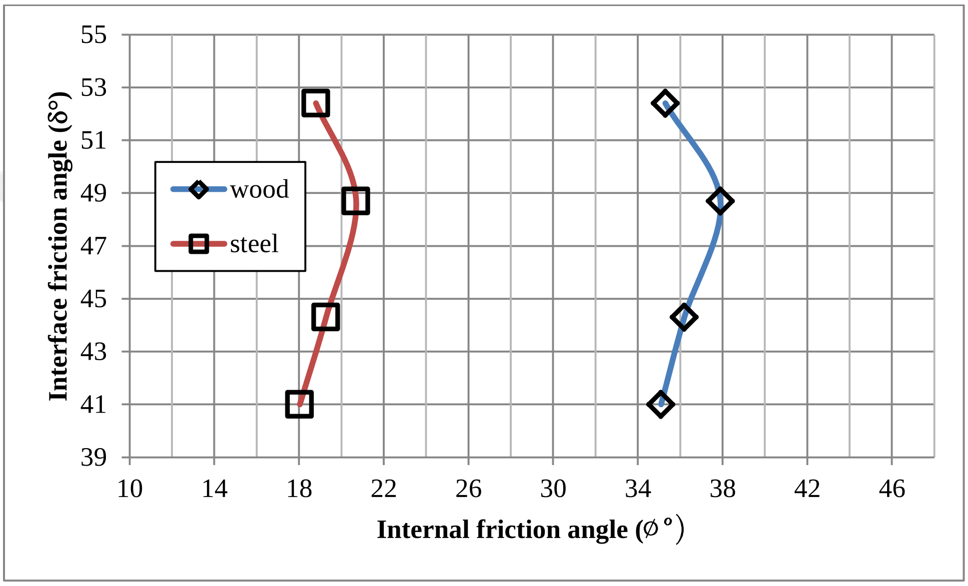

Figure 4.7. Relative density of the sand versus skin friction angle between sand and pile materials.

4.5. Pile Model Load Tests

4.5.1. Test Set Up

All laboratory pile model tests were performed by using the set up illustrated in Figure 4.8, it is consisted of soil tank with dimensions (75 cm x 75 cm x 100 cm), loading machine, and computer program system and pile models. Two model piles have been used in this study, timber and closed end steel pipe piles, piles diameter was 50 mm and length was 600 mm while the embedded length of the piles was L_b=500 mm, pile materials have the same surface roughness of the materials samples which had been used before in direct shear interface tests.

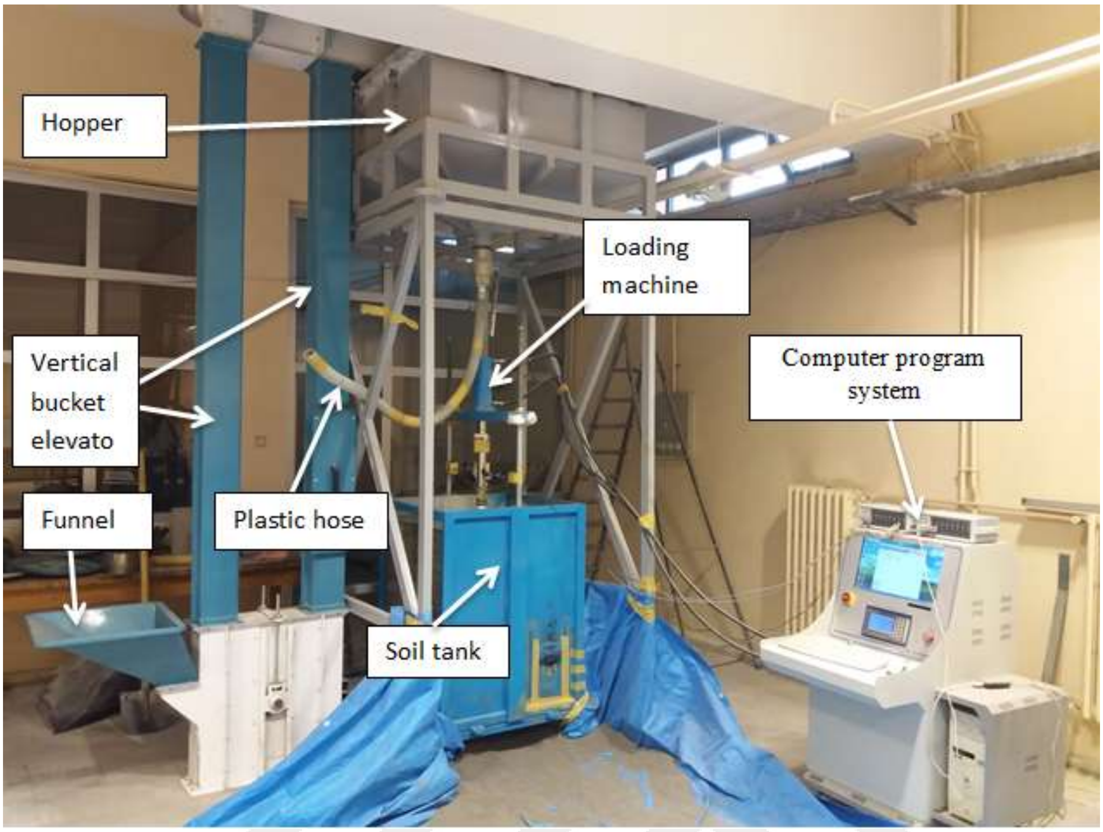

Figure 4.8. Pile model test set up

The soil tank which has been used manufactured of steel with dimensions mentioned above, the tank's dimensions were chosen like that to ensure that no interference occur between the failure region around the model pile and the walls of the tank.

Bolton et al,. (1999) suggested two guide lines to prevent the effect of boundary and scale on the bearing capacity of the model piles. They stated that to avoid these kinds of problems, the ratio of the soil tank diameter to the diameter of the model pile (D_{tank}/D_{pile}) must be greater than 8, and also the diameter of the model pile have to be greater than ($20*D_{50}$) average diameter of the soil particles.

In this study (D_{tank}/D_{pile}) = 15 which is greater than 8, and model pile diameter = 50 mm which is greater than ($20*D_{50}$=9.5 mm). Table 4.6 shows the various soil tanks and pile model dimensions which have been used by some researchers.

Table 4.6. Dimensions of soil model tank and model piles used by some researcher.

Reference	Soil model tank diameter (mm)	Model pile diameter (mm)	Soil model tank to model pile diameter ratio
Vesic (1963, 1964)*	2450	50.8 - 171.5	14.29 - 48.23
Hanna and Tan (1973)* Tan and Hanna (1974)*	610 x 610	15.7 - 38	16.05 – 38.85
Das et al. (1977)*	475 x 610	25.4	18.7
Chaudhuri and Symons (1983)*	1100	25.4 - 50	22 – 43.31
Kerisel (1964)*	6400	40 - 320	20 - 160
Robinsky and Morrison (1964)*	501 x 711	20.5 - 37.5	24.44 – 13.36
Shin et al. (1993)*	457 x 457	25.4	17.99
Al-Mhaidib (2001)*	450	30	15
Mayoral et al. (2005)*	510	51	10
Nanda and Patra (2011)*	750	32	23.44
Sheikhtaheri (2014)	300	38.3	7.8
		31.75	9.45
		19.25	15.6
Current Study	750x750	50	15
Note: the remarked references with (*) adopted from **(Taylan, 2013).**			

According to foundation engineering design the stress due to applied load on the foundation may effects on the soil layers up to a depth of (1.5B to 2B), B is the short dimension of the foundation. For this reason the mode piles were installed in a way that the bottom of the pile 400 mm above the bottom of the soil tank (400 mm >2B or 2D).

Although to avoid the effect of the material properties on the pile bearing capacities the galvanized steel plate is attached to the bottom pile, as shown in Figure 4.9

Figure 4.9. Galvanized steel plate at the bottom of the model piles

For installing model piles, the pile was connected to the detachable loading shaft by special types of epoxy adhesive (5 minutes), in each test the tank was filled with desired relative density up to 400 mm and after that pile was installed and pile was lowered until the bottom of the pile sits on the sand after that it's vertically was checked in all sides as shown in Figure 4.10 and tank was filled to the desired depth.

Figure 4.10. Checking vertically of the model pile

The axial load was applied to the single pile model by using loading machine; the loading machine used in this study is not strain deformation control that's why many trial tests have been done in laboratory to keep the rate of vertical displacement approximately (1 mm/min). The machine was connected to the computer program system to records the axial loads applied to the pile and displacement of the pile. To measure the displacement of the pile, a clamp was used with two L-shapes and two LVDT (Linear Variable Differential Transformation) were installed as shown in Figure 4.11. The LVDTs also were connected to the computer system, the interval time for recording the axial load and displacement was also controlled by a computer program. The data were recorded in computer system including; time interval, axial loads and displacement.

Figure 4.11. Installing LVDT on model pile.

4.5.2. Pile Model Test Procedures

4.5.2.1. Measuring Total Bearing Capacity of Single Model Pile

This section presents a procedures and methodology of filling tank with sand and conducting single model pile tests for steel and timber piles under axial loading and measuring their total bearing capacity.

1. In each relative density, for a complete soil experiment, the model soil tank is filled to a height of 90 cm. In the case of Dr=10% the model soil tank is filled by pouring model sand at a height of (15 cm) as shown (Figure 4.12.), For Dr=40% and Dr=65% (Figure 4.13.), the soil tank is filled in nine (9) layers, each layer is 10 cm in height with sand pouring at a height of (5 cm) and each soil layer is then compacted by hammer, the compaction period per soil layers is less than a second (for a moment only) for Dr= 40% and it is two seconds for Dr. 65%. But for Dr= 90% (Figure 4.14.), the soil tank is filled in eighteen (18) layers (i.e., each layer is 5 cm in height) with sand pouring at a height of (30 cm) and then each layer of soil is compacted for 8 seconds.

2. After the model soil tank was filled to depth of 40 cm. The model pile was installed which already have been attached to the detachable loading shaft by using epoxy adhesive. The pile was lowered down until the base of the pile was sat on the sand and plastic clamp and pile verticality was checked by water bubble level and filling tank was continued according to the procedures mentioned in the above points.

3. The axial applied load and the vertical displacement of the model piles are measured using the **Keli S beam-type 5 tons capacity** load cell and LVDTs. The data are recorded in the computer by the Data Acquisition System.

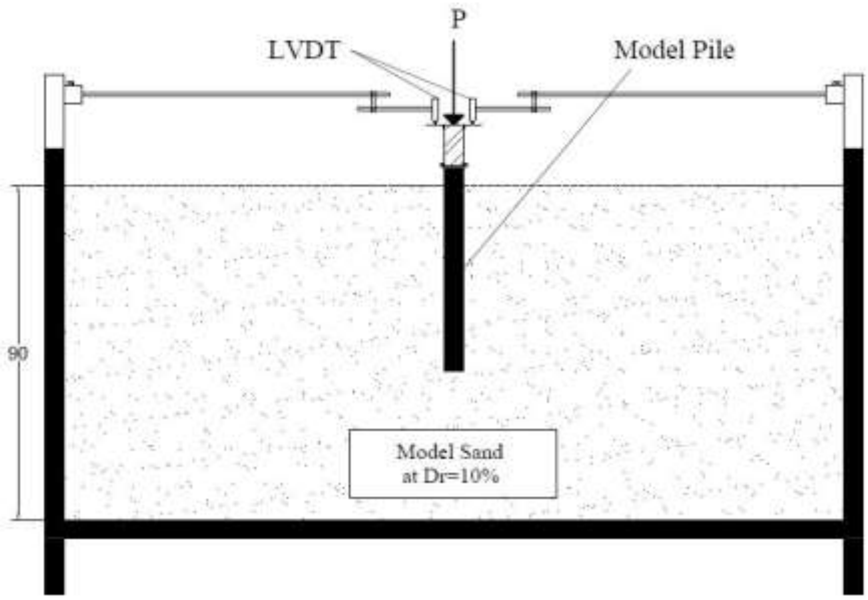

Figure 4.12. Model pile installed in the soil model tank for total bearing capacity test at Dr=10%.

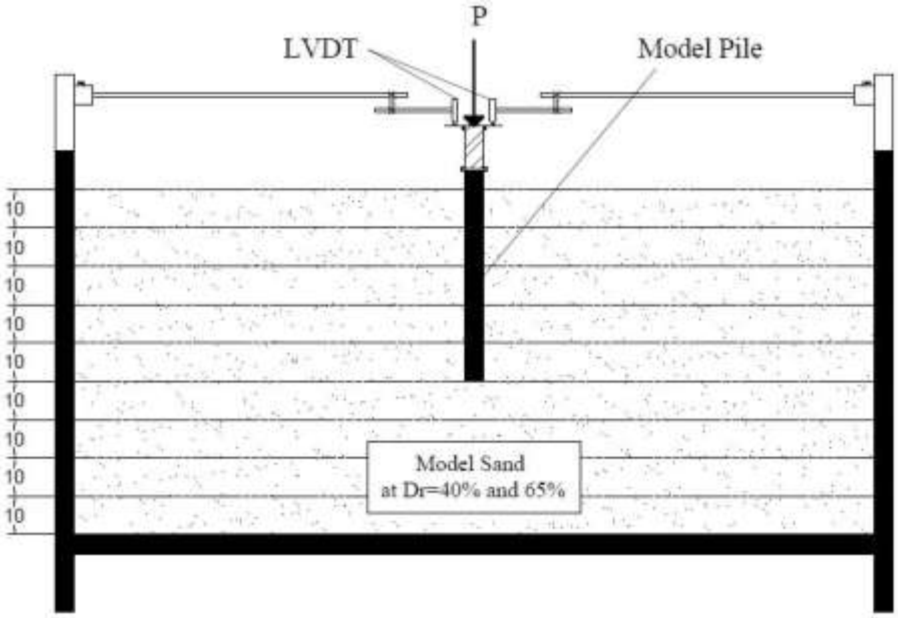

Figure 4.13. Model pile installed in the soil model tank for total bearing capacity test at Dr=40% and 65%.

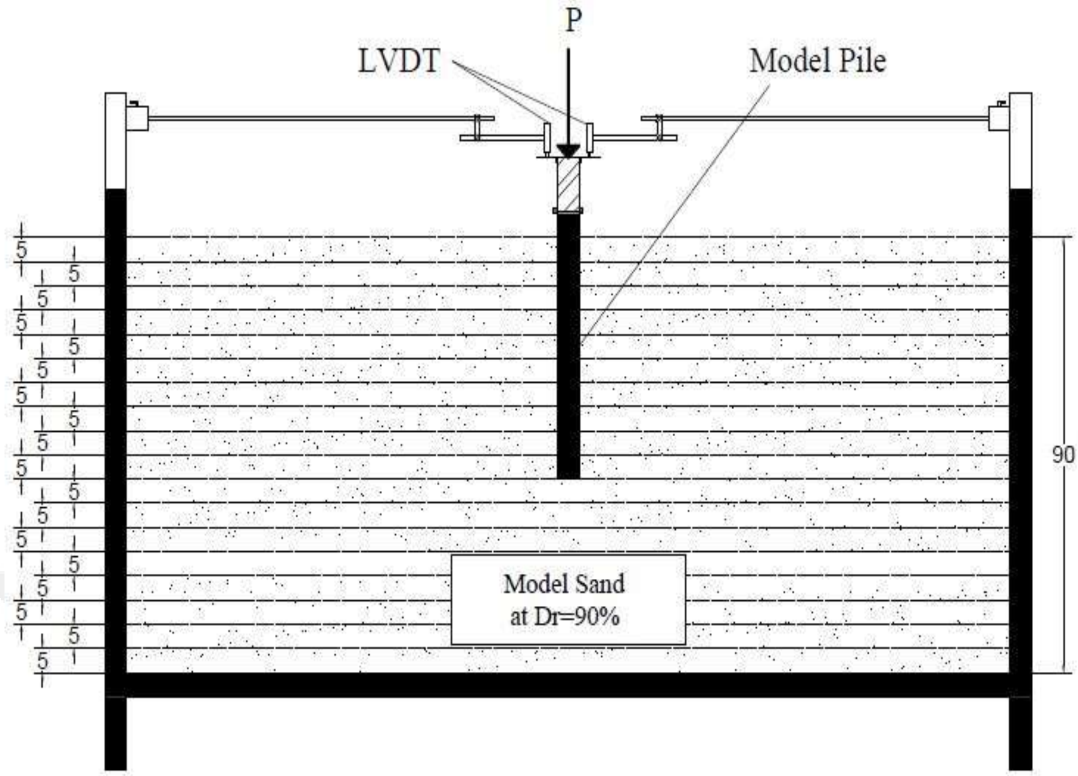

Figure 4.14. Model pile installed in the soil model tank for total bearing capacity test at Dr=90%.

4.5.2.2. Measuring the Base Bearing Capacity of Single Model Pile

To perform base bearing capacity of single model pile experimentally, the model tank was filled to a depth of 40 cm. The same procedures used as mentioned before for each relative density. When the model tank is filled to a depth of 40 cm, the piles are then lowered carefully to the level touched only on the sand and then the load is applied. Figure (4.15 to 4.17) show a pile installed at different relative densities to conduct model experiments of the base-bearing capacity.

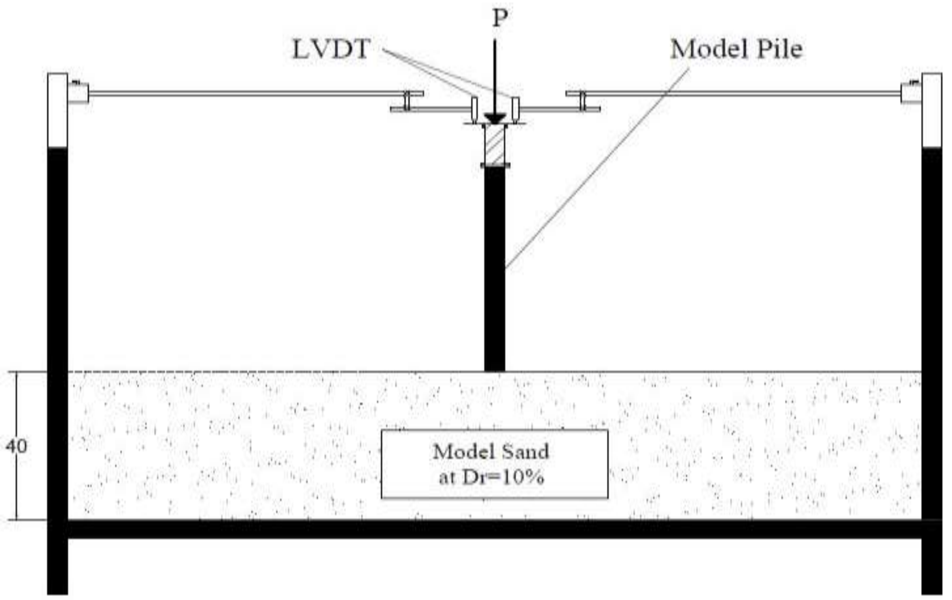

Figure 4.15. Model pile installed in the soil model tank for base bearing capacity test at Dr=10%.

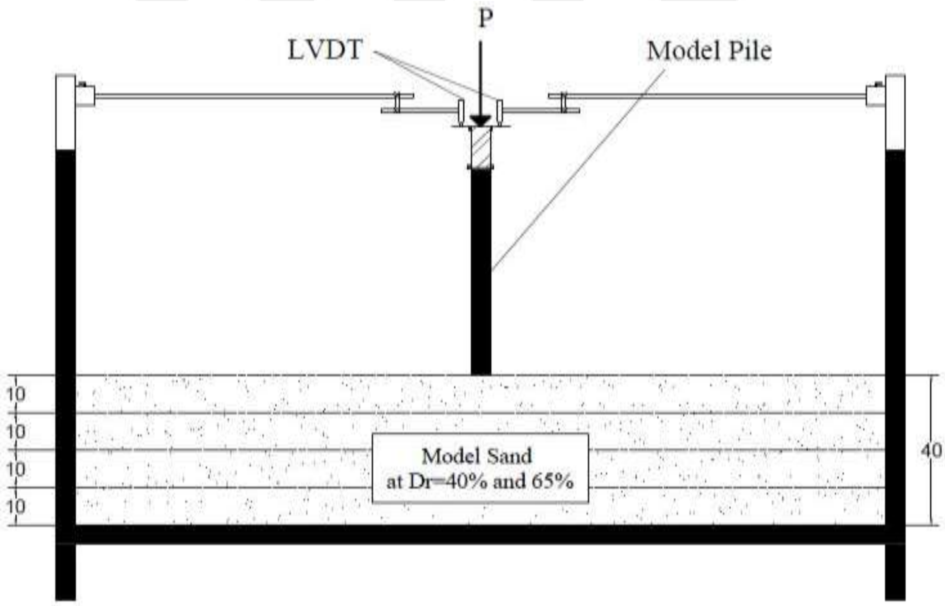

Figure 4.16. Model pile installed in the soil model tank for base bearing capacity test at Dr=40% and 65%.

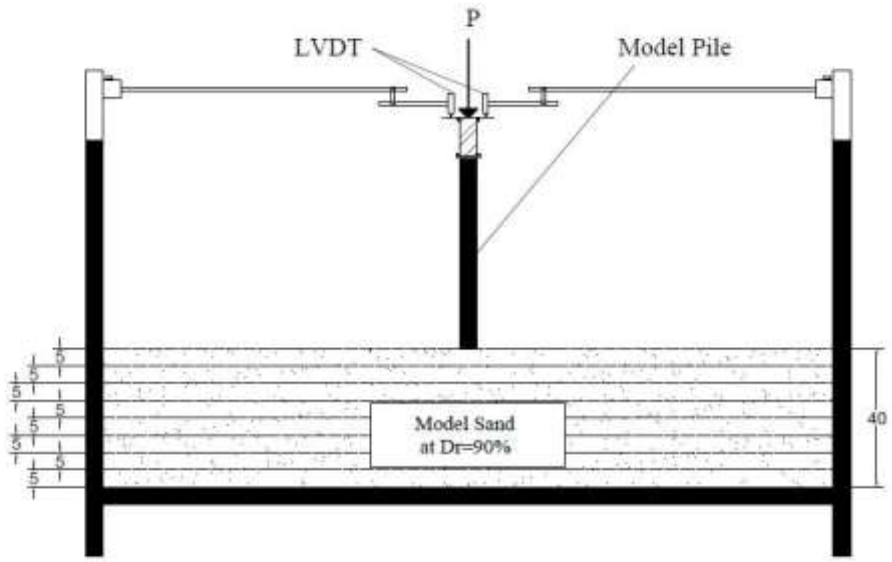

Figure 4.17. Model pile installed in the soil model tank for base bearing capacity test at Dr=90%.

4.5.2.3. Measuring the Shaft Resistance of Single Model Pile

The following procedures were performed to measure the pile shaft resistance of the pile experimentally.

1. A special type of Styrofoam as shown in Figure 4.18 was used with dimensions (12 x 12 x 8 cm). A hole of diameter 5 to 5.2 cm was made in the centre of the Styrofoam body to provide an adequate gap between the sides of the pile and the Styrofoam to avoid any contact during the experiments.

2. The model tank is filled to a depth of 40 cm under the same instructions that were previously provided in soil preparation for Dr. 90%. In the last layer of 40 cm depth, the Styrofoam body is placed in the center of the soil tank and the last layer is then compacted. Then the pile is then lowered to a depth of 2 cm in the pre-drilled hole inside the Styrofoam body.

3. A special type of sponge was wrapped around the pile close to the pile bottom by using a pipe clamp, and then the sponge-clamp system was covered with circular paper. A normal type of adhesive tape is also used to cover the top of the sponge-clamp and the Styrofoam body system, to prevent the fall and entry of any sand particles into the Styrofoam hole during the pile installation and pile load tests as shown in Figure 4.19.

4. For obtaining the desired relative density same procedure were used as for total and base bearing capacity.

Figure 4.18. Styrofoam prepared for the model pile shaft friction test

Figure 4.19. Timber model pile Prepared for a shaft friction resistance test.

Figures (4.20 to 4.22) show a pile installed at different relative densities to conduct model experiments of the shaft resistance for the model piles.

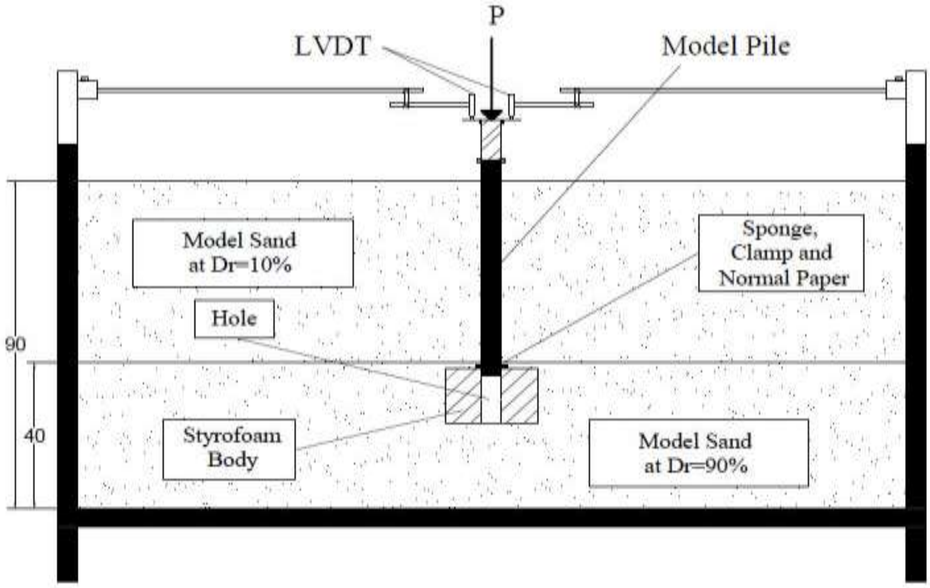

Figure 4.20. Model pile installed in the soil model tank for shaft friction resistance test at Dr=10%.

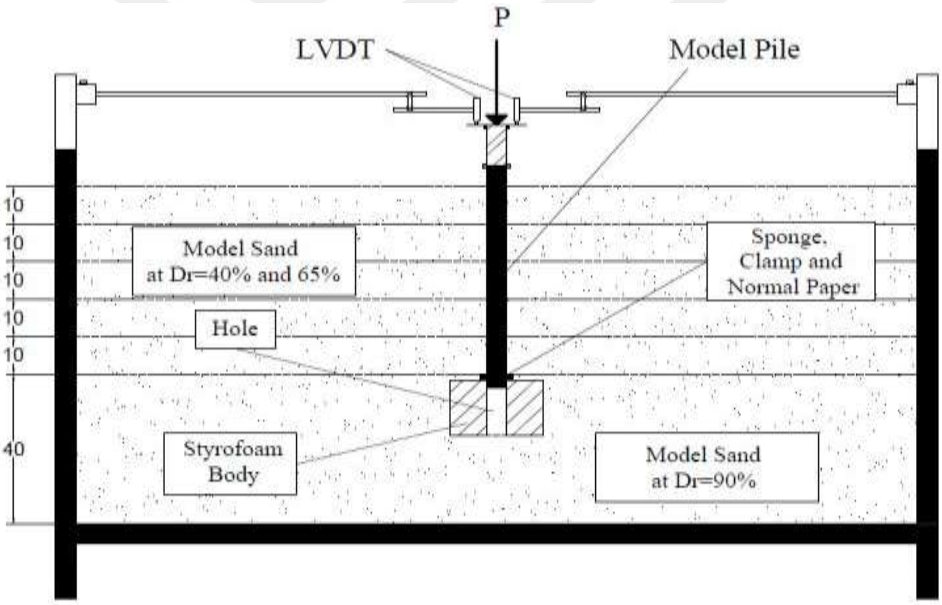

Figure 4.21. Model pile installed in the soil model tank for shaft friction resistance test at Dr=40% and 65%.

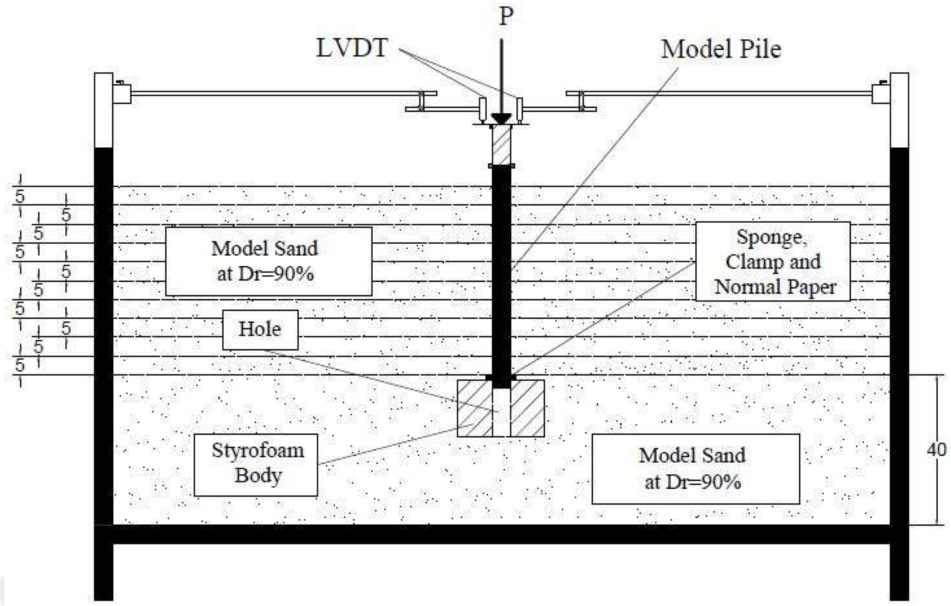

Figure 4.22. Model pile installed in the soil model tank for shaft friction resistance test at Dr=90%.

5. RESULTS AND DISCUSSION

5.1. Introduction

This chapter presents a detail of the experimental results of model piles and compares them to the theoretical results.

5.2. Experimental Results

5.2.1. Total Bearing Capacity

A pile load tests were conducted for both model piles steel and timber for the relative densities 10%, 40%, 65% and 90%. The results recorded in terms of load-settlement curves. Figures 5.1 to 5.4 show the total bearing capacity of the model piles consecutively.

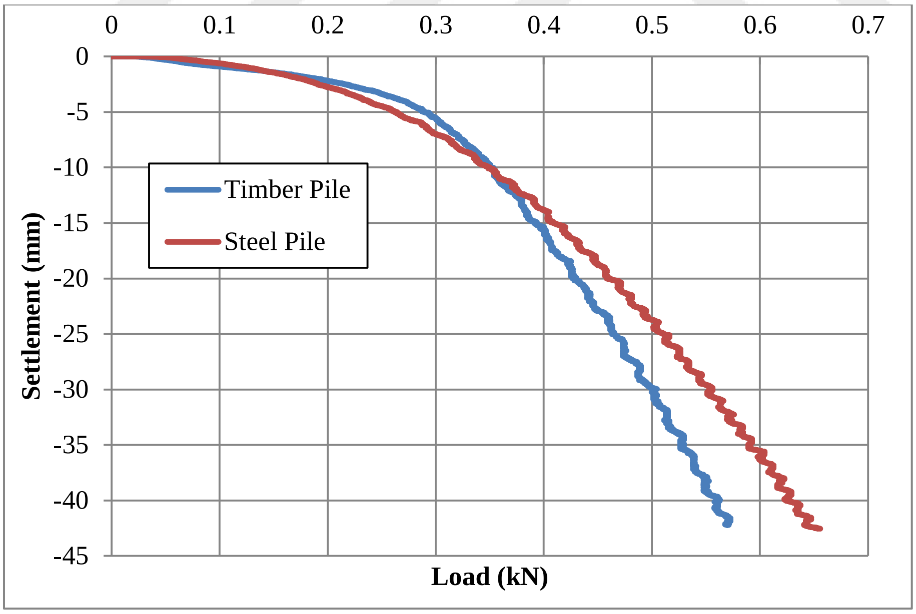

Figure 5.1. Load-displacement curves of model piles for total bearing capacity test at Dr = 10%.

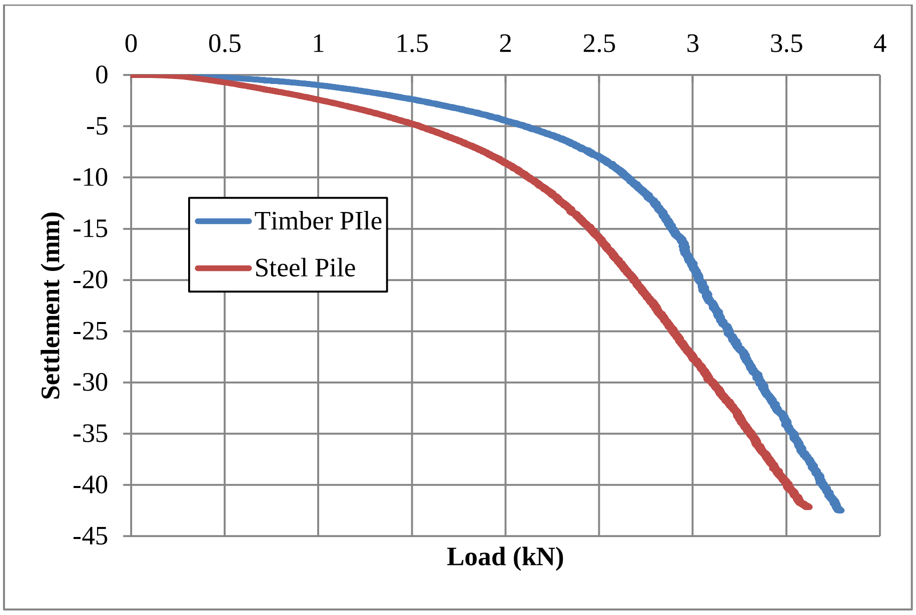

Figure 5.2. Load-displacement curves of model piles for total bearing capacity test at Dr = 40%.

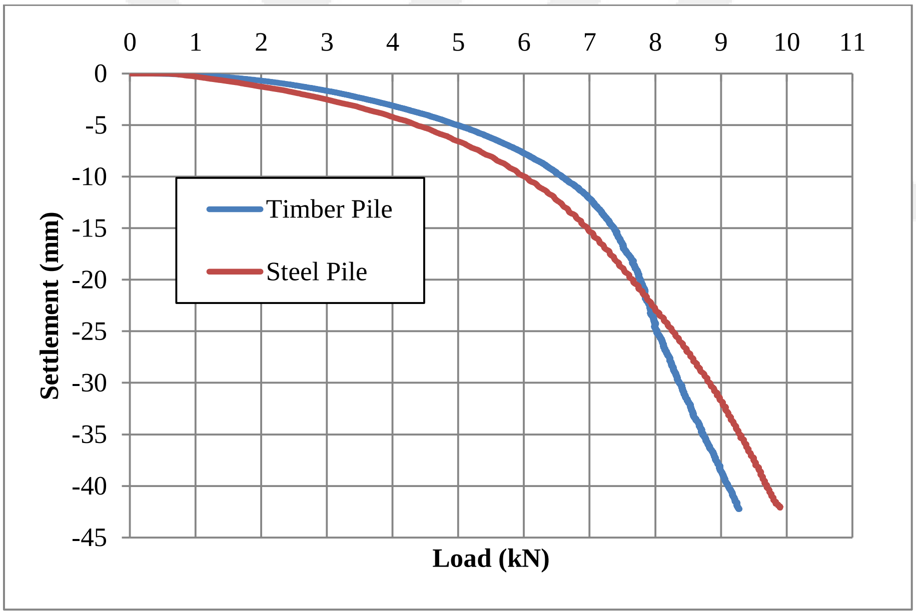

Figure 5.3. Load-displacement curves of model piles for total bearing capacity test at Dr = 65%.

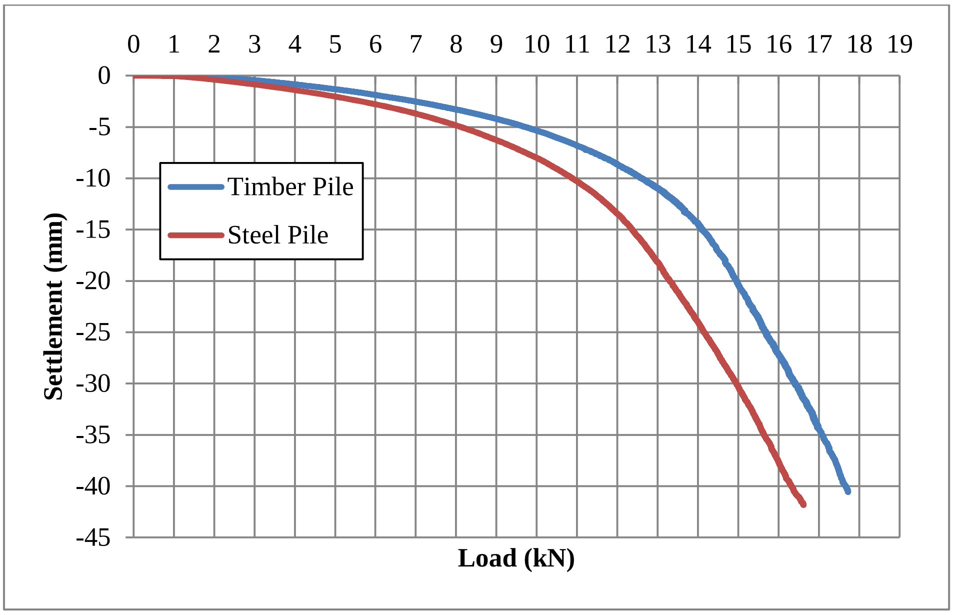

Figure 5.4. Load-displacement curves of model piles for total bearing capacity test at Dr = 90%.

Table 5.1 show the ultimate bearing capacity selected from the load-settlement curves of the model piles plus the weight of the detachable shaft used in the experiments.

Table 5.1. Experimental results of the total bearing capacity of the model piles.

	Model Sand							
	Dr=10%		Dr=40%		Dr=65%		Dr=90%	
Model Piles	Settlement (mm)	Load (kN)	Settlement (mm)	Load (kN)	Settlement (mm)	Load (kN)	Settlement (mm)	Load (kN)
Steel	4	0.28	7.6	1.95	9.32	5.88	10	10.92
Timber	5.3	0.31	9.5	2.64	11.65	6.95	12.5	13.52

Total bearing capacity of the model piles obtained in laboratory, the results showed that the total bearing capacity of single model piles (timber and steel) increases with increasing relative density of sand in a non-linear relationship. Furthermore the settlement which is required for mobilization of the total ultimate bearing capacity of the soil is also increases non-linearly with increasing relative density. The Figures (5.5 and 5.6) show the total ultimate bearing capacity and settlements of timber and steel piles versus the relative density of the sand consecutively.

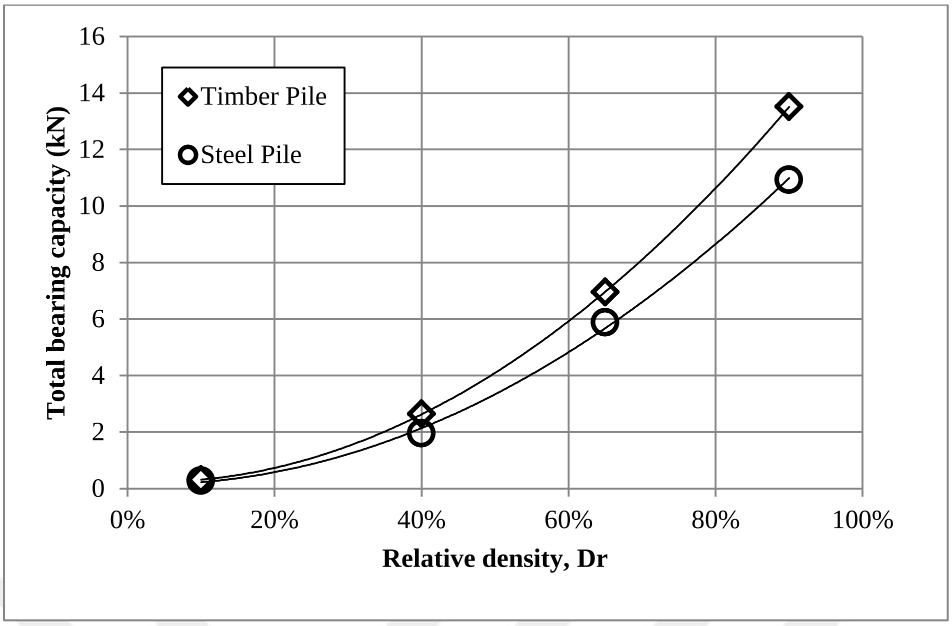

Figure 5.5. Total bearing capacity of model piles versus relative density.

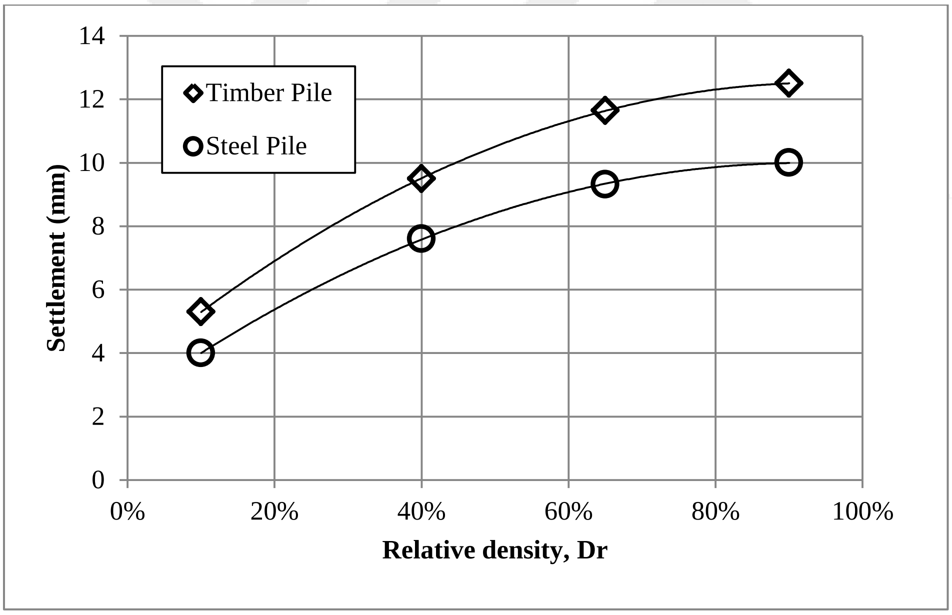

Figure 5.6. Displacement versus relative density for the total bearing capacity of model piles.

5.2.2. Base Bearing Capacity

A pile load test was performed also to measure the base bearing capacity of the model piles, the term base bearing capacity means that there is no over burden pressure above the pile. The results showed that the model piles approximately have the same bearing capacity despite of the weight of the model piles are different. Table 5.2 shows the base bearing capacity of the model piles (timber and steel). Figure 5.7 shows the base bearing capacity curves of the model piles in term of load versus settlement.

Table 5.2. Experimental results of the base-bearing capacity of the model piles.

	Model Sand							
	Dr=10%		Dr=40%		Dr=65%		Dr=90%	
Model Piles	Settlement (mm)	Load (kN)	Settlement (mm)	Load (kN)	Settlement (mm)	Load (kN)	Settlement (mm)	Load (kN)
Timber and Steel Pile	5.5	0.035	3.99	0.231	3.19	0.501	2.80	0.84

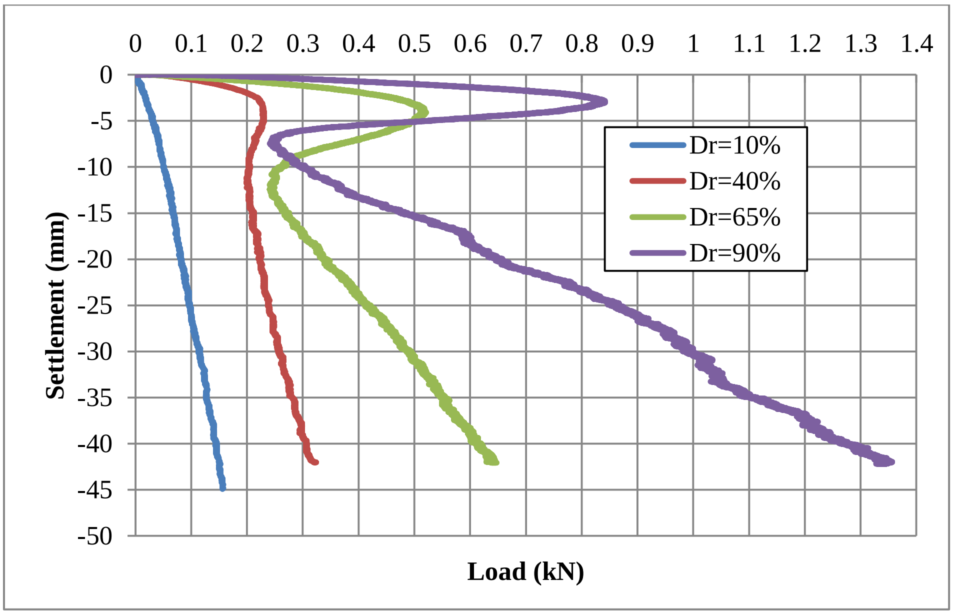

Figure 5.7. Load-displacement curves of model piles for base bearing capacity.

The results of the model piles indicated that the base resistance increases with relative density of the sand but the settlement decreases with increasing relative density of the sand Figures (5.8 and 5.9) show the base resistance and settlement versus relative density of the sand.

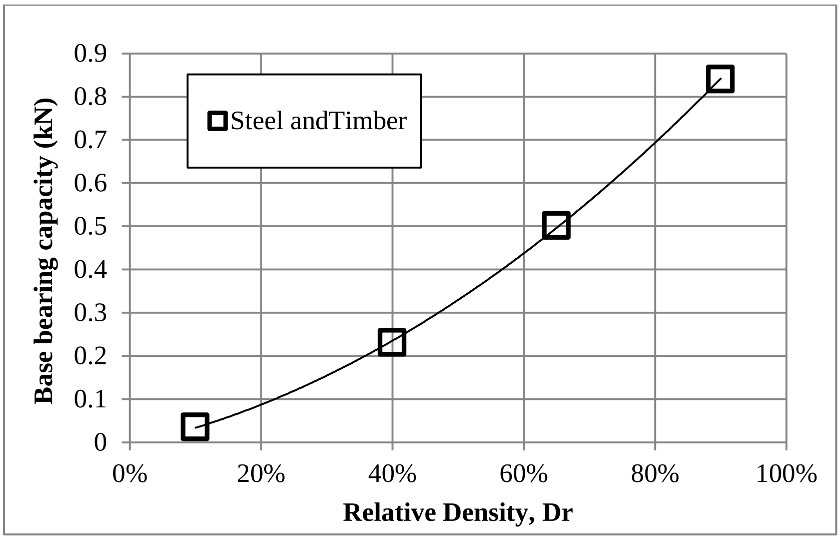

Figure 5.8. Base bearing capacity of model piles versus relative density.

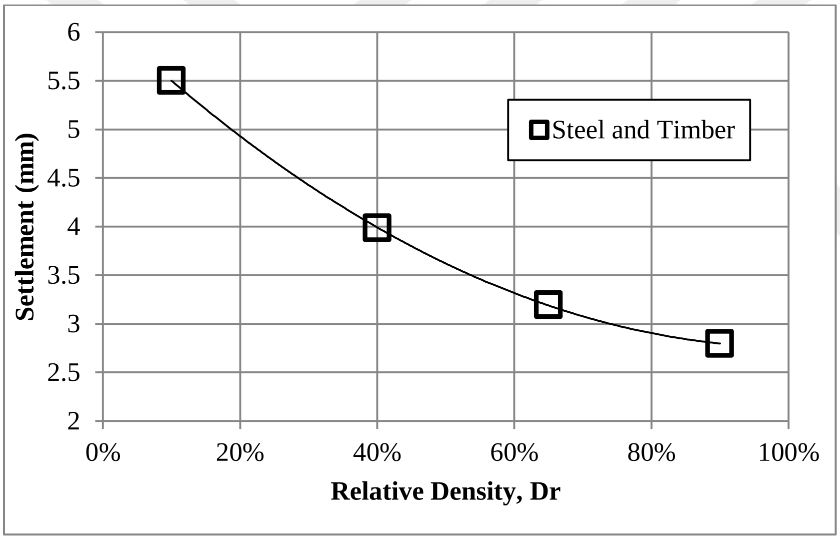

Figure 5.9. Displacement versus relative density of the model piles for the base bearing capacity.

5.2.3. Shaft Friction Resistance

In addition to the total bearing capacity and base bearing capacity of the model piles tests, several tests were conducted to measure the shaft friction resistance of the model piles in four relative densities including 10%, 40%, 65% and 90%, to get the net shaft resistance of the model piles, the Styrofoam friction resistance was also measured in the same procedure as described in chapter three. After that Styrofoam friction resistance was subtracted from the the shaft resistance of the model piles.

The shaft friction resistance of model piles and settlement necessary for mobilization of friction resistance increases with increasing the relative density of the sand. Figures 5.10 to 5.14 show the total shaft resistance of the mode piles (timber and steel) in term of load versus settlement for relative densities 10%, 40%, 65% and 90%.

Table 5.3 show the ultimate shaft resistance selected from the load-settlement curves of the model piles minus the Styrofoam penetration resistance.

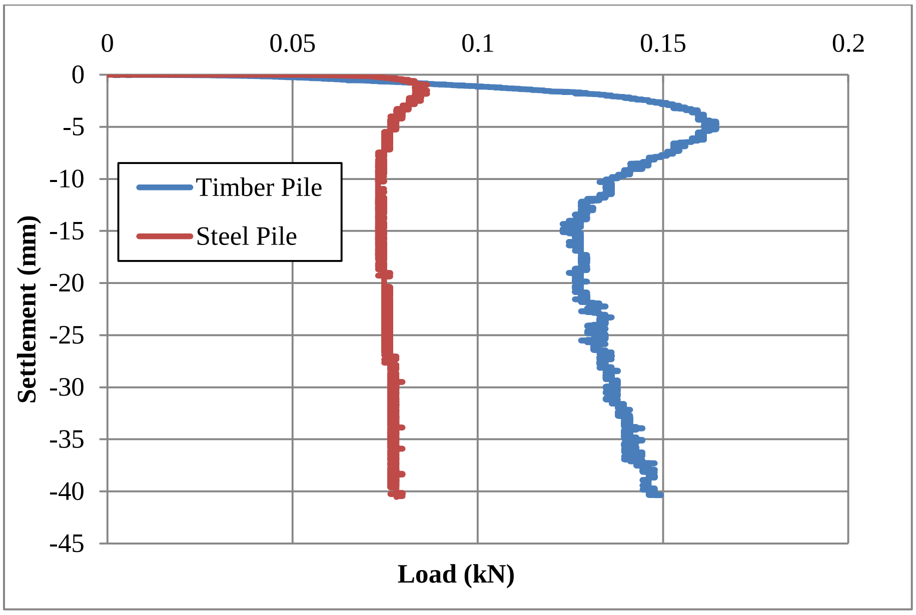

Figure 5.10. Load-displacement curves of model piles for shaft friction resistance test at Dr = 10%.

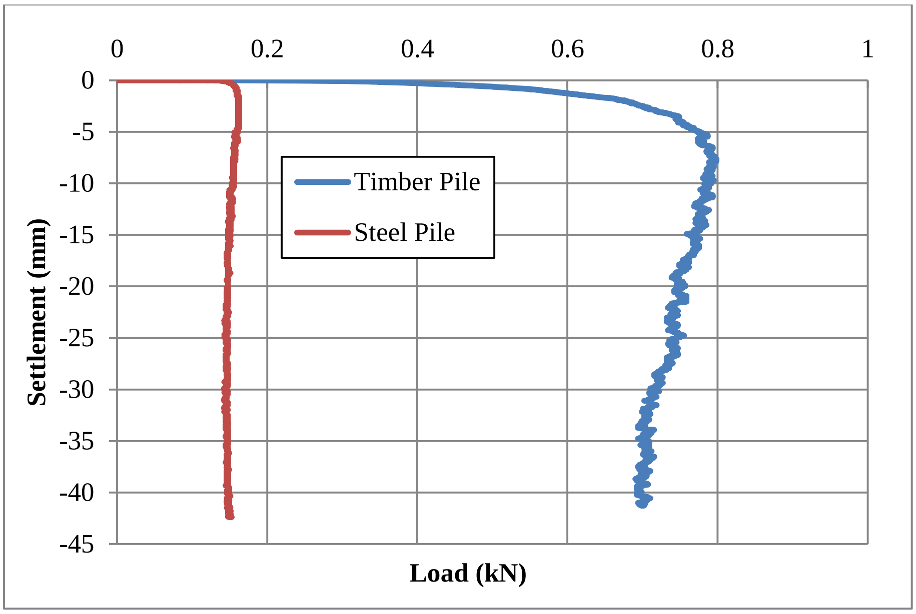

Figure 5.11. Load-displacement curves of model piles for shaft friction resistance test at Dr = 40%.

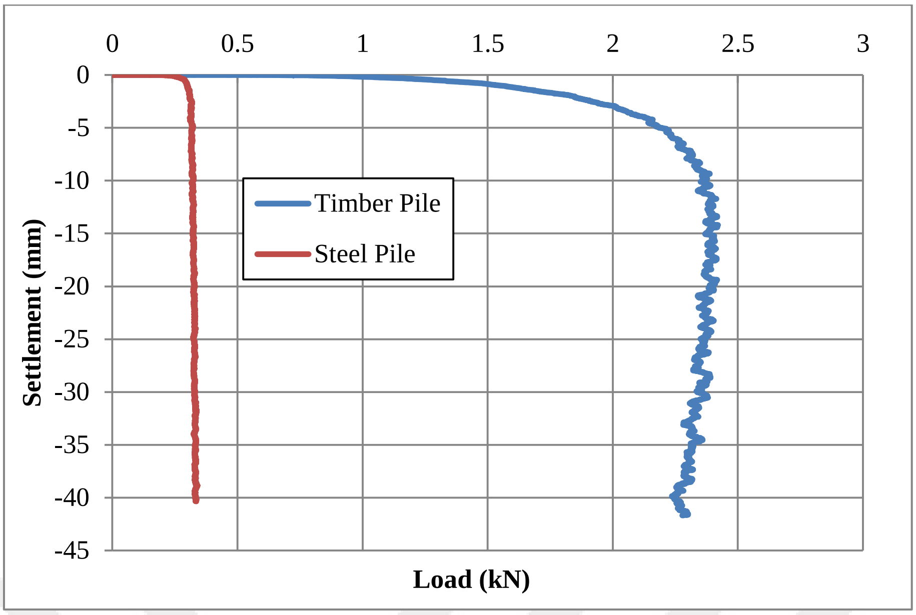

Figure 5.12. Load-displacement curves of model piles for shaft friction resistance test at Dr = 65%.

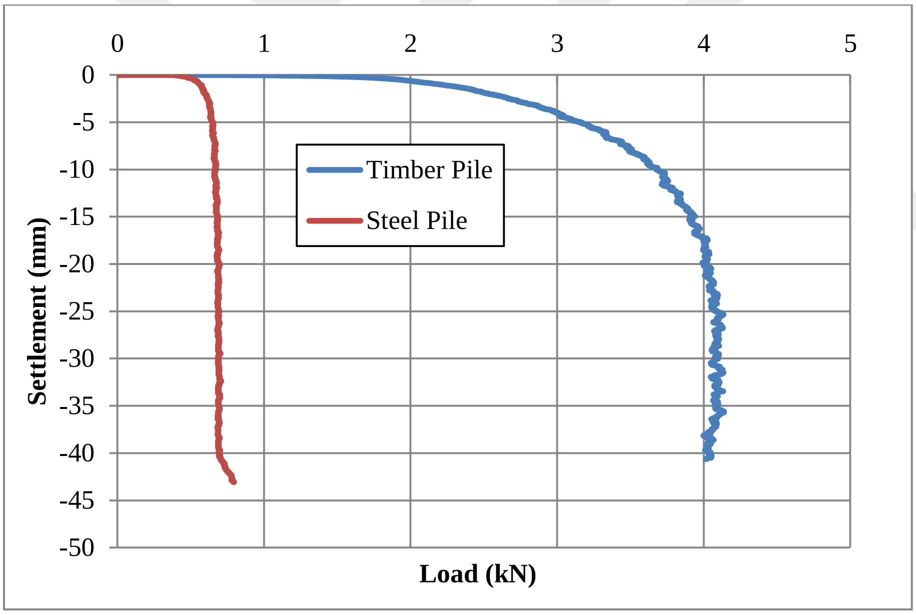

Figure 5.13. Load-displacement curves of model piles for shaft friction resistance test at Dr = 90%.

Table 5.3. Experimental results of the shaft friction resistance the model piles.

	Model Sand							
	Dr=10%		Dr=40%		Dr=65%		Dr=90%	
Model Piles	Settlement (mm)	Load (kN)	Settlement (mm)	Load (kN)	Settlement (mm)	Load (kN)	Settlement (mm)	Load (kN)
Steel Pile	2.2	0.047	4.15	0.125	5.34	0.279	6	0.614
Timber Pile	4.7	0.154	9.50	0.75	11.65	2.37	12.50	3.81

It is obvious from the shaft resistance curves of the model piles that the steel model pile has a low shaft friction resistance even it can be neglected, which means most of the bearing capacity is achieved from the end bearing capacity of the mode pile. Figure 5.14 show the ultimate shaft friction resistance of the model piles versus relative density and Figure 5.15 also show the settlement which is required for mobilization of the shaft friction resistance corresponding to the relative densities of the sand.

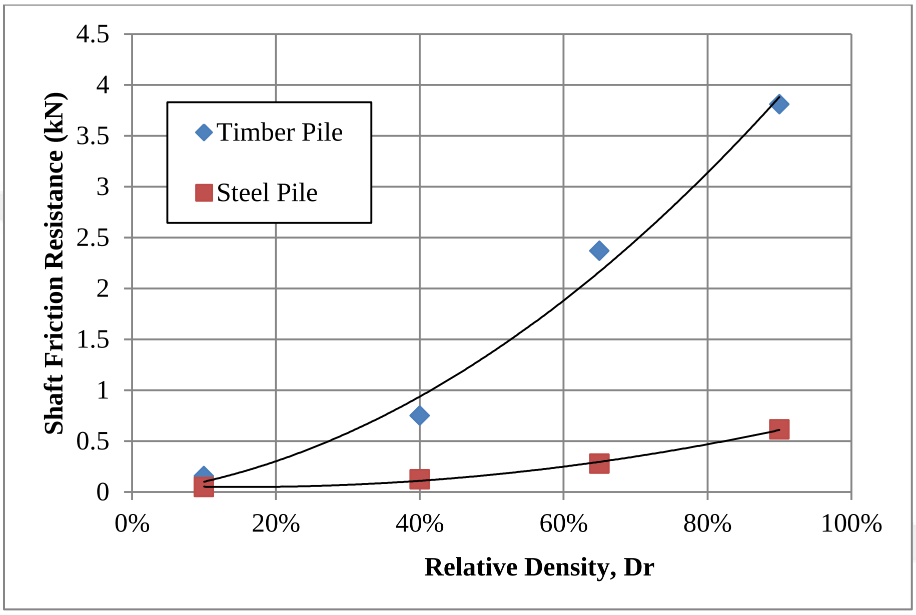

Figure 5.14. Shaft friction resistance capacity of the model piles versus relative density

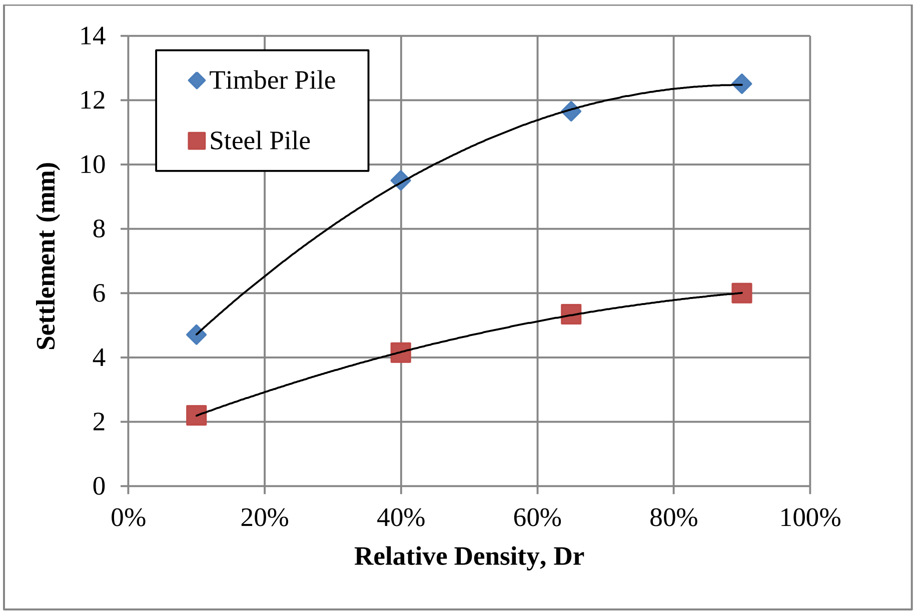

Figure 5.15. Displacement versus relative density of the model piles for the shaft friction resistance.

5.3. Theoretical Results

5.3.1. Pile Base Capacity

The base bearing capacity (Q_b) of the model piles is calculated by using common methods such as Terzaghi (1943), Meyerhof (1963) and Hansen (1970) method. The calculated theoretical results of the base capacity of the model piles are given in Table 5.4.

Table 5.4. Theoretically calculated results of base bearing capacity for model piles (Q_b, kN).

Timber & Steel Pile	Terzaghi (1943)	Meyerhof * (1963)	Hansen (1970)	Experiment
Dr, 10%	0.05	0.39	0.041	0.035
Dr, 40%	0.12	0.913	0.081	0.231
Dr, 65%	0.426	3.152	0.207	0.501
Dr, 90%	1.003	10.749	0.510	0.84

Meyerhof * = from Meyerhof's general bearing capacity equation for shallow foundation.

5.3.2. Pile End (Point) Bearing Capacity

The end-bearing capacity (Q_p) of the model piles is found using the method of Terzaghi (1943), Meyerhof (1976), Coyle & Castello (1981), Janbu (1976) and Hansen (1970). The theoretically calculated results of the model piles end-bearing capacity are given in table 5.5. and 5.6. The experimental end bearing capacity obtained by subtracting shaft friction resistance of the model piles from total bearing capacity of the model piles,

Table 5.5. Theoretically calculated results of end-bearing capacity for the Steel model pile (Q_p, kN).

Steel Pile	Terzaghi (1943)	Meyerhof (1976)	Coyle & Castello (1981)	Janbu (1976)	Hansen (1970)	Experiment
Dr, 10%	1.56	6.023	1.58	0.580	2.339	0.233
Dr, 40%	2.506	12.483	2.416	1.406	4.042	1.890
Dr, 65%	5.038	26.735	3.888	4.047	8.779	5.601
Dr, 90%	9.385	40.269	5.866	11.447	18.748	10.306

Table 5.6. Theoretically calculated results of end-bearing capacity for the Timber model pile (Q_p, kN).

Timber Pile	Terzaghi (1943)	Meyerhof (1976)	Coyle & Castello (1981)	Janbu (1976)	Hansen (1970)	Experiment
Dr, 10%	1.56	6.023	1.58	0.580	2.339	0.156
Dr, 40%	2.506	12.483	2.416	1.406	4.042	1.99
Dr, 65%	5.038	26.735	3.888	4.047	8.779	4.58
Dr, 90%	9.385	40.269	5.866	11.447	18.748	9.71

5.3.3. Pile Shaft Capacity

In our study, in order to estimate pile shaft capacity resistance of the model piles (steel and timber) theoretically, the general equation used for estimating the skin friction pile capacity suggested by Burland (1973) has been used with different considerations of K values, in addition the Coyle and Castello's (1981) method. Table 5.7 and 5.8 show the results of pile shaft friction resistance consecutively.

Table 5.7. Theoretically calculated results of shaft friction resistance for the steel model pile (Q_f, kN).

	Burland Method			Coyle and Castello's method	Experiments
Model Sand	Q_f ($K = K_0$)	Q_f ($K = 1.4\ K_0$)	Q_f ($K = K_p$)	Q_f (Coyle and Castello's K)	Q_f (experiment)
Dr, 10%	0.032	0.045	0.451	0.699	0.047
Dr, 40%	0.032	0.045	0.602	1.267	0.125
Dr, 65%	0.030	0.042	0.855	2.361	0.279
Dr, 90%	0.024	0.034	1.002	3.178	0.614

Table 5.8. Theoretically calculated results of shaft friction resistance for the timber model pile (Q_f, kN).

	Burland Method			Coyle and Castello's	Experiments
Model Sand	Q_f (K = K_0)	Q_f (K = 1.4 K_0)	Q_f (K = K_p)	Q_f (Coyle and Castello's K)	Q_f (experiment)
Dr, 10%	0.069	0.097	0.973	1.508	0.154
Dr, 40%	0.067	0.094	1.259	2.651	0.75
Dr, 65%	0.062	0.087	1.761	4.866	2.37
Dr, 90%	0.050	0.07	2.084	6.611	3.81

5.4. Comparison of Experimental and Theoretical Results

In this section, the experimental results of the model piles will be compared to the calculated theoretical results. The comparison is made by plotting the results in graphs representing the theoretical and experimental results.

5.4.1. Base Bearing Capacity

The base bearing capacity of model piles (steel and timber) were calculated by using Terzaghi (1943), Meyerhof (1963) and Hansen (1970). Comparisons of the results are shown in (Figure 5.16).

From Figure 5.16, it is observed that the results calculated by Meyerhof don't have good agreement with experimental and other two method's results. Figure 5.17 shows the comparison among the results of the experimental with Terzaghi (1943) and Hansen (1970). From Figure 5.17 it is seen that the calculated results by Terzaghi and Hansen are close to the experimental results. However, most of the researchers who worked on pile bearing capacity stated that the Terzaghi method is not suitable for use in estimating pile bearing capacity. But in this study, his method gave the values closest to the experimental results.

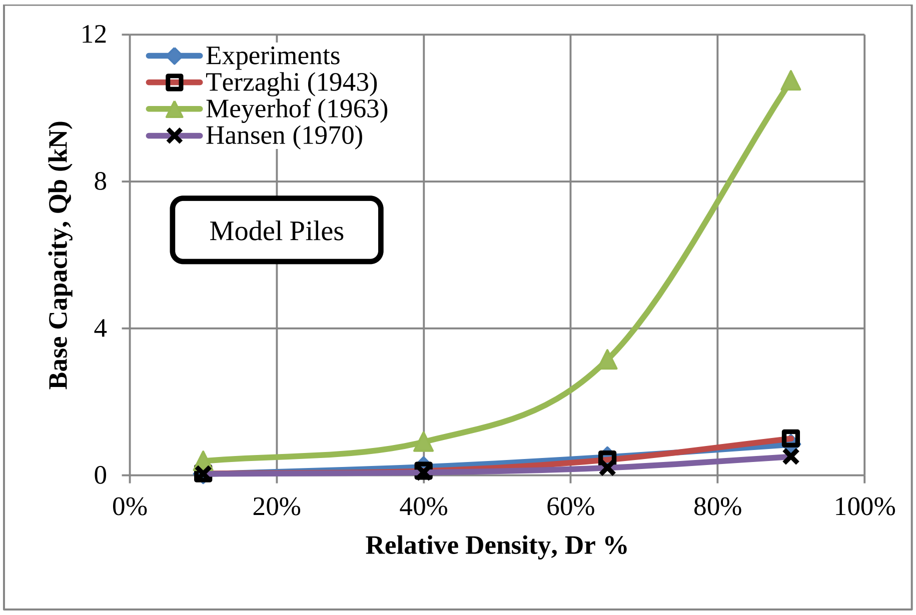

Figure 5.16. Comparison between experimental and theoretical results of base bearing capacity.

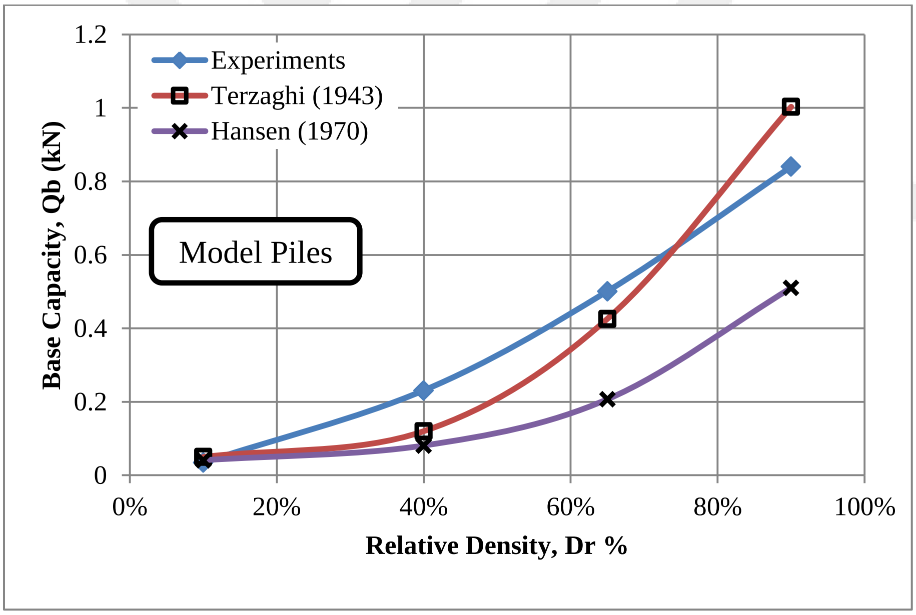

Figure 5.17. Comparison between experimental and theoretical results of base bearing capacity excluding Meyerhof, Q_b (kN).

5.4.2. Pile End (Point) Bearing Capacity

The most common methods used in estimating the pile end bearing capacity are Terzaghi (1943), Meyerhof (1976), Coyle and Castello (1981), Janbu (1976), Hansen (1970). The experimental end bearing capacity of the model piles were calculated by subtracting the friction of the shaft resistance from total bearing capacity. From table 5.5 it is observed that there are significant differences between the experimental results and those of the Meyerhof and Hansen method. Therefore, the results of the Meyerhof and Hansen methods are excluded from the comparative graphs for the model piles. Figure 5.18 and 5.19 show the comparison of the experimental end bearing results of the model piles (steel and timber) with other three methods consecutively.

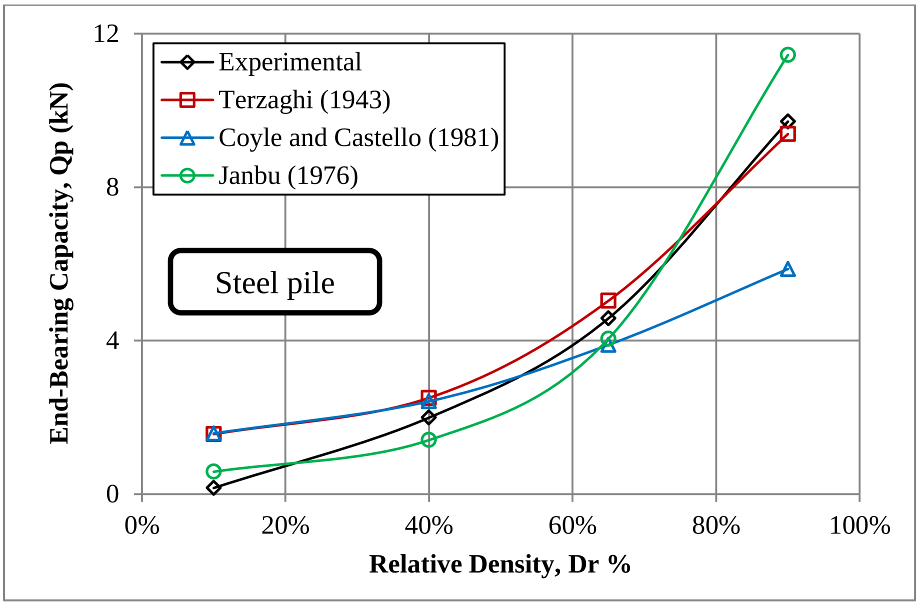

Figure 5.18. Comparison between experimental and theoretical results of end bearing capacity for steel pile.

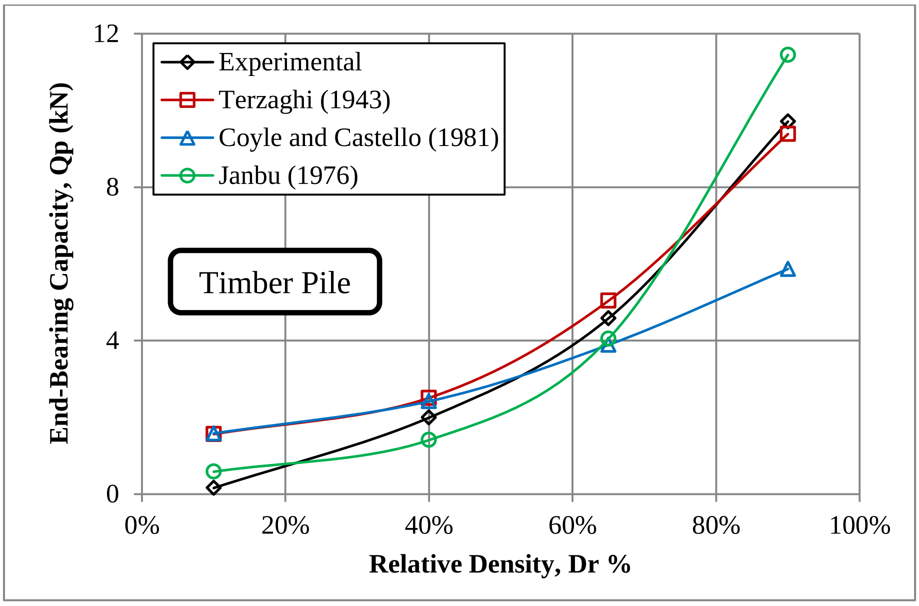

Figure 5.19. Comparison between experimental and theoretical results of end bearing capacity for timber pile.

5.4.3. Pile shaft Capacity

In calculation of shaft resistance of pile, the most difficult factors to estimate are the coefficient of the earth pressure K and the skin friction angle δ between pile materials and soil. The skin friction angle δ is usually measured by using the modified direct shear test, while its interface friction behavior is different from that of the pile model tests. The general equation suggested by Burland (1973) which is mentioned in chapter one equation 1.2 was used to estimate the shaft friction resistance of the model piles. Two methods were used for estimating the K parameter including Kp and one which was invented by Coyle and Castello.

Figures 5.19 and 5.20 show the graphical Comparison between experimental and theoretical shaft resistance results of Steel and timber piles.

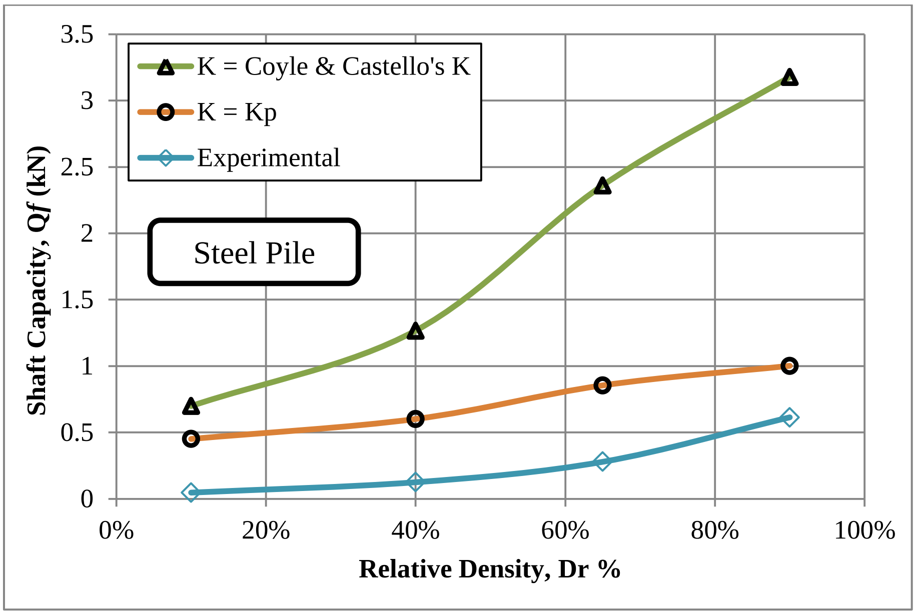

Figure 5.20. Comparison between experimental and theoretical results of shaft friction resistance for steel pile.

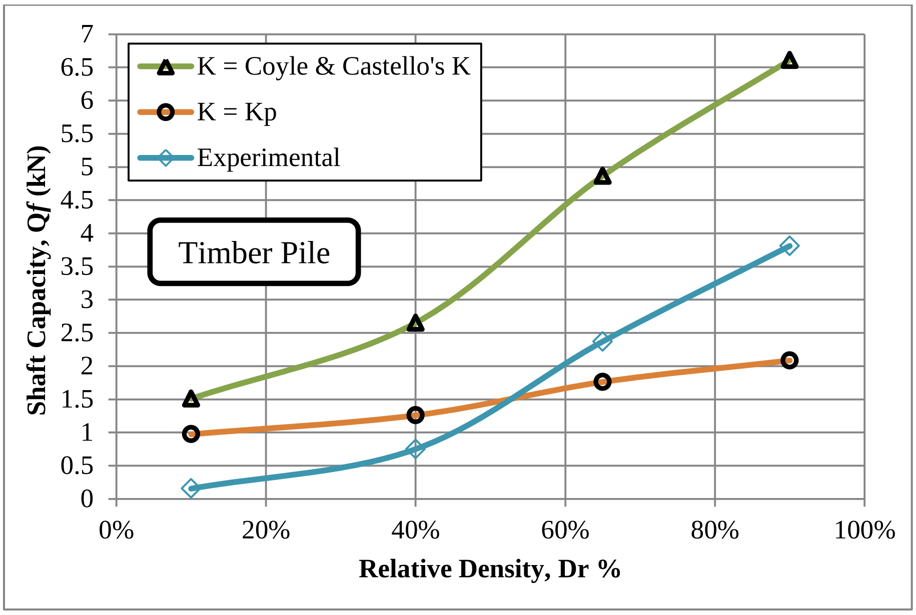

Figure 5.21. Comparison between experimental and theoretical results of shaft friction resistance for timber pile.

5.5. Back Calculation

In this section the coefficient of earth pressure K has been back calculated by substituting experimental results in equation 1.3 in chapter one section 1.5. Also skin friction angle has been calculated by the same equation by substitution passive earth pressure coefficient Kp.

Table 5.9. Back calculation of earth pressure coefficient (K) factor for timber pile

Dr (%)	Timber pile				
	D_f (m)	γ (kN/m^3)	Q_f (kN)	$\delta°$	K
10	0.5	14.6	0.154	35.1	0.76
40	0.5	15.5	0.750	36.2	3.37
65	0.5	16.3	2.370	37.9	9.51
90	0.5	17.3	3.810	35.3	15.83

Table 5.10. Back calculation of earth pressure coefficient (K) factor for steel pile

Dr (%)	Steel pile				
	D_f (m)	γ (kN/m^3)	Q_f (kN)	δ^o	K
10	0.5	14.6	0.047	18.04	0.50
40	0.5	15.5	0.125	19.28	1.17
65	0.5	16.3	0.279	20.7	2.31
90	0.5	17.3	0.614	18.8	5.31

Table 5.11. Back calculation of skin friction angle (δ^o) for timber pile

Dr (%)	Timber pile						
	D_f (m)	γ (kN/m^3)	Q_f (kN)	Kp	δ^o (back)	δ^o (IST)	Difference (%)
10	0.5	14.6	0.154	4.815	6.36	35.1	+452
40	0.5	15.5	0.750	5.632	23.63	36.2	+53
65	0.5	16.3	2.370	7.041	46.43	37.9	-18
90	0.5	17.3	3.810	8.629	52.42	35.3	-33

Table 5.12. Back calculation of skin friction angle (δ^o) for steel pile

Dr (%)	Steel pile						
	D_f (m)	γ (kN/m^3)	Q_f (kN)	Kp	δ^o (back)	δ^o (IST)	Difference (%)
10	0.5	14.6	0.047	4.815	1.95	18.04	+825
40	0.5	15.5	0.125	5.632	4.17	19.28	+362
65	0.5	16.3	0.279	7.041	7.06	20.7	+193
90	0.5	17.3	0.614	8.629	11.83	18.8	+59

6. FINITE ELEMENT ANALYSIS

6.1. Introduction

Usually, the geotechnical engineering problems can be very difficult and complicated because of their boundary conditions. However, there are some simplified theories invented by some researchers can be used to solve these kinds of problems. Because of soil variability, these problems can be more complex and in this case numerical analysis can be very useful.

Numerical modeling analysis has turn out to be extra popular in the analysis and design of geotechnical structures such as retaining walls, foundation and dams, etc. Important projects sometimes are analyzed by numerical modeling analysis and it is also very effective in analysis of soil-structures interaction.

In finite element analysis technique, the domain of the problems are meshed into a small elements which is composed of hundreds or thousands of small elements and nodes, suitable boundary conditions and proper essential models such as Mohr-Coulomb and linear elastic are applied, for all of the nodes equations are made and by solving theses equations every variables are found at the nodes.

Some people write a special finite element program for their self which can be used in solving geotechnical engineering problems. There are also some popular numerical finite element programs which are used by geotechnical engineers very often such as PLAXIS, GEO-SLOPE. Besides, there some other software which are more powerful such as ABAQUS and ANSYS and these programs can be used in many engineering aspects such as materials, structures, concrete and also can be used in analysis of geotechnical engineering problems. And those two programs are also utilized in many universities they are effective for teaching and research purposes.

6.2. Plaxis 3D Program

PLAXIS 3D is the most popular graphical user interface geotechnical program which is based on the finite element analysis and very often used by geotechnical engineers especially in modeling and analysis of soil-structure interaction such as foundation, retaining walls, soil slope stability, etc. The program has been designed in a way that the user can easily model any soil-structure interaction problems and study the behavior of the structure under loading.

Recently, many researchers use finite element technique for analysis and study soil-structure interaction problems. In this study, finite element analysis has been conducted by PLAXIS 3D package software. The model piles (timber and steel) are modeled and axial load applied the results were obtained in term of settlement versus bearing capacity and the finite element results were compared to the experimental results.

6.3. Model Pile Analysis

In this study the numerical finite element software PLAXIS 3D has been used for analysis of single model piles (steel and timber). The Mohr-Coulomb failure criteria were used to conduct finite element analysis and the dry condition was considered for the model sand. The totally eight model pile load tests were analyzed with four relative density of the sand mentioned in this study before. In each test the results obtained in term of pile displacement versus axial load.

6.3.1. Boundary Conditions

In analysis of model piles in Plaxis 3D "Standard Fixities" has defined for the boundary condition which is made automatically by the software. Furthermore, rigid interfaces were defined, that means, there is no relative movement between the nodes of the finite elements which represent the model pile and those of the finite elements which represent the ground soil. In the three-dimensional analysis, 15-node wedge elements are generally used. The schematic representation of the 15-node elements used in the analysis is shown in Figure 6.1

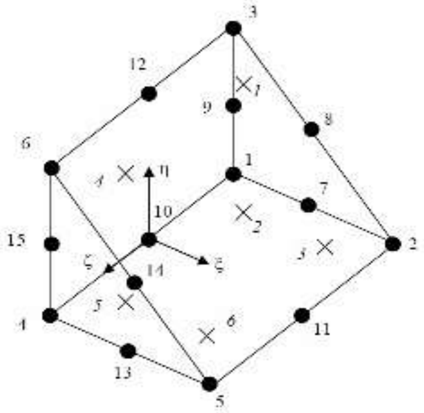

Nodes (●) and strain points (x)

Figure 6.1. Node Wedge Elements in 3D Analysis (Plaxis 3D Foundation Tutorial Manual, 2007)

6.3.2. The Mesh Generation

In Plaxis 3D, a two-dimensional top-view mesh is generated first, after that the three-dimensional mesh is generated with the standard procedure of the software. Figure 6.2 shows the two and three dimensional mesh generated in the program.

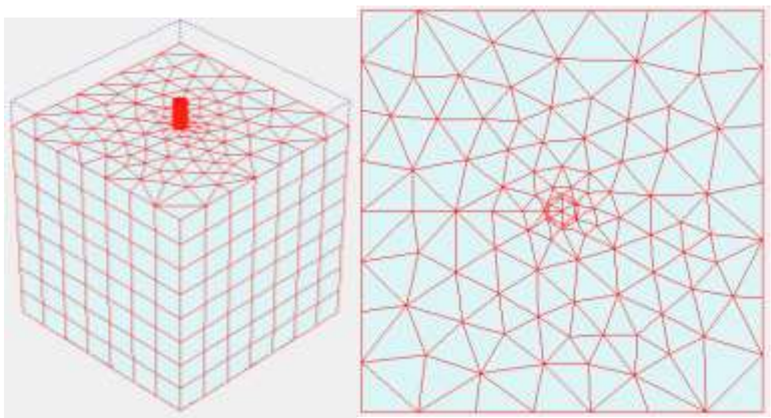

Figure 6.2. 2D and 3D dimensional mesh generated in Plaxis 3D program

6.4. The Material Parameters Used in the Analysis

The sand was modelled to obey Mohr-Coulomb failure criterion under drained conditions, the dry unit weight of the sand corresponding to relative density was input to the Plaxis 3D. The model piles (wood and steel) were modelled to obey linear elastic and non-porous and their unit weight also were given to Plaxis 3D program. Table 6.1 and 6.2 shows the parameters of the sand and pile materials used in Paxis 3D.

Table 6.1. The parameters of the sand used in Plaxis 3D program

Relative Density (Dr,%)	Average Dry Unit Weight (γ_d), (kN/m^3)	Modulus of Elasticity of the Sand (E) (kN/m^2)	Poisson's ratio	Internal friction angle of the sand (ϕ)°	Dialatancy angle of the sand (ψ)°	R_{int}	Cohesion kN/m^2
10	14.6	800	0.3	41	11	0.67	0.001
40	15.5	6300	0.3	44.3	14.3	0.67	0.1
65	16.3	12000	0.3	48.7	18.7	0.67	0.3
90	17.3	15500	0.3	52.4	22.4	0.67	0.5

Table 6.2. The parameters of the model piles (wood and steel) used in Plaxis 3D program

Model Pile	Average Dry Unit Weight (γ_d), (kN/m^3)	Modulus of Elasticity of the Piles (E) (kN/m^2)	Poisson's ratio
Wood Pile	6.077	$123*10^5$	0.369
Steel Pile	30.79	$2*10^8$	0.3

6.5. Results from Finite Element Program

After the sand and model piles were modelled in the Plaxis 3D, the total bearing capacity chosen from the experimental load-settlement, the same load value applied to the pile in Plaxis 3D by using the parameters mentioned above. The results showed that there is a good agreement of the Plaxis 3D finite element program compared to the experimental results.

Table 6.3. Comparison of the experimental results with Plaxis 3D for wood pile

Dr	Load (kN)	Experimental Settlement (mm)	Plaxis 3D Settlement (mm)
10%	0.32	5.3	4.95
40%	2.64	9.5	9.02
65%	6.95	11.65	10.71
90%	13.52	12.5	11.70

Table 6.4. Comparison of the experimental results with Plaxis 3D for steel pile

Dr	Load (kN)	Experimental Settlement (mm)	Plaxis 3D Settlement (mm)
10%	0.27	4	4.28
40%	1.95	7.6	6.25
65%	5.88	9.32	8.82
90%	10.92	10	9.30

To get a better view and easily compare the results of the experimental tests with results achieved from Plaxis 3D finite element, the results from experimental and Plaxis 3D combined in a graphical figure together. The graphical comparisons between experimental results with Plaxis 3D results are shown in Figures 6.3 and 6.4. Figure 6.5 show the typical vertical displacement contours of the pile. Figures 6.6 through 6.13 show the load-displacement curves of the model piles analysis by Plaxis 3D.

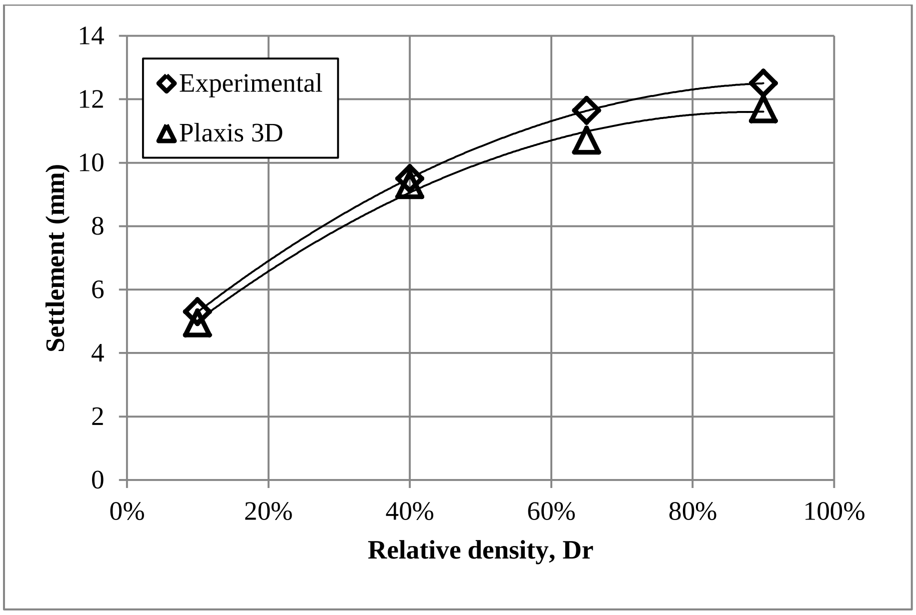

Figure 6.3. Comparison of the experimental results with Paxis 3D for wood pile

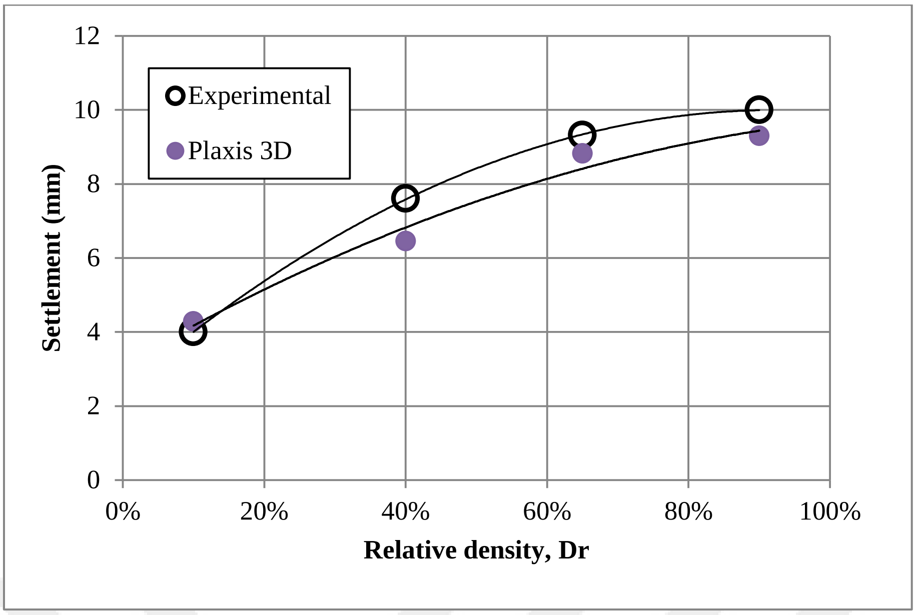

Figure 6.4. Comparison of the experimental results with Paxis 3D for steel pile

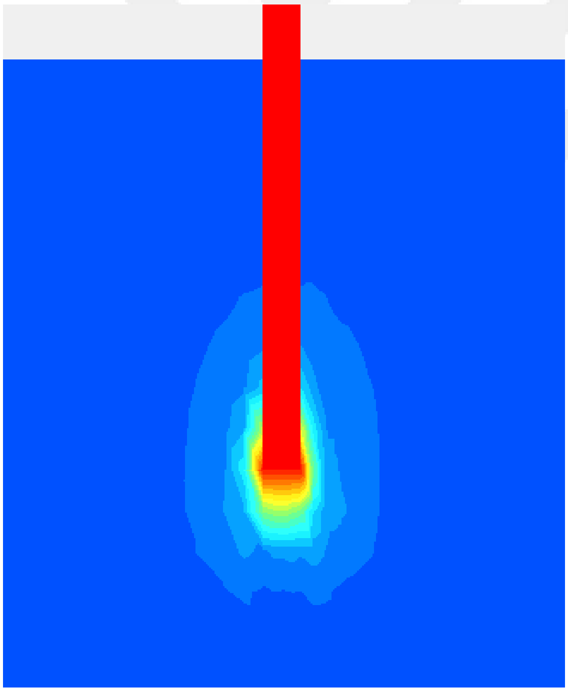

Figure 6.5. Typical vertical displacement contours of the pile analyzed by Plaxis 3D

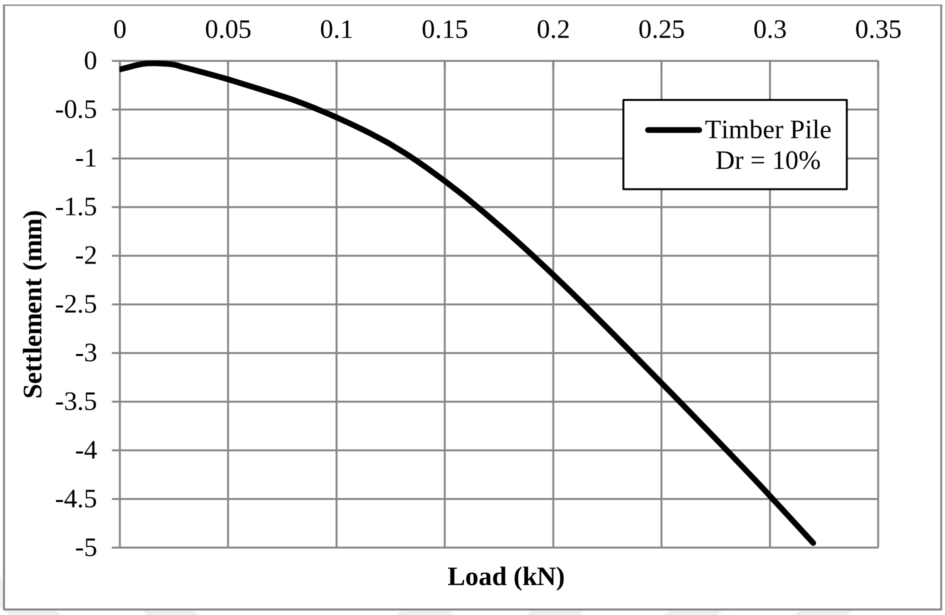

Figure 6.6. Load- displacement curve of timber model pile by Plaxis 3D for Dr = 10%

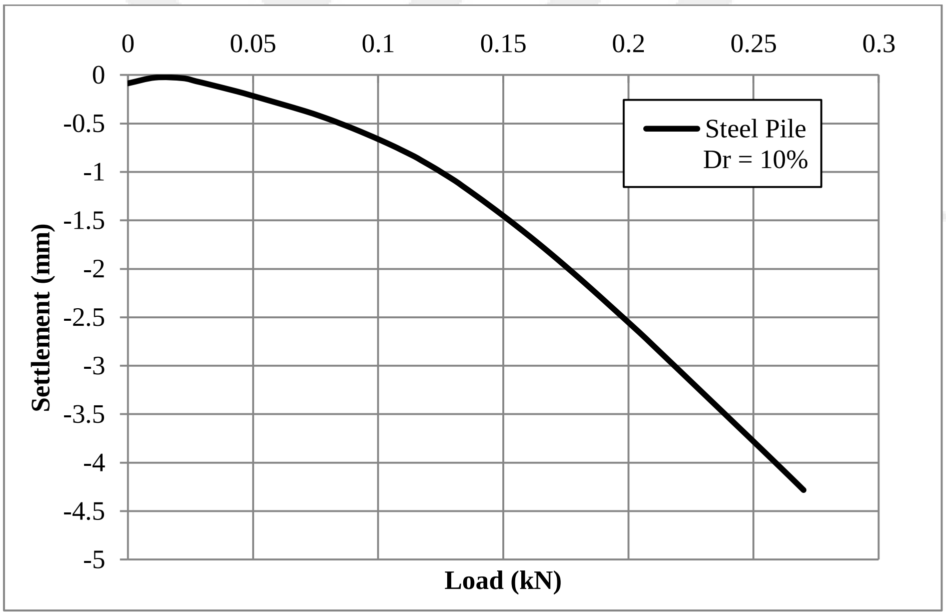

Figure 6.7. Load- displacement curve of steel model pile by Plaxis 3D for Dr = 10%

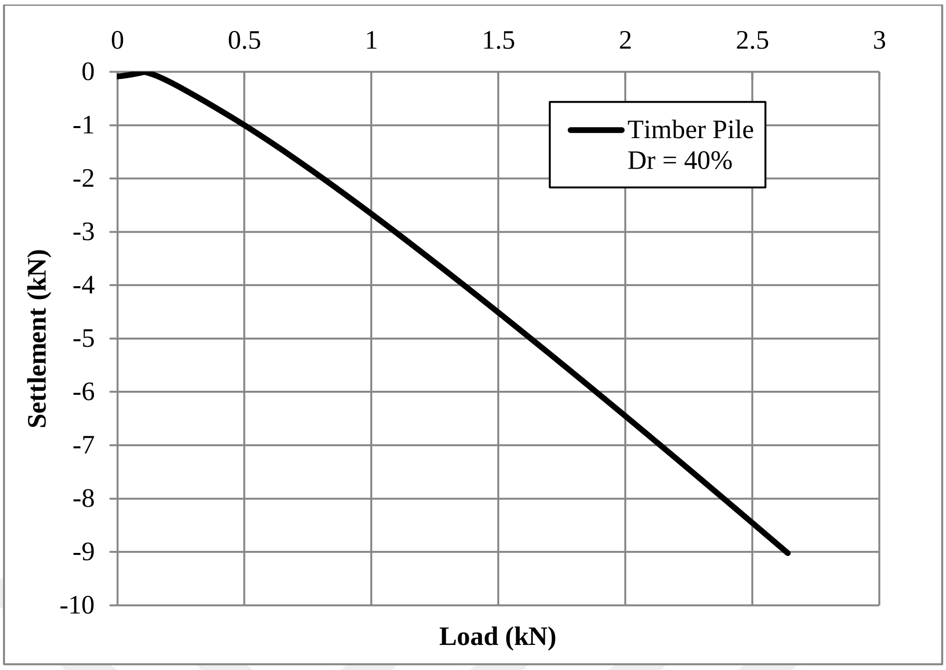

Figure 6.8. Load- displacement curve of timber model pile by Plaxis 3D for Dr = 40%

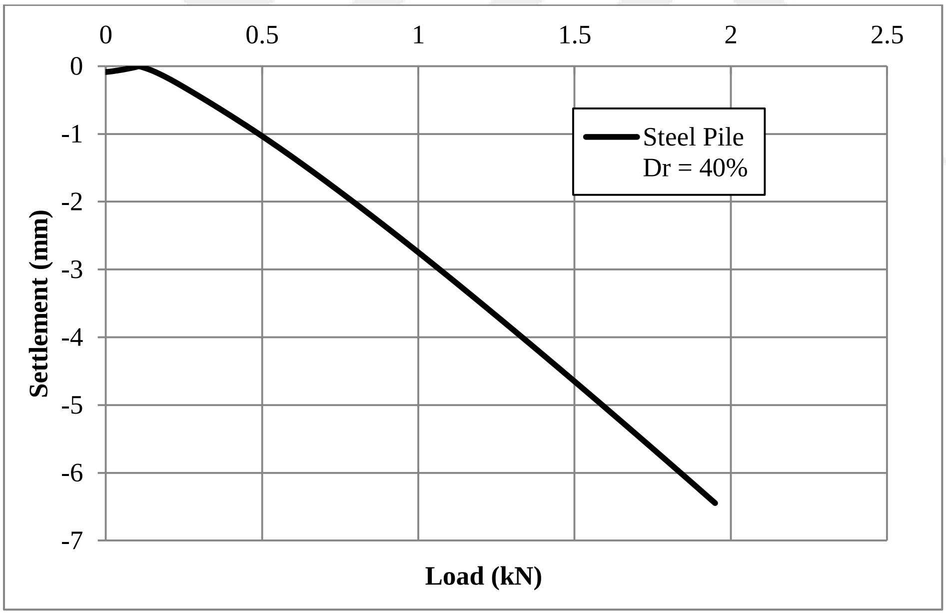

Figure 6.9. Load- displacement curve of steel model pile by Plaxis 3D for Dr = 40%

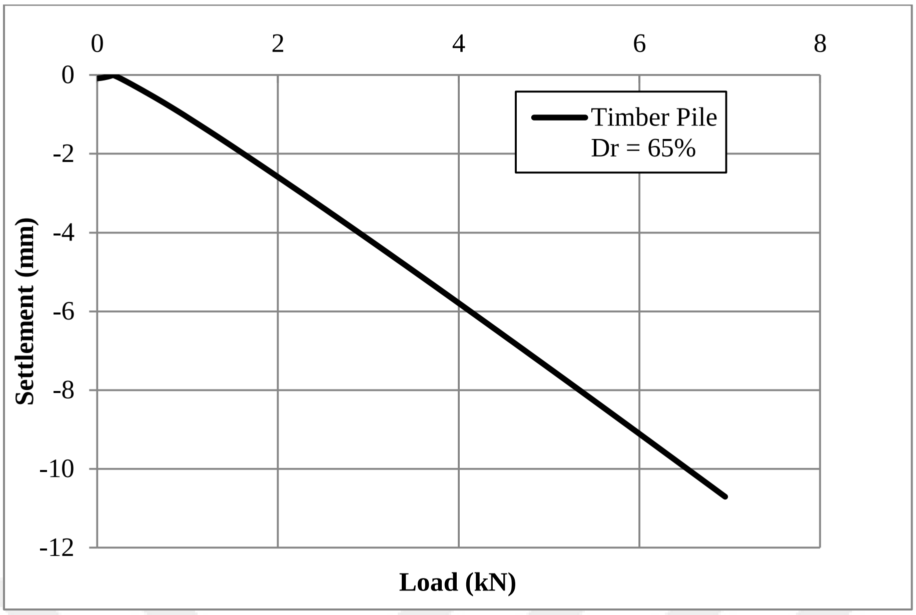

Figure 6.10. Load- displacement curve of timber model pile by Plaxis 3D for Dr = 65%

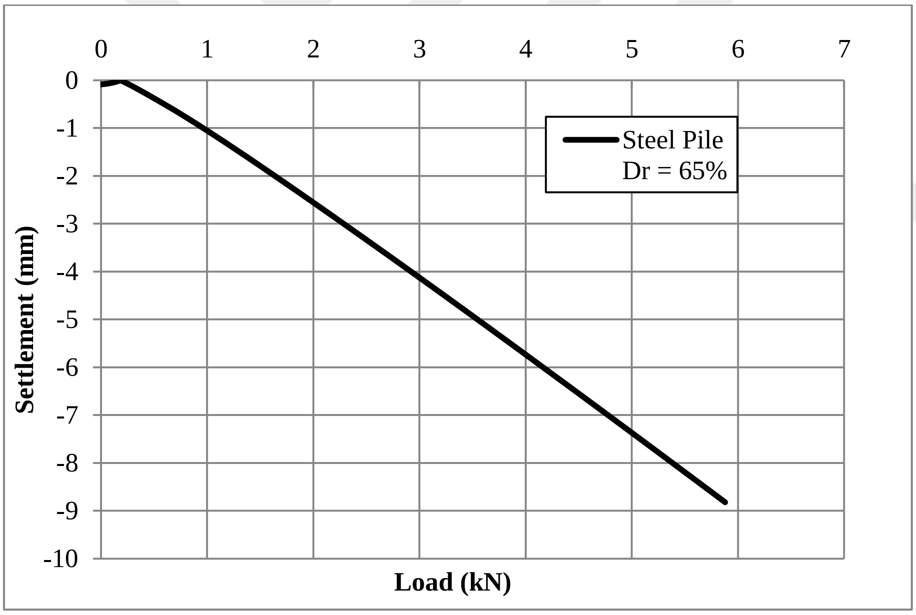

Figure 6.11. Load- displacement curve of steel model pile by Plaxis 3D for Dr = 65%

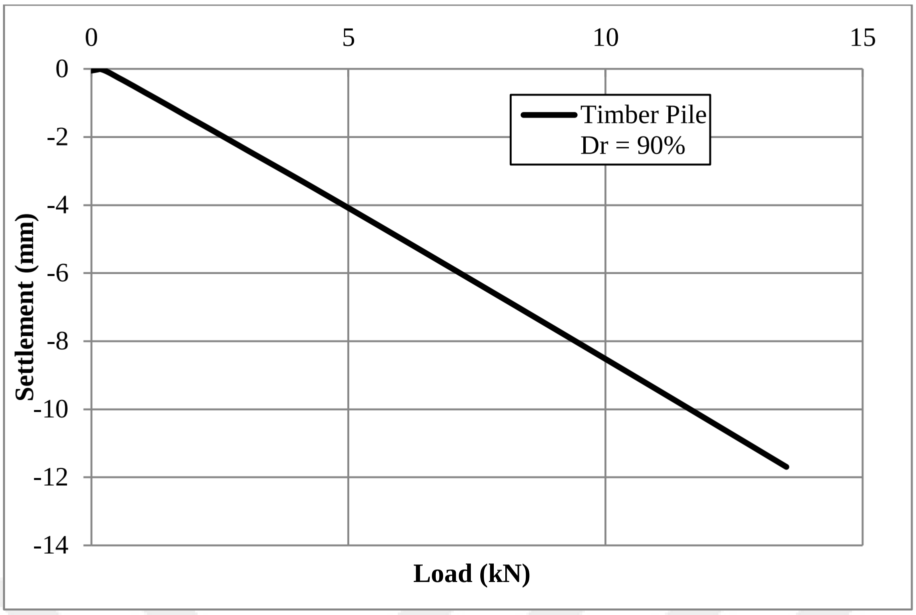

Figure 6.12. Load- displacement curve of timber model pile by Plaxis 3D for Dr = 90%

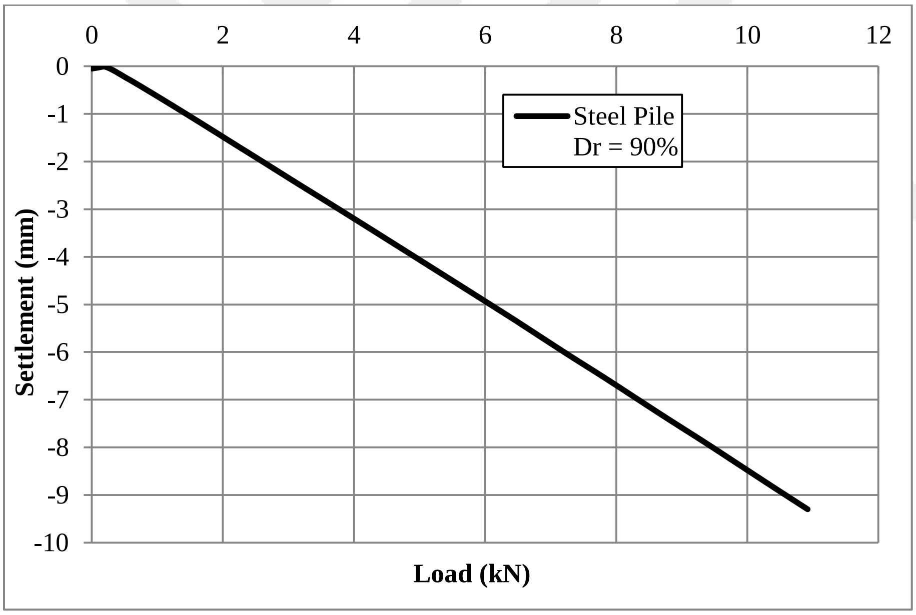

Figure 6.13. Load- displacement curve of steel model pile by Plaxis 3D for Dr = 90%

7. CONCLUSION

Direct shear tests were performed to estimate the internal friction angle of the sand in different relative densities. Interface shear tests were also conducted to estimate the skin friction angle between sand and pile materials (wood and steel) in four different relative densities. The direct shear tests and interface shear tests were done under three different normal stresses with constant shearing rate 0.5 mm/min. Besides, the behavior of the single model piles were studied under axial loading, the pile materials were same to those materials used in direct shear tests. The rate of the pile displacement was approximately kept 1 mm/min. Finite element program Plaxis 3D was also used to study the behavior of same model piles under axial loading. The following conclusions achieved from the test results.

- From the direct shear tests it was discovered that the internal friction angle of the sand increases with increasing relative density.
- From the interface shear tests between sand and pile materials it was observed that the skin friction angle increases with increasing relative density up to 65%, but it started to decrease in relative density 90%.
- From the pile model load tests, it was found that the total bearing capacity of the model pile increases with increasing relative density in a non-linear relationship. The settlement corresponding to the total bearing capacity also increases with increasing relative density. But in pile base bearing capacity it was noticed that the settlement corresponding the failure load decreases with increasing relative density. The shaft friction resistance of the model piles also increases with increasing relative density, and the settlement which is required for mobilization the shaft resistance also goes high with increasing relative density. From the pile shaft friction load tests it was observed that the friction resistance of the steel model pile is very low compare to the wood model pile.
- Among the theoretical results, it was found that the Terzaghi's results are very close to the experimental results of our study. While there is a big difference between experimental results compared to other theories. However, many researchers say that the Terzaghi's equation is very conservative and give very low results.

- From the comparisons of the shaft friction resistance of the model piles to the theoretical methods, it was found that there is a considerable difference between experimental results and theoretical results. Considering K_p as a coefficient of earth pressure in calculation of shaft friction resistance gives more reasonable results.
- From back calculation of the earth pressure coefficient by using experimental results, it was discovered that it increases with increasing relative density, and also depends on the degree of stress, the density and angle of friction of the soil, the roughness and the diameter of the pile.
- It is noticed from the total bearing capacity load-settlement curves, the total bearing capacity mobilized at the settlement about (10-25)% of the pile model diameter.
- From the finite element analysis like the experimental results the bearing capacity of the model pile increases with increasing relative density. The most parameter which influences the settlement is the modulus of elasticity and the unit weight of the soil. The load-settlement curve achieved from the Plaxis 3D programs is different from the experimental load-settlement curves. In relative density 10% the load-settlement curve from Plaxis 3D and experimental are non-linear. But in relative density 40%, 65% and 90% the load-settlement curves from plaxis 3D are linear, while they are no-linear from experimental results.

REFERENCES

Adejumo, T.W., 2015. Research Article Effects of Shape and Technology of Installation on the Bearing Capacity of Pile Foundations in Layered Soil, *Sch. J. Eng. Tech.*, **3**(2A), 104-111.

Aksoy, H.S., Gör, M. and İnal, E., 2016. A new design chart for estimating friction angle between soil and pile materials, *Geomechanics and Engineering*, **10**(3), 315-324.

American Petroleum Institute, 1989. Recommended practice for planning, designing, and constructing fixed offshore platforms (Vol. 2). American Petroleum Institute.

American Society of Civil Engineers, 1959. Timber Piles and Construction Timbers, Manual of Practice, No. 17, *American Society of Civil Engineers*, New York.

ASTM D3080/D3080M-11, 2011, Standard test method for direct shear test of soils under consolidated drained conditions, ASTM International, West Conshohocken, PA, USA.

ASTM D422-63, 2007. Standard Test Method for Particle-Size Analysis of Soils, American Test Methods Standards, West Conshohocken, PA.

ASTM D4254-16, 2016. Standard Test Methods for Minimum Index Density, and Unit Weight of Soils and Calculation of Relative Density, American Test Methods Standards, West Conshohocken, PA.

ASTM D854-14, 2014. Standard Test Methods for Specific Gravity of Soil Solids by Water Pycnometer, American Test Methods Standards, West Conshohocken, PA.

Awoshika, K. and Reese, L.C., 1971.Analysis of Foundations with Widely Spaced Piles. *Research Report **No.*** **117-3**, Center for Highway Research, The University of Texas at Austin.

Bank, L.C., 2006. Composites for construction: structural design with FRP materials, *John Wiley & Sons.*

Beringen, F. L., Windle, D., and Van Hooydonk, W. R., 1980. Results of loading tests on driven piles in sand. In *Recent developments in the design and construction of piles*, 213-225, Thomas Telford Publishing.

Bolton, M.D., and Lau, C.K., 1993. Vertical bearing capacity factors for circular and strip footings on Mohr–Coulomb soil, *Canadian Geotechnical Journal*, ***30***(6), 1024-1033.

Bolton, M.D., Gui, M.W., Garnier, J., Corte, J.F., Bagge, G., Laue, J. and Renzi, R., 1999. Centrifuge cone penetration tests in sand, *Géotechnique*, **49**(4), 543-552.

Bowles, L.E., 1996. Foundation analysis and design, *5th edition McGraw Hill*, New York.

Briaud, J.L., and Tucker, L.M., 1988. Measured and predicted axial response of 98 piles, *Journal of Geotechnical Engineering*, **114**(9), 984-1001.

Buenfeld, N.R. and Newman, J.B., 1986. The development and stability of surface layers on concrete exposed to sea-water, *Cement and Concrete Research*, **16**(5), 721-732.

Bullen, F.R., 1958. Phenomena Connected with the Settlement Driven Piles, *Geotechnique*, **8**(3), 121-133.

Burland, J., 1973. Shaft friction of piles in clay--a simple fundamental approach. *Publication of Ground Engineering*/UK/, **6**(3), 30-42.

Chaudhuri, K.P.R. and Symons, M.V., 1983. Uplift resistance of model single piles, In *Geotechnical Practice in Offshore Engineering*, ASCE , 335-355.

Chellis, R.D., 1961. Pile foundations, *2nd edition McGraw Hill*, New York.

Chen, L.Y., Chen, Y.M. and Zhang, W.M., 2006. Time-effect on vertical bearing capacity of single drilled grouting pile in saturated soft soil, *Yantu Lixue(Rock and Soil Mechanics)*, **27**(3), 471-474.

Chen, W.F., 1975. Limit analysis and soil plasticity, 1st edition, Elsevier, 638.

Chow, F. C., Jardine, R. J., Brucy, F. & Nauroy, J. F., 1996. The effect of time on the capacity of pipe piles in sand, *Proceeding 28th Offshore Technology Conference, Houston.*

Coduto Donald P., 2016. Foundation design: principles and practices. 3rd ed. New Jersey Prentice Hall, 2016.

Coyle, H.M. and Reese, L.C., 1966. Load transfer for axially loaded piles in clay, *Journal of the Soil Mechanics and Foundations Division*, **92**(2), 1-26.

Coyle, H.M. and Sulaiman, I.H., 1967. Skin friction for steel piles in sand, *Journal of Soil Mechanics & Foundations Div*, 92(SM5, Proc Paper 490).

Coyle, H.M., and Castello, R.R., 1981. New design correlations for piles in sand, *Journal of Geotechnical and Geoenvironmental Engineering*, ***107***(ASCE 16379).

Das, B.M. and Sivakugan, N., 2016. Fundamentals of geotechnical engineering, *Cengage Learning.*

Das, B.M., Seeley, G.R. and Pfeifle, T.W., 1977. Pullout resistance of rough rigid piles in granular soils, *Soils and Foundations*, **17**(3), 72-77.

F. M. Lea, N. Davey., 1949. The deterioration of concrete in Structures, *J. Inst. C.E.* No. **7**, 248-95, London.

Fleming, K., Weltman, A., Randolph, M. and Elson, K., 2014. Piling engineering, *CRC press.*

Gavin, K. and Gallagher, D., 2005. Development of shaft friction on driven piles in sand and clay, *Geotechnical Society of the Institution of Civil Engineers of Ireland. Dublin* Institution of Civil Engineers of Ireland.

Goodell, B., 2000. Wood products: deterioration by insects and marine organisms, *Encyclopedia of materials science and technology*, Elsevier, New York.

Han, F., Salgado, R., Prezzi, M. and Lim, J., 2017. Shaft and base resistance of non-displacement piles in sand, *Computers and Geotechnics*, **83**, 184-197.

Han, J., Frost, J. and Brown, V., 2003. Design of fiber-reinforced polymer composite piles under vertical and lateral loads, Transportation Research Record, *Journal of the Transportation Research Board*, (1849).71-80.

Hanna, T. H., and Tan, R. H. S., 1973. The behavior of long piles under compressive loads in sand, *Canadian Geotechnical Journal*, ***10***(3), 311-340.

Hansen, J.B., 1970. A revised and extended formula for bearing capacity.

Igoe, D. J. P., Gavin, K. G., and O'Kelly, B. C., 2011. Shaft capacity of open-ended piles in sand, *Journal of Geotechnical and Geoenvironmental Engineering*, ***137***(10), 903-913.

Janbu, N., 1976. Static bearing capacity of friction piles, In *Sechste Europaeische Konferenz Fuer Bodenmechanik Und Grundbau*,**1**.

Kerisel, J., 1964. Deep foundations basic experimental facts, *In Proceedings of a Conference on Deep Foundations, Mexico City*, 5-44.

Kishanrao, W.M., Arun Prasad, A., 2016. Numerical Modeling Of Single Pile In A Two-Layered Soil. *International Journal of Mechanical and Production Engineering*, Volume- 4, Issue-6,

Kraft Jr, L. M., 1991. Performance of axially loaded pipe piles in sand, *Journal of Geotechnical Engineering*, ***117***(2), 272-296.

Loehr, J., Bowders, J., Owen, J., Sommers, L. and Liew, W., 2000. Slope stabilization with recycled plastic pins. Transportation Research Record*: Journal of the Transportation Research Board*, (1714), 1-8.

Lopez-Anido, R., Michael, A. P., and Sandford, T. C., 2004. FRP composite-wood pile interface characterization by push-out tests. *J. Compos. Constr., in press.*

Lopez-Anido, R., Michael, A.P. and Sandford, T.C., 2003. Experimental characterization of FRP composite-wood pile structural response by bending tests, *Marine Structures*, **16**(4), 257-274.

Lopez-Anido, R., Michael, A.P., Sandford, T.C. and Goodell, B., 2004. 'Repair of wood piles using prefabricated FRP composite shells. *J. Perform. Constr. Facil*.

Mansur, C.I. and Hunter, A.H., 1970. Pile tests-Arkansas river project. *Journal of Soil Mechanics & Division, American Society of Civil Engineers*, Vol. **96**, No. SM6, 1545–1582.

Mayerhof, G.G., 1976. Bearing capacity and settlement of pile foundations, *Journal of Geotechnical and Geoenvironmental Engineering*, ***102***(ASCE# 11962).

Mayoral, J.M., Pestana, J.M. and Seed, R.B., 2005. Determination of multidirectional p-y curves for soft clays, *Geotechnical testing journal*, ***28*****(**3), 253-263.

Mazurkiewicz, B.K., 1968. Skin friction on model piles in sand, Bulletin No. **25**, *The Danish Geotechnical Institute*, Copenhagen. 13.

Meyerhof, G. G., 1959. Compaction of sands and bearing capacity of piles, *Journal of the Soil Mechanics and Foundations Division*, ***85***(6), 1-30.

Meyerhof, G.G., 1948. An investigation of the bearing capacity of shallow footings on dry sand, In *Proc. 2nd ICSMFE,* **1**, 238-243.

Meyerhof, G.G., 1961. Compaction of Sands and Bearing Capacities of Piles, *American Society of Civil Engineers, Transactions.* **126**, 1292 – 1323

Meyerhof, G.G., 1963. Some recent research on the bearing capacity of foundations, *Canadian Geotechnical Journal*, ***1***(1), 16-26.

Mijena, E.H., 2012. A comparison of friction piles bearing capacity based on theoretical and empirical mathematical models (*Master's thesis*, Institutt for bygg, anlegg og transport).

Naghibi, F., Fenton, G.A. and Griffiths, D.V., 2014. Prediction of pile settlement in an elastic soil, *Computers and Geotechnics*, **60**, 29-32.

Nanda, S. and Patra, N.R., 2011. Shaft resistance of piles in normally consolidating marine clay subjected to compressive and uplift load, In *Geo-Frontiers 2011: Advances in Geotechnical Engineering*, 263-272.

OKAHARA, M., NAKATANI, S., TAGUCHI, K. and MATSUI, K., 1990. A study on vertical bearing characteristics of piles. *Doboku Gakkai Ronbunshu*, (**418)**, 257-266.

Olson, R.E., and Denis, N.D., 1982. Review and compilation of pile test results, axial pile capacity, Geo*technical Engineering Center, Department of Civil Engineering, University of Texas*.

O'Neill, M.W. and Raines, R.D., 1991. Load transfer for pipe piles in highly pressured dense sand, *Journal of Geotechnical Engineering*, **117**(8), 1208-1226.

Paik, K., Salgado, R., Lee, J. and Kim, B., 2003. Behavior of open-and closed-ended piles driven into sands, *Journal of Geotechnical and Geoenvironmental Engineering*, **129**(4), 296-306.

Paikowsky, S.G., Player, C.M. and Connors, P.J., 1995. A dual interface apparatus for testing unrestricted friction of soil along solid surfaces. *Geotechnical Testing Journal*, **18**(2), 168-193.

Pecce, M., 2001. Structural behaviour of FRP profiles, *In Composites in Construction*: A Reality, 241-249.

Perkins, R., 2009. Creosote Treated Timber in the Alaskan Marine Environment. *Alaska University Transportation Center.*

Potyondy, J.G., 1961. Skin friction between various soils and construction materials. *Geotechnique*, **11**(4), 339-353.

Rahil, F.H., Al-Neami, M.A. and Al-Zaho, K.A.N., 2016. Effect of Relative Density on Behavior of Single Pile and Piles Groups Embedded with Different Lengths in Sand, *Engineering and Technology Journal*, **34**(6 Part (A) Engineering),1206-1220.

Rahil, F.H., Al-Neami, M.A. and Al-Zaho, K.A.N., 2016. Effect of Relative Density on Behavior of Single Pile and Piles Groups Embedded with Different Lengths in Sand. *Engineering and Technology Journal*, 34(6 Part (A) Engineering), 1206-1220.

Randolph, M. F., Dolwin, R., and Beck, R., 1994. Design of driven piles in sand, *Géotechnique*, ***44***(3), 427-448.

Reddy, E.S., Chapman, D.N. and O'Reilly, M., 1998. Design and performance of soil-pile-slip test apparatus for tension piles. *Geotechnical testing journal*, **21**(2), 132-139.

Reddy, E.S., Chapman, D.N. and Sastry, V.V.R.N., 2000. Direct shear interface test for shaft capacity of piles in sand. *Geotechnical Testing Journal*, **23**(2), 199-205.

Robinsky, E.I. and Morrison, C.F., 1964. Sand displacement and compaction around model friction piles, *Canadian Geotechnical Journal*, **1**(2), 81-93.

Schmertmann, J.H., 1991. The mechanical aging of soils. *Journal of Geotechnical Engineering*, **117**(9), 1288-1330.

Shin, E.C., Das, B.M., Puri, V.K., Yen, S.C. and Cook, E.E., 1993. Ultimate uplift capacity of model rigid metal piles in clay. *Geotechnical & Geological Engineering*, ***11*(**3), 203-215.

Sosa, M., Pérez-López, T., Reyes, J., Corvo, F., Camacho-Chab, R., Quintana, P. and Aguilar, D., 2011. Influence of the marine environment on reinforced concrete degradation depending on exposure conditions. *Int. J. Electrochem*. Sci, **6**, 6300-6318.

Tan, R. H. S., and Hanna, T. H., 1974. 'Long piles under tensile loads in sand, *Geotech. Engrg*, ***5***(2), 109-124.

Tavenas, F.A., 1971. Load tests results on friction piles in sand, Canadian Geotechnical Journal, **8**(1), 7-22.

Terzaghi, K. and Peck, R.B., 1948. Soil Mechanics in Engineering Practice, *John Wiley and Sons*, New York, NY, USA.

Thomann, T.G., Zoli, T. and Volk, J., 2004. Lateral load test on large diameter composite piles. *In Geotechnical Engineering for Transportation Projects*, 1239-1247.

Uesugi, M. and Kishida, H., 1986. Influential factors of friction between steel and dry sands. *Soils and foundations*, **26**(2), 33-46.

Ukritchon, B., Whittle, A.J., and Klangvijit, C., 2003. Calculations of bearing capacity factor Nγ using numerical limit analyses, *Journal of Geotechnical and Geoenvironmental Engineering*, ***129***(5), 468-474.

Vesic, A.S., 1963. Bearing capacity of deep foundation in sand, Highway Research Record. *National Academy of Sciences, National Research Council*, ***39***, 113-151.

Vesic, A.S., 1977. Design of pile foundations. *NCHRP synthesis of highway practice*, (42).

Wada, A., 2004. Skin Friction and Pile Design. *International Conference on Case Histories in Geotechnical Engineering*.

Yasufuku, N., and Ochiai, H., 2005. Sand-Steel Interface Friction Related to Soil Crushability. Geotechnical Special Publication. 627-641.

Yasufuku, N., and Ochiai, H., 2005. Sand-steel interface friction related to soil crushability, In *Geomechanics: Testing, Modeling, and Simulation*, 627-641.

Yazdanbod, A., O'Neill, M.W., and Aurora, R.P., 1984. Phenomenological study of model piles in sand, *Geotechnical Testing Journal*, ***7***(3), 135-144.

APPENDIX

APPENDIX-1 (Experimental Time-Load and Time-Displacement Curves of Total Bearing Capacity of Timber Model Pile)

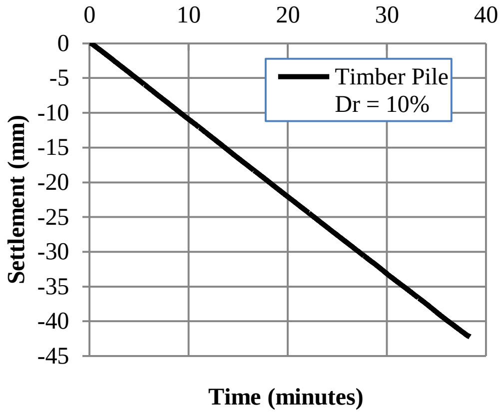

a) Time-Settlement Behavior

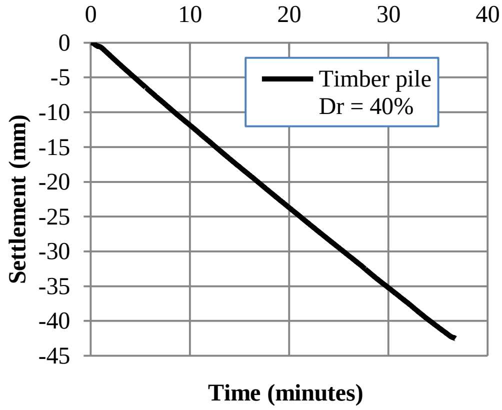

b) Time-Settlement Behavior

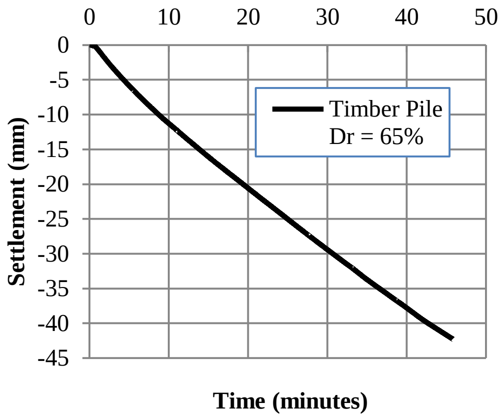

c) Time-Settlement Behavior

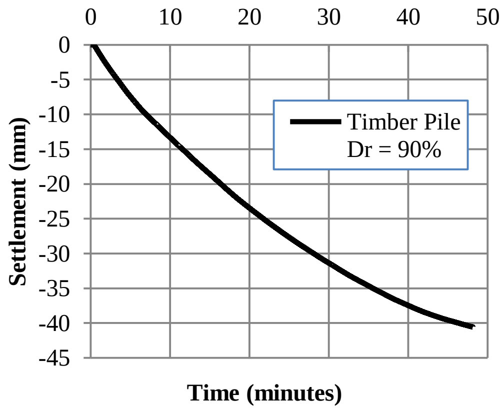

d) Time-Settlement Behavior

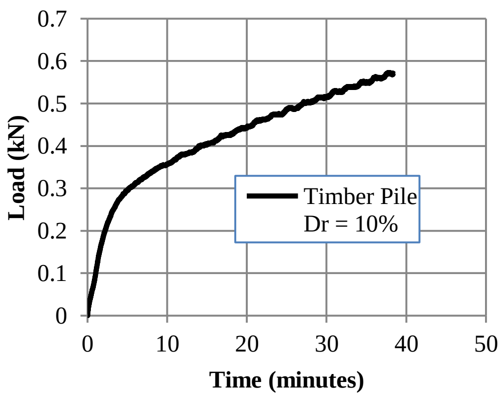

e) Time-Load Behavior

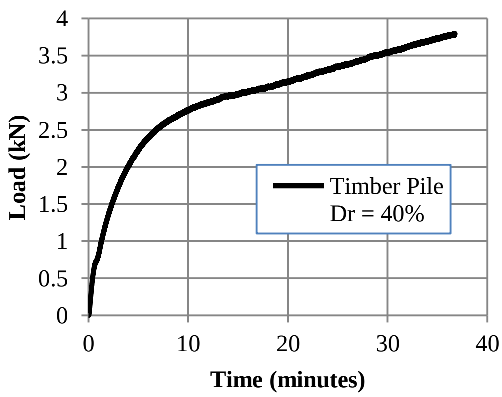

f) Time-Load Behavior

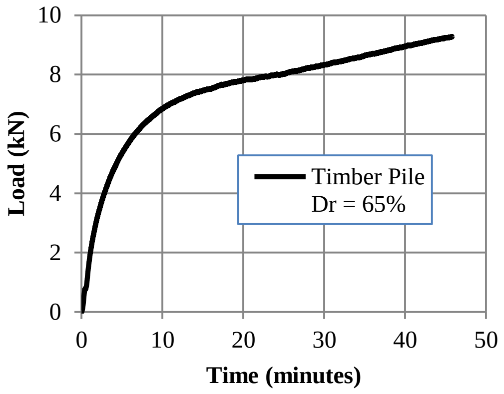

g) Time-Load Behavior

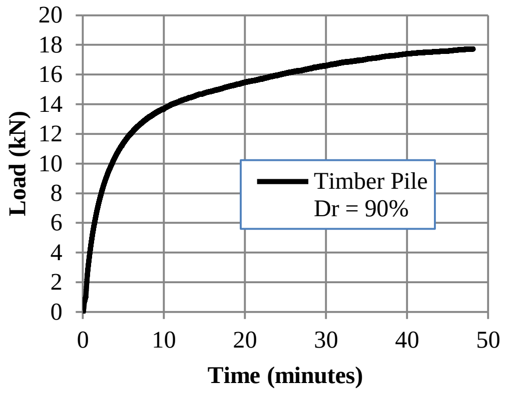

h) Time-Load Behavior

Figure A.1. a), b), c), d); Time-settlement behavior, and e), f), g), h); time-load behavior curves of timber pile at (Dr=10%, 40%, 65% and 90%), respectively.

APPENDIX-2 (Experimental Time-Load and Time-Displacement Curves of Total Bearing Capacity of Steel Model Pile)

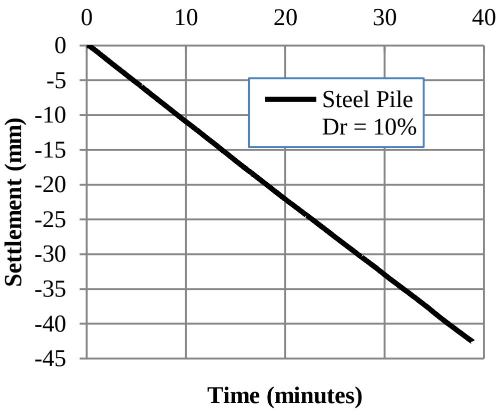

a) Time-Settlement Behavior

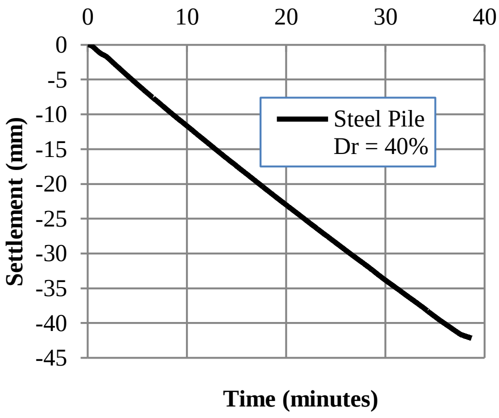

b) Time-Settlement Behavior

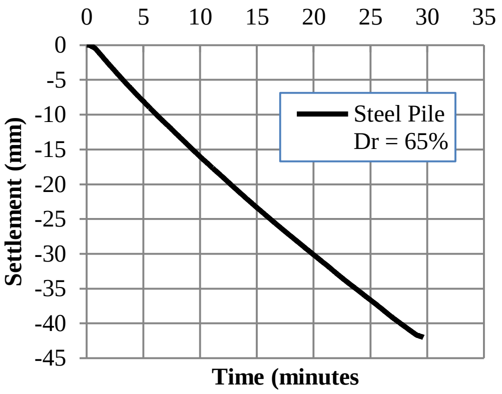

c) Time-Settlement Behavior

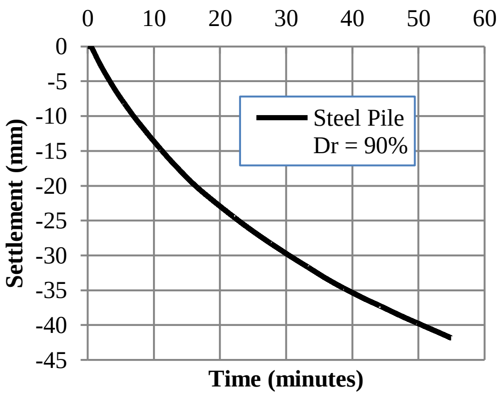

d) Time-Settlement Behavior

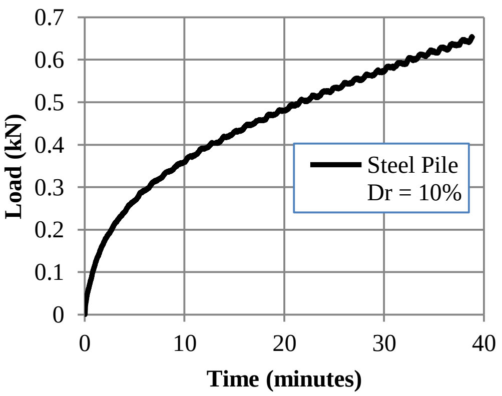

e) Time-Load Behavior

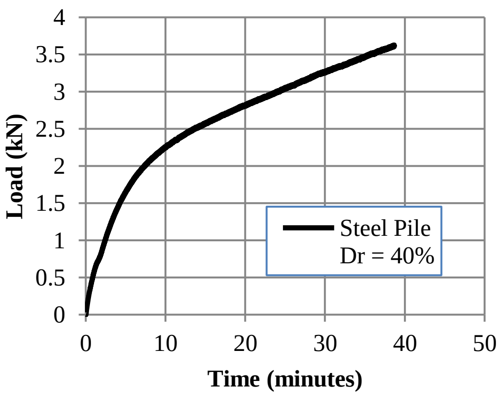

f) Time-Load Behavior

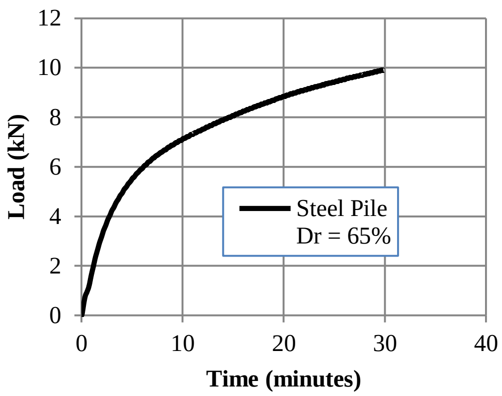

g) Time-Load Behavior

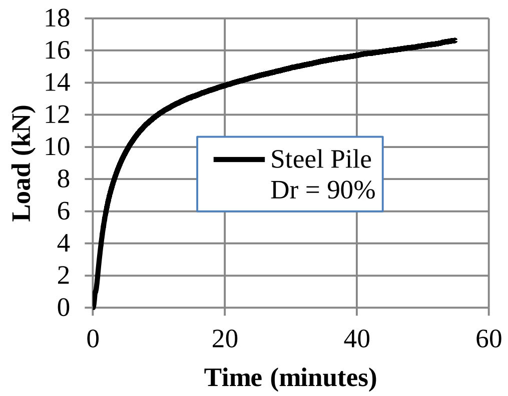

h) Time-Load Behavior

Figure A.2. a), b), c), d); Time-settlement, and e), f),g), h); behavior time-load behavior curves of steel pile at (Dr=10%, 40%, 65% and 90%), respectively.

APPENDIX-3 (Experimental Time-Load and Time-Displacement Curves of Base Bearing Capacity of Model-Piles)

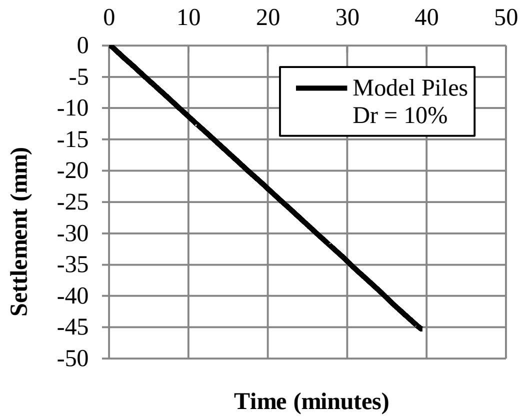

a) Time-Settlement Behavior

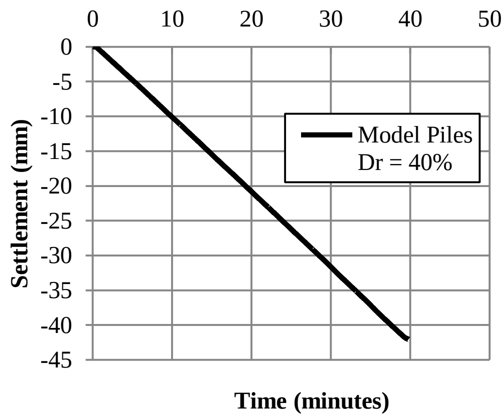

b) Time-Settlement Behavior

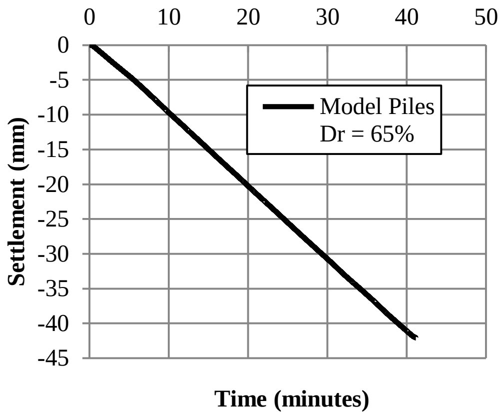

c) Time-Settlement Behavior

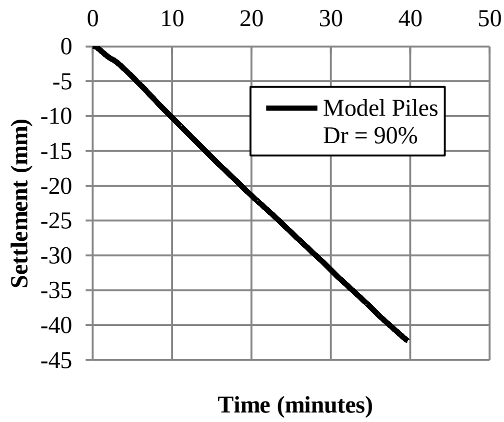

d) Time-Settlement Behavior

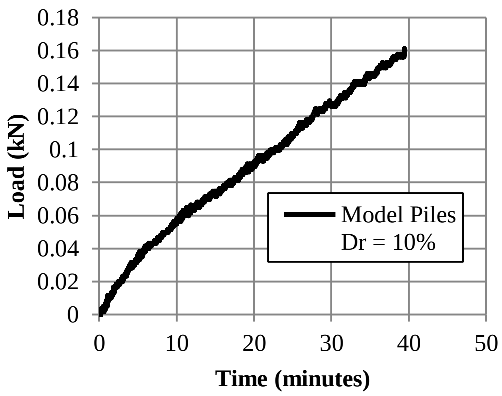

e) Time-Load Behavior

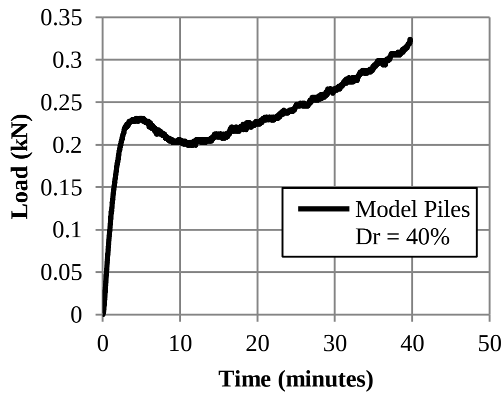

f) Time-Load Behavior

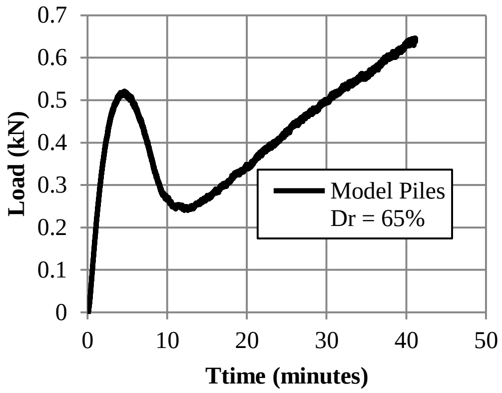

g) Time-Load Behavior

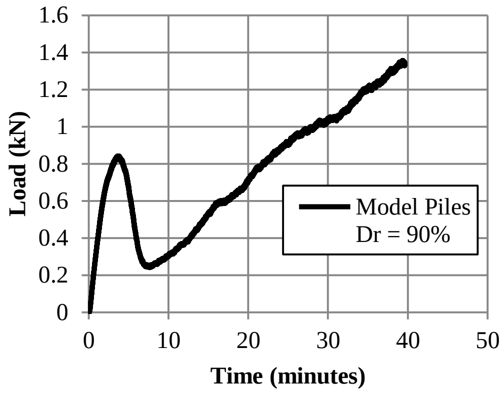

h) Time-Load Behavior

Figure A.3. a), b), c), d); Time-settlement behavior, and e), f), g), h); time-load behavior curves of base bearing capacity of model piles at (Dr=10%, 40%, 65% and 90%), respectively.

APPENDIX-4 (Experimental Time-Load and Time-Displacement Curves of Shaft Friction Resistance of Timber Pile, and Styrofoam-Filter Penetration Resistance)

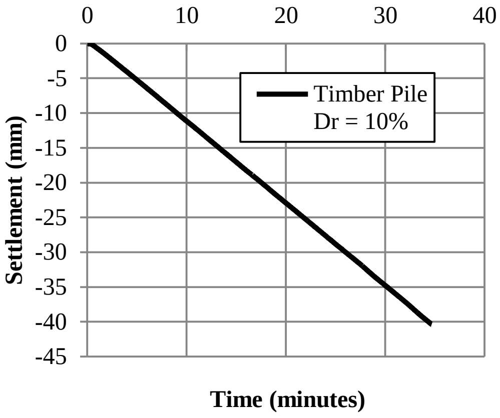

a) Time-Settlement Behavior

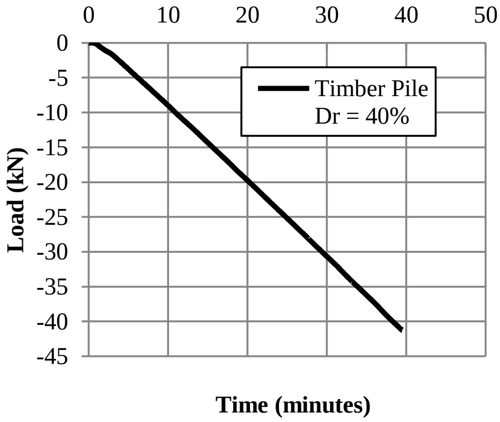

b) Time-Settlement Behavior

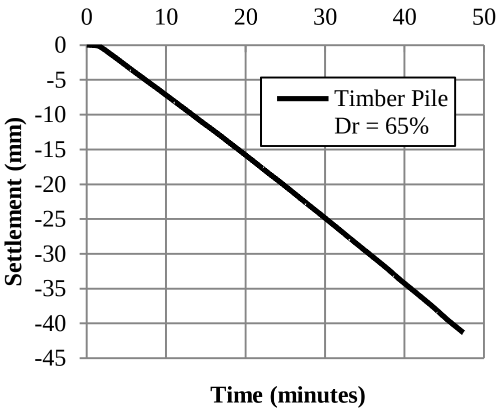

c) Time-Settlement Behavior

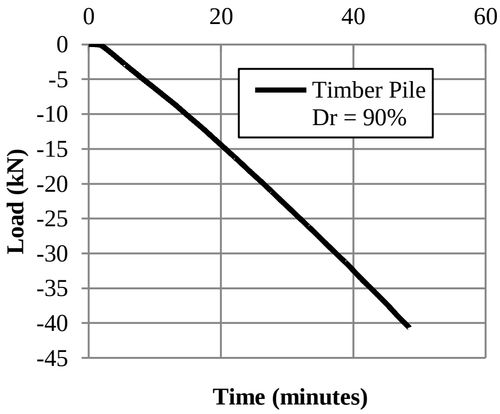

d) Time-Settlement Behavior

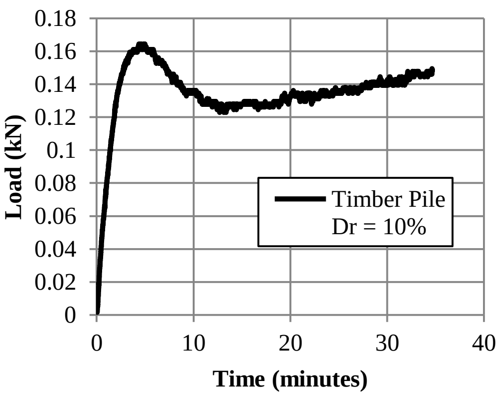

e) Time-Load Behavior

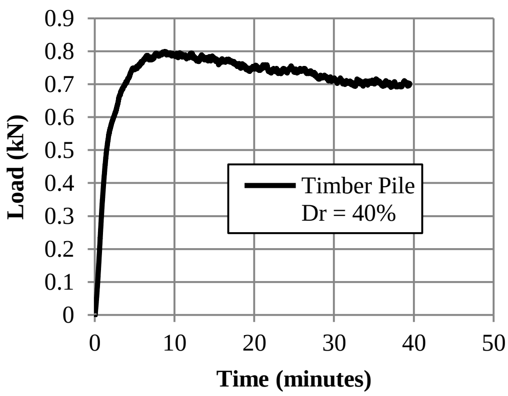

f) Time-Load Behavior

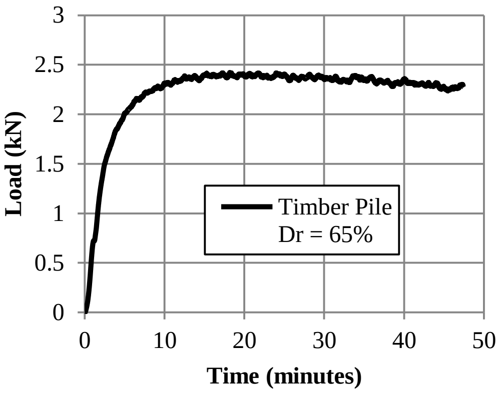

g) Time-Load Behavior

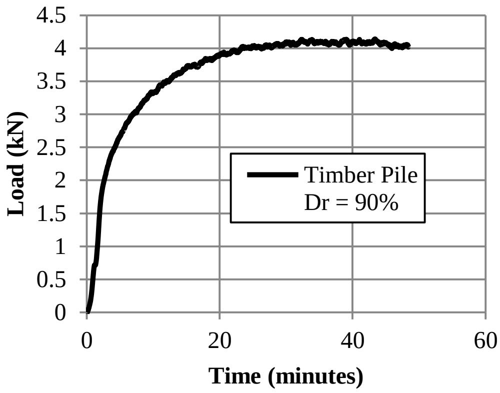

h) Time-Load Behavior

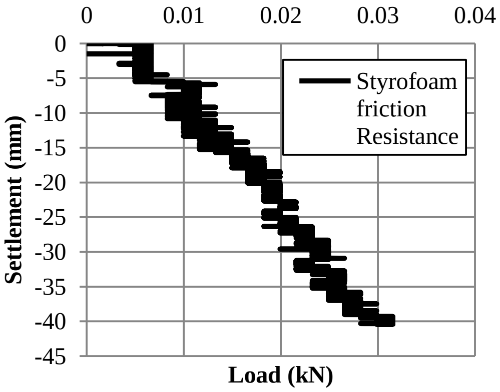

i) Load-Displacement Behavior

Figure A.4. a), b), c),d); Time-settlement behavior curves,, and e), f), g), h); time-load behavior curves of shaft friction resistance of timber pile at (Dr=10%, 40%, 65% and 90%), respectively., and i); load-displacement behavior of Styrofoam-filter penetration resistance with timber pile.

APPENDIX-5 (Experimental Time-Load and Time-Displacement Curves of Shaft Friction Resistance of Steel Pile, and Styrofoam-Filter Penetration Resistance)

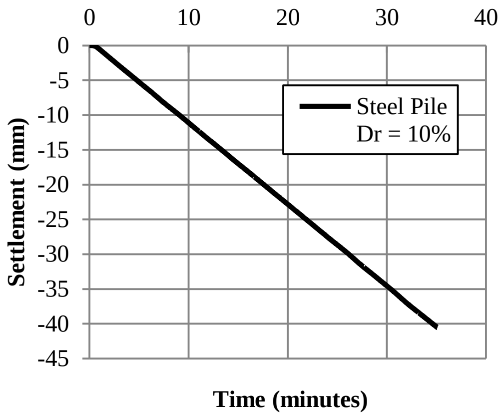

a) Time-Settlement Behavior

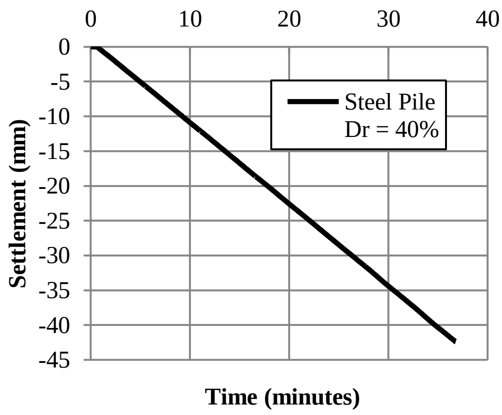

b) Time-Settlement Behavior

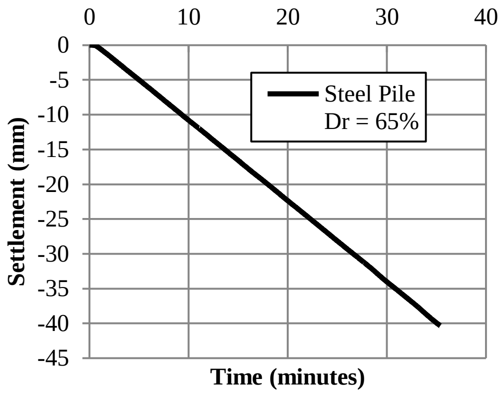

c) Time-Settlement Behavior

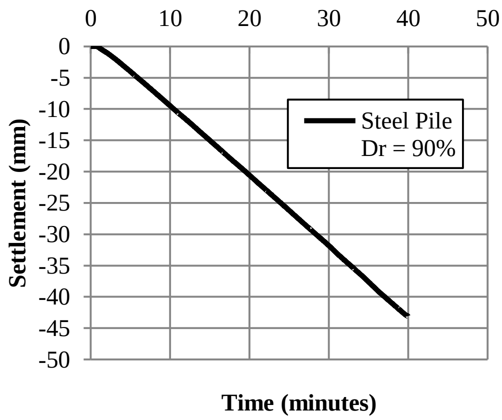

d) Time-Settlement Behavior

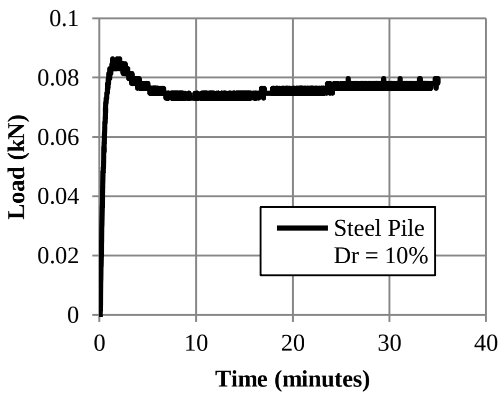

e) Time-Load Behavior

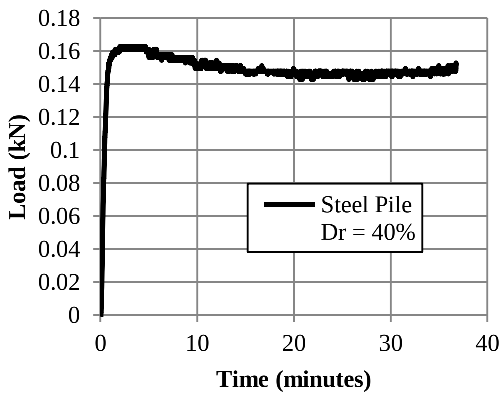

f) Time-Load Behavior

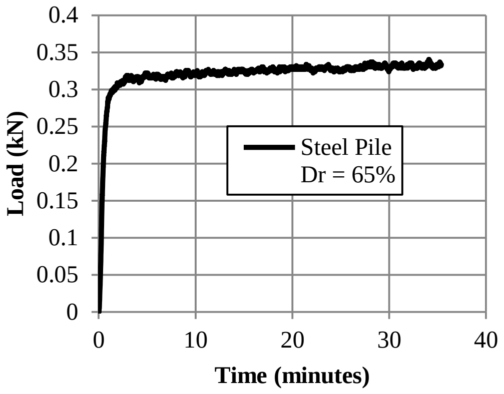

g) Time-Load Behavior

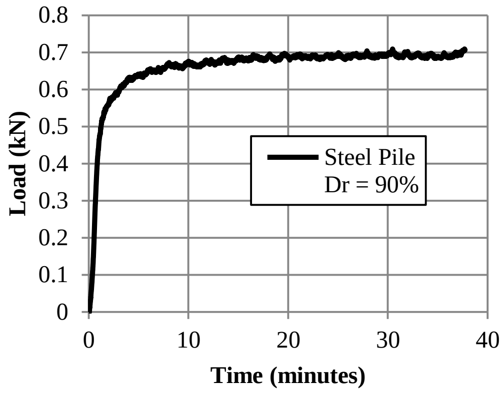

h) Time-Load Behavior

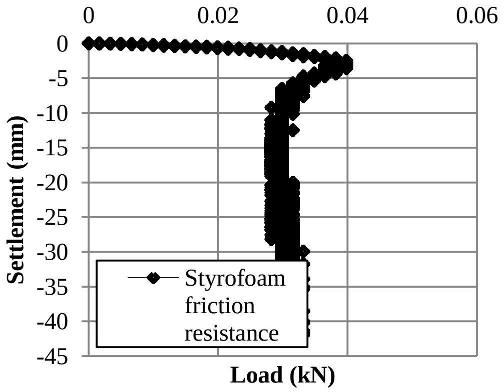

i) Load-Displacement Behavior

Figure A.5 a), b), c),d); Time-settlement behavior curves,, and e), f), g), h); time-load behavior curves of shaft friction resistance of steel pile at (Dr=10%, 40%, 65% and 90%), respectively., and i); load-displacement behavior of Styrofoam-filter penetration resistance with steel pile.

RESUME

Personal Information

Nationality	: Iraqi
Date of birth	: July 14, 1989
Place of Birth	: Zakho, Iraq
Gender	: Male
Marital Status	: Sıngle
Email Address	: eng.nechervan@gmail.com
Phone No.	: +9647504262428
	: +905530469618